Three essays on trade policy, commodity trade and deforestation

by

Manoj Sharma

B.S., Tribhuvan University, Nepal, 2017

M.S., Agriculture and Forestry University, Nepal, 2020

AN ABSTRACT OF A DISSERTATION

submitted in partial fulfillment of the
requirements for the degree

DOCTOR OF PHILOSOPHY

Department of Agricultural Economics
College of Agriculture

KANSAS STATE UNIVERSITY
Manhattan, Kansas

2026

Abstract

This dissertation examines the complex relationship between environmental regulation incorporating trade restriction policy, agricultural expansion, including deforestation, and transport infrastructure. It is composed of three essays that investigate these dynamics using the combination of structural and reduced form approaches.

The first chapter, "Costly Regulation, Minimal Results: The EU's Deforestation Regulation Effect on Global Soy Trade", analyzes the impact of the European Union Deforestation Regulation (EUDR). The EUDR aims to reduce deforestation by restricting market access to soy products that are deforestation-embodied in the EU market. The primary concern is that such restrictions could shift the soy trade to unregulated markets. To shed light on this issue, we employ a gravity model, treating the EUDR compliance costs as additional trade costs for exports to the EU. We find that stricter compliance costs reallocate soy exports from South America toward non-EU markets, mainly China, and divert the EU imports towards North America. Under the counterfactual scenario in which South America does not comply with the regulation, EU consumers face even larger price increases, while South American countries experience minimal terms-of-trade losses. Our analysis suggests that trade reallocation to an unregulated market could potentially dilute the impact of the EUDR, making it less effective in directly reducing deforestation linked to soy production.

The second chapter, "Exports and Deforestation: A Commodity-Level Analysis", quantifies the extent to which international demand for agricultural commodities drives deforestation. Using panel data for 138 countries and 18 commodity groups during 2001–2022, we estimate commodity-specific elasticities of deforestation with respect to exports. To address the potential endogeneity between exports and supply-driven deforestation, we instrument exports with an export share-weighted average of destination-market import demands, constructed from a gravity model of bilateral trade. We find that a 10% increase in exports of agricultural commodities increases

commodities-associated deforestation by 2.96%. We also find heterogeneous effects across commodities and regions, with the largest effects for perennial and tree crops, livestock, soybeans, and sugar crops. Back-of-the-envelope calculations suggest that increases in international demand account for approximately 53 million hectares of agricultural expansion into forests between 2001 and 2022, corresponding to 49% of the observed forest-to-agriculture conversion.

The third chapter, “Domestic Market Access and Cropland Expansion in Brazil”, examines how improvements in domestic market access shape agricultural production and land use across Brazilian municipalities over 2015 to 2023. We construct a measure of domestic market access from Dijkstra least-cost routing on Brazil’s road, rail, and waterway networks. We find that a 10% improvement in domestic market access raises production value by 0.6 to 0.8% and expands the area under temporary crops by about 0.5%. By contrast, we find no robust long-run change in land productivity, measured as value per harvested hectare. The pattern points to an extensive-margin response in which a better transport network expands the cultivated area. We find heterogeneous effects across municipalities. In the North, greater market access is associated with declining value per hectare alongside area expansion, consistent with cultivation moving onto marginal frontier land, while in the Cerrado biome, it raises production value and harvested area.

Three essays on trade policy, commodity trade and deforestation

by

Manoj Sharma

B.S., Tribhuvan University, Nepal, 2017

M.S., Agriculture and Forestry University, Nepal, 2020

A DISSERTATION

submitted in partial fulfillment of the
requirements for the degree

DOCTOR OF PHILOSOPHY

Department of Agricultural Economics
College of Agriculture

KANSAS STATE UNIVERSITY
Manhattan, Kansas

2026

Approved by:

Major Professor
Nelson B. Villoria

Copyright

Abstract

This dissertation examines the complex relationship between environmental regulation incorporating trade restriction policy, agricultural expansion, including deforestation, and transport infrastructure. It is composed of three essays that investigate these dynamics using the combination of structural and reduced form approaches.

The first chapter, “Costly Regulation, Minimal Results: The EU’s Deforestation Regulation Effect on Global Soy Trade”, analyzes the impact of the European Union Deforestation Regulation (EUDR). The EUDR aims to reduce deforestation by restricting market access to soy products that are deforestation-embodied in the EU market. The primary concern is that such restrictions could shift the soy trade to unregulated markets. To shed light on this issue, we employ a gravity model, treating the EUDR compliance costs as additional trade costs for exports to the EU. We find that stricter compliance costs reallocate soy exports from South America toward non-EU markets, mainly China, and divert the EU imports towards North America. Under the counterfactual scenario in which South America does not comply with the regulation, EU consumers face even larger price increases, while South American countries experience minimal terms-of-trade losses. Our analysis suggests that trade reallocation to an unregulated market could potentially dilute the impact of the EUDR, making it less effective in directly reducing deforestation linked to soy production.

The second chapter, “Exports and Deforestation: A Commodity-Level Analysis”, quantifies the extent to which international demand for agricultural commodities drives deforestation. Using panel data for 138 countries and 18 commodity groups during 2001–2022, we estimate commodity-specific elasticities of deforestation with respect to exports. To address the potential endogeneity between exports and supply-driven deforestation, we instrument exports with an export share-weighted average of destination-market import demands, constructed from a gravity model of bilateral trade. We find that a 10% increase in exports of agricultural commodities increases

commodities-associated deforestation by 2.96%. We also find heterogeneous effects across commodities and regions, with the largest effects for perennial and tree crops, livestock, soybeans, and sugar crops. Back-of-the-envelope calculations suggest that increases in international demand account for approximately 53 million hectares of agricultural expansion into forests between 2001 and 2022, corresponding to 49% of the observed forest-to-agriculture conversion.

The third chapter, “Domestic Market Access and Cropland Expansion in Brazil”, examines how improvements in domestic market access shape agricultural production and land use across Brazilian municipalities over 2015 to 2023. We construct a measure of domestic market access from Dijkstra least-cost routing on Brazil’s road, rail, and waterway networks. We find that a 10% improvement in domestic market access raises production value by 0.6 to 0.8% and expands the area under temporary crops by about 0.5%. By contrast, we find no robust long-run change in land productivity, measured as value per harvested hectare. The pattern points to an extensive-margin response in which a better transport network expands the cultivated area. We find heterogeneous effects across municipalities. In the North, greater market access is associated with declining value per hectare alongside area expansion, consistent with cultivation moving onto marginal frontier land, while in the Cerrado biome, it raises production value and harvested area.

Table of Contents

List of Figures

List of Tables

Acknowledgments

I am deeply grateful to my major advisor, Professor Nelson B. Villoria, for his guidance in shaping my research direction, arousing my intellectual curiosity, and providing academic support throughout the journey. His insights and commitment to rigorous scholarship have shaped my development as a researcher in ways I will carry throughout my career.

I also extend my sincere gratitude to the members of my advisory committee — Professor Nathan Hendricks, Professor Peri da Silva, and Professor Jisang Yu — for their valuable comments, constructive feedback, and encouragement during both my proposal defense and my PhD dissertation defense. Their diverse perspectives greatly strengthened this research.

I am profoundly thankful to my wife, Sadiksha Dhakal, for her understanding, and support throughout this journey. Her encouragement sustained me through the most challenging moments of my doctoral studies.

Finally, I am deeply indebted to my parents, Chitra Kumari Ghimire and Toyanath Sharma, whose sacrifices, love, and belief in education made this achievement possible. Their support has been the foundation upon which everything else rests.

Last, but not least, I am grateful to my sister-in-law, Suvechha Dhakal, and my parents-in-law, Sapana Pandit and Murali Dhakal, for their love and support.

Dedication

To my elder brother, Santosh Poudel,

whose soul left this world far too soon at the age of twenty-six.

You are forever in my heart.

And to my younger sister, Maya Poudel,

with love and gratitude.

Chapter 1

Costly Regulation, Minimal Results: The EU's Deforestation Regulation Effect on Global Soy Trade

1.1 Introduction

The European Union Deforestation Regulation (EUDR) prohibits the trade of seven commodities (including their derivatives)—namely, palm oil, cattle, soy, cocoa, coffee, rubber, and wood—collectively known as forest risk commodities (FRCs), in the EU market unless they meet three criteria: being deforestation-free, compliant with source country legislation, and covered by a due diligence statement (European Union 2023). These requirements act as a non-tariff measure (NTM) to trade with an environmental objective by imposing deforestation-free production and traceability obligations on suppliers- a very similar NTM under the WTO's Technical Barriers to Trade (TBT)/ Sanitary and Phytosanitary (SPS) agreements. The regulation supports the EU's international climate change commitments, such as the EU Green Deal and the Paris Agreement. The implementation of the EUDR is anticipated to reduce tropical deforestation by 71.92 thousand hectares per year (the equivalent of ~101 thousand football pitches, which is 0.72% of annual global deforestation), avoiding the emissions of 32 million tons of carbon per year (~0.09% of annual global emissions) (KPMG 2023).

The EUDR can also inherit the well-documented ambiguity of NTM's trade effects. Technical barriers can either disrupt or facilitate trade, with effects being heterogeneous across products, measure types, country-pairs, and even with empirical design (Li and Beghin 2012; Santeramo and Lamonaca 2019). In particular, regarding environmental technical measures in food and agricultural products, several multi-country evidence points towards trade reducing effects (Santeramo and Lamonaca 2019; Fontagné, Kirchbach and Mimouni 2005). Globally, the environmental TBTs have been expanding rapidly, increasing the coverage of 3% to 16% of world trade between 2010 and 2020, and on average, reducing trade with effects varying by sector and exporter characteristics (Santeramo, Lamonaca and Emlinger 2025). Together, this motivates understanding EUDR compliance in the context of a technical barrier that can have potentially sizable and heterogeneous effects across soy products and trading partners.

Beyond trade effects, the EUDR's unilateral and market access reduction approach to curb deforestation has raised concerns about its effectiveness. The studies of climate policy and environmental trade policies have consistently shown that the carbon and market leakage effects, whether occurring within or across borders, undermine policy effectiveness, creating tension between environment and trade goals (e.g., Aichele and Felbermayr 2015; Shapiro 2021; Villoria et al. 2022). In the soy sector, Villoria et al. (2022) reveal that within-border displacement of deforestation is a notable risk in Brazil, as exports exposed to restrictions in one sub-region shift deforestation pressures elsewhere within the country. More broadly, the global commodity market often reallocates deforestation pressure, particularly when relatively smaller destination markets implement regulatory measures (Muradian et al. 2025). Given that the EUDR is a new regulation, it is important to assess whether its market access restrictions can truly reduce deforestation.

We analyze the impact of the proposed EU trade restrictions on the soy sector, using separate gravity models of soybeans, soybean oil, and soybean cake. We focus on the soy sector because (i) soybean expansion is an important driver of deforestation in South America, particularly Brazil (Song et al. 2021); (ii) the EU is the second-largest global importer of soybeans, accounting for 9.88% of global exports, and the largest importer of soybean meals—which constitutes 23.82% of global soy trade—with approximately 24% of global exports (Comtrade 2024); (iii) the EU's consumption accounts for 32.80% of the deforestation associated with soybean production (Pendrill et al. 2022; European Union 2023). We estimate the trade elasticity of each product and simulate the EUDR implementation by modeling the EUDR compliance costs as increased trade frictions, consistent with the NTM literature's treatment of technical measures as ad valorem tariff-equivalent frictions (e.g., Fontagné et al. 2005; Santeramo and Lamonaca 2019; Santeramo et al. 2025). We develop two scenarios: one in which all countries comply with the EUDR, and another in which three major deforestation-risk countries- Brazil, Argentina and Paraguay (BAP)- do not comply. These countries account for 59.3%, 6%, and 4.4% of deforestation-linked to soybean production, respectively (Persson et al. 2024). We estimate the counterfactual trade flows under these scenarios using the procedure developed by Anderson, Larch and Yotov (2018), which holds supplies and expenditures constant while allowing domestic and bilateral trade to adjust in response to changes in multilateral resistances stemming from the compliance costs. This approach enables us to evaluate the EUDR's effects on trade flows and price indexes.

Three key findings emerge from our analysis. First, the EUDR is largely ineffective at reducing soy exports from the focus countries. This is because the EU accounts for only a small share of exports from BAP (~8%), while demand from China is strong. Any entry restriction into the EU faced by BAP is offset by increased Chinese imports, while the EU can substitute with soy originating in the US and Canada. As a result, deforestation-embodied trade shifts from the EU to China. Second, the EU incurs a significant increase in soy prices, as much as 51%. In contrast, China and other Asian countries benefit from lower prices. Third, major exporters see no change in their terms of trade.

Our study makes two main contributions. First, we provide direct evidence of trade reallocation in the soy sector under the EUDR. Specifically, we show that soy trade shifts from the EU market to China, pointing towards little to no change in deforestation pressure and supporting the minimal cross-border leakage revealed by Villoria et al. (2022). Moreover, this points towards the domestic leakage patterns identified by Villoria et al. (2022) when sub-regions within a country (i.e., BAP) that are directly exposed to EU demand may shift deforestation pressure to sub-regions exposed to Chinese demand. This finding reinforces concerns raised in research (e.g., Aichele and Felbermayr 2015; Copeland, Shapiro and Taylor 2022; Villoria et al. 2022) about the limited effectiveness of unilateral trade policies covering relatively smaller markets. Second, our analysis highlights the broader challenges of using trade restrictions to achieve environmental goals, contributing to the literature of environmental-trade relations (Shapiro 2021; Felbermayr, Peterson and Wanner 2024). This issue underscores two tensions in the multilateral trade system: concerns from deforestation-risk countries about the discriminatory nature of the EUDR restrictions, and policy trade-offs between environmental objectives and market access (Larch and Wanner 2017; Farrokhi and Lashkaripour 2024). The experience with the EU's REACH suggests that, over time, stringent European technical regulations can diffuse as trading partners harmonize to retain market access (Cha and Koo 2021), but the short run is characterized by compliance burdens and trade reallocation; the very dynamics we document for soy under the EUDR.

1.2 The EUDR, the global soy market and implication to deforestation

The EUDR—Regulation (EU) 2023/1115 adopted on June 2023, and postponed to come into effect on December, 2025—repeals the EU Timber Regulation (EUTR) and goes beyond timber (wood) legality standards by including the six additional agricultural commodities (including their derivatives based on Harmonized System (HS) of classification): oil palm, cattle, soy, cocoa, coffee, and rubber (European Union 2023). The EUDR prohibits the trade of products whose supply chain is linked to either deforestation or forest degradation and mandates due diligence for tracing the origin of their products and providing evidence that they are sourced from non-deforested land. The regulation applies directly to the soy processors and supply companies that must verify the lack of deforestation along the supply chain, using geospatial data, land tenure documents, and compliance records with local laws. Enforcement of the regulation is the responsibility of the EU member states, which must establish robust monitoring and evaluation mechanisms, requiring the companies to submit due diligence statements and maintain traceability throughout the supply chain. When companies are found to breach diligence statements, the member state can charge penalties up to at least 4% of the annual turnover, confiscate the soy products or revenue, impose a temporary exclusion from public procurement, and impose a temporary prohibition from placing soy products on the EU market. Further, member states will conduct checks based on the risk benchmarking of the country of origin, including document reviews and field inspections. For example, major soy-producing South American countries, such as Brazil, Argentina, Paraguay, and Bolivia, fall under the standard risk category, and the member states conduct compliance checks at least 3% of companies sourcing soy products from these countries annually.

Four soy products based on the HS codes are subject to the EUDR: HS 1201 (soybeans whether or not broken), HS 120810 (Soybean flour and meal), HS 1507 (Soybean oil and its fractions, whether or not refined, but not chemically modified) and HS 2304 (oilcake and other solid residues, whether or not ground or in the form of pellets, resulting from the extraction of soybean oil). Soybeans account for 64.91% (USD 90.97 billion) of these products, followed by 0.36%, 10.34%, and 24.39%,

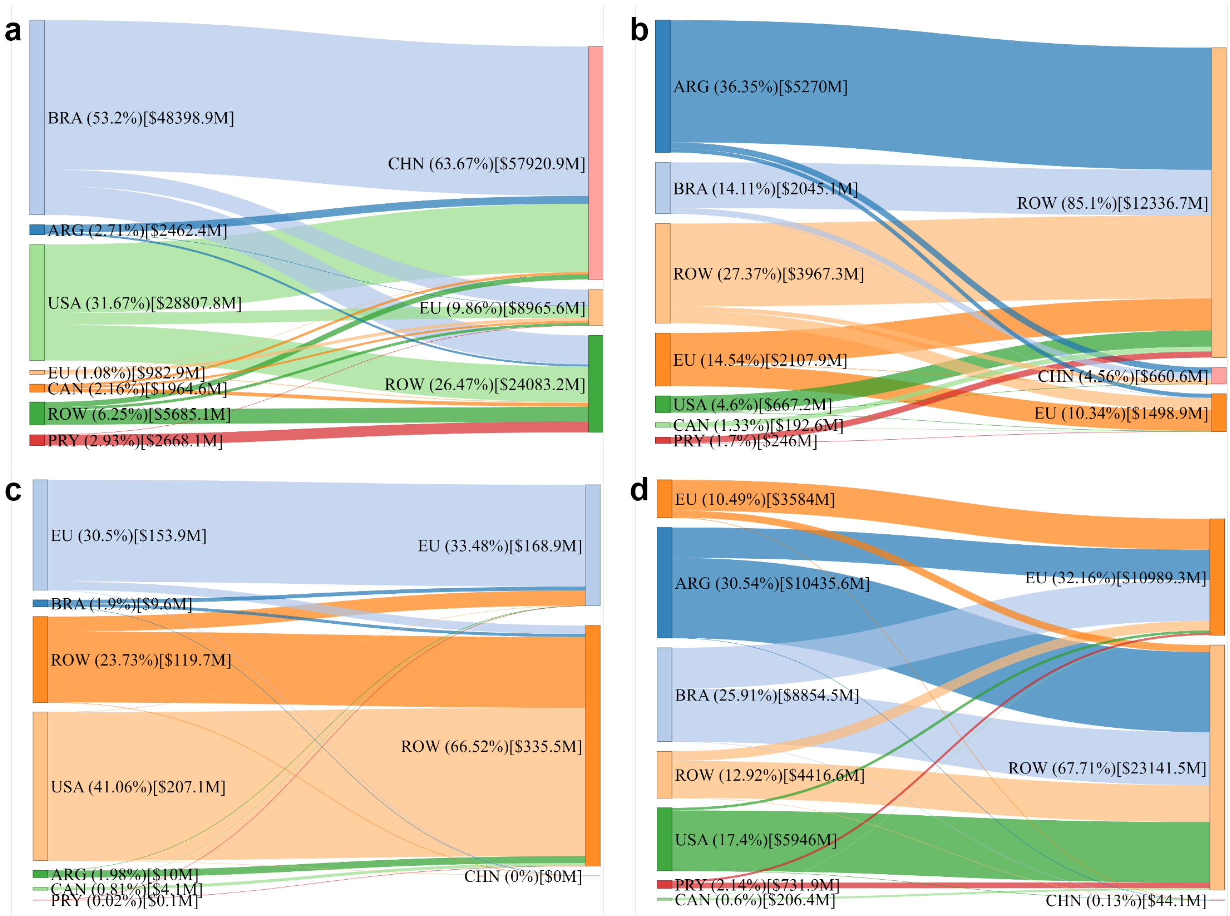

Figure 1.1: Global trade flows of soy market.

Notes. (a) Soybean (HS1201) trade flow which share 64.91% of total soy trade. (b) Soybean oil (HS1507) trade flows which shares 10.34% of total soy trade. (c) Soybean flour and meal (HS120810) trade flows which share 0.36% of total soy trade. (d) Soybean oil cake (HS2304) trade flows which shares 24.39% of total soy trade. Trade flows are based on cumulative values from 2021 to 2023. The values in the brackets represent the average export and import values over the same period. The left side of the plots indicates exporters, while the right side indicates importers. Source: UN Comtrade Database (Comtrade 2024).

respectively.

The global soybean market is characterized by three important features: (1) The increased production of soybeans is largely attributed to expanded land area. Between 2010 and 2021, the global harvested area for soybeans increased by 20.59%, leading to an 18% rise in production. This growth was driven primarily by land expansion (85%) and, to a lesser extent, yield improvements (15%) (Cassman and Grassini 2020). In Brazil, soybean production increased ninefold between 1990 and 2020, with much of this expansion occurring at the expense of natural ecosystems such as the Amazon and Cerrado (Umburanas et al. 2022; Fehlenberg et al. 2017). (2) The global soybean market represents one of the largest and most concentrated agricultural commodity trades, dominated by three major players: the US, Brazil, and China (Gale, Valdes and Ash 2019). Brazil and the US collectively account for over 80% of global soybean exports, while China alone imports more than 60% of global soybean imports, as illustrated in Figure 2.2. Although a relatively minor player in raw soybean and soybean oil imports, at 9.88% and 10.34%, respectively, the EU remains the leading importer of the global soybean meal and oilcake market, representing 32.16% of the imports (see table 4.1 for details on the EU's trade share). In addition, the soybean oil market is relatively fragmented than the soybean cake and soybeans market, balancing market leverage among multiple sources and destinations. (3) Few companies control the global soy supply chain (Heron, Prado and West 2018; Gouveris 2024). In Brazil, six multinational corporations—Archer Daniels Midland (ADM), Bunge, Cargill, Louis Dreyfus Company (LDC), Glencore, and Amaggi—together were responsible for 56.6% of soy exports and 66.3% of export-related soy deforestation risk over 2008 and 2017 (Ermgassen et al. 2020). These companies play a pivotal role in shaping supply chains and compliance with regulations.

The EUDR has faced criticism despite its aim to reduce tropical deforestation. Producer countries argue that the regulation is imposed unilaterally, ignoring their forest protection efforts (Noordwijk, Leimona and Minang 2025; Fisher et al. 2024). The regulation's data-intensive compliance is a major challenge, especially for multinational companies that struggle to trace commodity origins. For instance, although about 95% of soy from the Amazon and Cerrado in 2020 was deforestation-free, verifying this for EU compliance remains difficult (Vasconcelos et al. 2023). Similar administrative burdens for data verification of foreign emissions are a central concern in the EU's Carbon Border Adjustment Mechanism (CABM) debate (see Bellora and Fontagné 2023), highlighting that data collection costs matter a lot for environmental-cum-trade regulations. Such rules may also exclude smallholder farmers, including indigenous and local communities, as collecting geospatial data and land-tenure documents is costly and complex (Bürgi and Oberlack 2023; Noordwijk et al. 2025; Fisher et al. 2024), with mapping costs estimated at \$30–\$40 per plot (Gilbert 2024). Finally, since the EU represents a small share of the global soybean market, its influence is limited. This could result in segregated supply chains, with compliant soy sent to the EU and non-compliant ones sold elsewhere, leading to no change in deforestation (Oliveira et al. 2024; AgUnity 2023).

1.3 Data and Empirical Strategy

1.3.1 Data

To conduct empirical analyses, we construct a panel dataset for 90 countries (see appendix A1) covering 2007-2022. We choose this period because the data on effective applied tariffs are available only after 2007 onward and the bilateral and domestic sales data needed to construct intranational trade flows are available through 2022. Our data cover four key components: (i) international trade flows, (ii) intra-national trade flows, (iii) effectively applied tariffs, and (iv) standard gravity variables.

International trade flows. We compile a dataset on bilateral trade flows for soy products using the CEPII-BACI database, which is recognized for its detailed and reliable dataset. The BACI database offers several key advantages: (i) it provides data at the product level, categorized using Harmonized System (HS) codes, and (ii) it is more reliable than raw data from Comtrade as it reconciles mirror figures to address discrepancies and improve accuracy (Gaulier and Zignago 2010). For soybeans, the data is constructed using HS code 1200100 for the period before 2012, and HS codes 120110 and 120190 for the period from 2012 onward. Similarly, the trade flows for soybean oil are based on HS codes 150710 and 150790, while those for soybean cake are based on HS code 230400.

Intra-national trade flows. Following Villoria (2025), we estimate intranational trade quantity as production minus exports plus stock variation, using the FAOSTAT Food Balance Sheets database (FAOSTAT 2024). We convert intranational trade quantities to values using prices from the World Bank's Pink Sheet (World Bank 2025). Because the International Trade and Production Database for Estimation (ITPDE) (Larch, Shikher and Yotov 2025) includes only soybean intranational trade flows, our soybean intranational trade values correlate with ITPDE's at 0.95.

Effectively applied tariffs. We use bilateral effectively applied tariff rates obtained from the ITC MacMap database, which ensures accurate representation of tariff rates applied to a particular import during the study period (International Trade Centre 2024). If a preferential tariff exists, it is used as the effectively applied tariff, otherwise the most favored nation (MFN) applied tariff is used.

Standard gravity variables. In addition to trade and tariff data, we include variables capturing geographic and historical relationships between trading partners. These variables—such as distance, shared language, contiguity, and colonial ties—are sourced from CEPII's gravity database, which is a standard reference for gravity model analyses in international trade (Conte, Cotterlaz and Mayer 2023).

Table 1.1 presents summary statistics for our dataset, which covers 90 countries as both exporters and importers, resulting in 129600 observations. In our sample, average tariff rates are approximately 10.6% for soybeans, 8.8% for soybean oil, and 4.2% for soybean cake. Figure 1.2 displays the average tariffs imposed by EU countries on major exporters from 2007 to 2022. Notably, EU tariffs on soybean and soybean cake imports from Brazil, Argentina, Paraguay, and the USA are zero, and tariffs on soybean oil are also very low. Additionally, about 2.9% of country pairs in the sample share a border, 8.2% share a common language, and 3% have colonial ties.

Table 1.1: Summary statistics of variables used in the study

Variable	**Mean or Proportion**	**Standard Deviation**	**Minimum**	**Maximum**
Year	-	-	2007	2022
Soybean (000' USD)	16442.776	486355.389	0.000	35442703.415
Soyoil (000' USD)	5576.757	194287.663	0.000	26468744.300
Soycake (000' USD)	9865.004	311705.833	0.000	40749116.550
Tariff Soybean	0.106	0.684	0.000	7.574

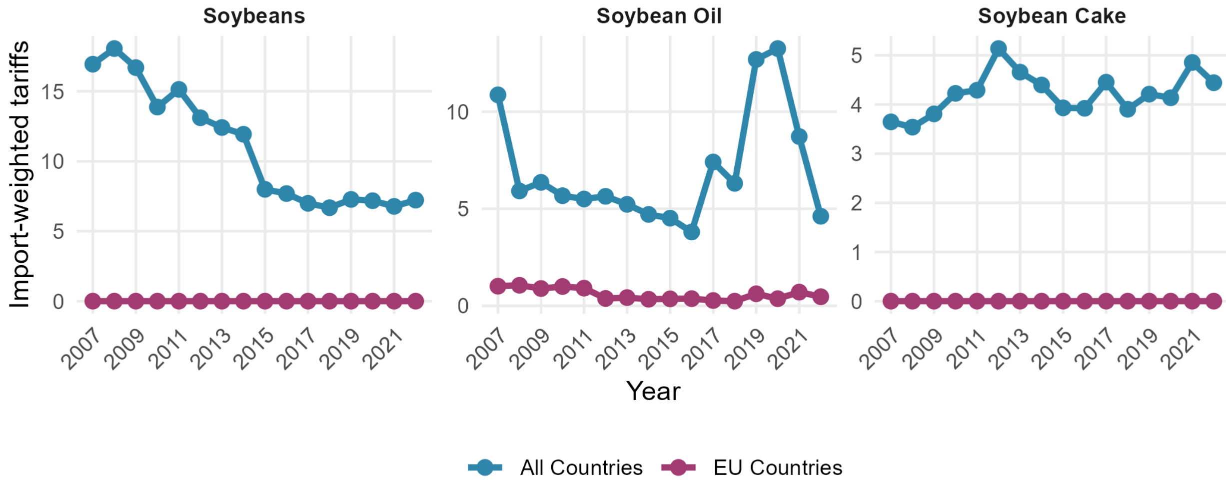

Figure 1.2: Import-weighted tariffs (%) by all countries and EU countries.

Variable	**Mean or Proportion**	**Standard Deviation**	**Minimum**	**Maximum**
Tariff Soybean oil	0.088	0.179	0.000	1.900
Tariff Soybean cake	0.042	0.102	0.000	0.715
Distance (KM)	7496.085	4761.858	7.000	19845.000
Contiguity	2.9%	-	0.000	1.000
Common Language	8.2%	-	0.000	1.000
Colonial Ties	3.0%	-	0.000	1.000

Notes: The total number of observations is 129600 (90 exporters * 90 importers * 16 years).

Source: Own illustration based on trade data from the BACI database (Gaulier and Zignago 2010) and tariffs data from the ITC MacMap (International Trade Centre 2024).

Note: The spikes in import-weighted tariffs for all countries for soybean oil in 2017–2020 reflect increased tariffs by India from 4% in 2016 to 36% in 2020.

1.3.2 The EUDR simulation

We conduct the EUDR simulation by employing a conditional equilibrium framework based on Anderson et al. (2018). This approach estimates conditional counterfactuals that keep sales and expenditures of each country unchanged, with the change in trade pattern driven directly from compliance costs and indirectly from shifts in trade patterns with third countries via multilateral resistance terms (see appendix A1.4 for the decomposition). Further, we model the EUDR as a destination-specific measure that raises the marginal cost of delivering soy from origin to the EU. As the legal obligation falls on 'operators' (importers, traders, and processors), these firm-level expenditures can be passed on to upstream and downstream depending on marketing structure, creating an effective ad valorem (iceberg) wedge on the EU-bounded flow. In a structural gravity framework, what matters for bilateral trade is this price wedge, which we represent in the form of 'tariff-equivalent". Our focus is the EUDR's effectiveness in mitigating soybean-related deforestation by examining economic pressure faced by high-risk countries, particularly Brazil and other South American countries. If these countries experience unfavorable changes in export potential, price indexes, producer prices, and terms of trade, it suggests that compliance pressures can incentivize anti-deforestation practices. The methodology for measuring these effects is described below:

Step 1: Estimation of Armington elasticities

We estimate separate gravity models for soybeans, soybean oil, and soybean cake. Our empirical model employs the PPML-gravity specification (see appendix 2 for details), as shown in below:

$$X_{ijt}^{s} = \exp(\gamma_{it}^{s} + \gamma_{jt}^{s} + \gamma_{ij}^{s} + \gamma_{1}^{s} \log(1 + \tau_{ijt}^{s}))\varepsilon_{ijt}^{s}, \quad (1)$$

where s indexes the soy products, with $s \in \{\text{soybean}, \text{soyoil}, \text{soycake}\}$. X_{ijt}^{s} is the exports of soy products country i to country j at time t and τ_{ijt}^{s} is the corresponding effectively applied ad valorem tariff rate. γ_{it}, γ_{jt} and γ_{ij} are exporter-year fixed effects, importer-year fixed effects and country-pairs fixed effects, respectively. The purpose of using effectively applied tariffs is two-fold: first, to estimate Armington elasticities; and second; to incorporate an ad valorem tariff-equivalent of the EUDR compliance cost on the EU imports, which facilitates counterfactual computations in the absence of separate non-tariff elasticities. Following Anderson et al. (2018) and Fontagné, Guimbard and Orefice (2022), the elasticity estimation of any price shifter (i.e. tariff) in the gravity model can be used to recover Armington elsticities which are $1 - \gamma_1^s$ is our case.

Step 2: Estimation of baseline trade costs

Using the trade elasticities derived from equation (1), we estimate the country-pair fixed effects, exporter fixed effects, and importer fixed effects. We then fit these fixed effects, taking the base year 2022, as shown in equation 6. For the ease of notation, we omit product superscripts, s:

$$X_{ij} = \exp(\tilde{\gamma}_1 \log(1 + \tau_{ij}) + \tilde{\gamma}_i^{[BLN]} + \tilde{\gamma}_j^{[BLN]} + \tilde{\gamma}_{ij}^{[BLN]}). \quad (2)$$

Using the expenditure, sales and PPML fixed effects, we recover OMR and IMR consistent with the structural gravity terms, as demonstrated by Fally (2015). The PPML ensures that the fixed effects adjust so that corresponding multilateral resistances are consistent with tariff elasticity. A unique feature of the PPML is that fitted expenditures (or sales) equal observed expenditures (sales), resulting in: $\sum_j \tilde{X}_{ij} = \sum_j X_{ij} = \tilde{Y}_i^{BLN}$ and $\sum_i \tilde{X}_{ij} = \sum_i X_{ij} = \tilde{E}_j^{BLN}$.

To construct baseline OMR and IMR, we normalize all the fixed effects relative to Australia, denoted as E_0. According to Yotov et al. (2016), the reference country should be the one that is presumably not significantly affected by the counterfactual shock. This idea is to make the "relative" counterfactual changes in multilateral resistances closer to their "absolute" counterparts as possible.

$$[\Pi_i^{\widetilde{1-\sigma}}]^{BLN} = \frac{\tilde{E}_0}{\tilde{Y}_i} \exp(-\tilde{\gamma}_i^{[BLN]}), \quad (3)$$

$$[P_j^{\widetilde{1-\sigma}}]^{BLN} = \frac{\tilde{E}_j}{\tilde{E}_0} \exp(-\tilde{\gamma}_j^{[BLN]}). \quad (4)$$

Practically, many country pairs involve zero trade flows. For such pairs, $\exp(\tilde{\gamma}_{ij})$ is not available. To recover the fixed effects of all country pairs, we conduct the regression using equation (5) for those with available country pair fixed effects. We then estimate all γ parameters and predict $\exp(\tilde{\gamma}_{ij})$ for the missing country pair fixed effects.

$$\exp(\tilde{\gamma}_{ij}) = \exp[\gamma_i + \gamma_j + \gamma_2 \ln(DIST_{ij}) + \gamma_3 CNTG_{ij} + \gamma_4 LANG_{ij} + \gamma_5 CLNY_{ij}] \cdot \varepsilon_{ij}. \quad (5)$$

Therefore, the baseline trade cost is estimated as below:

$$[\tilde{t_{ij}^{1-\sigma}}]^{BLN} = \begin{cases} \exp(\tilde{\gamma}_{ij}) \exp(\tilde{\gamma}_1 \log(1+\tau_{ij})), & \text{if } X_{ij} > 0 \text{ for at least one period,} \\ \exp(\tilde{\tilde{\ }}_{ij}) \exp(\tilde{\gamma}_1 \log(1+\tau_{ij})), & \text{if } X_{ij} = 0 \text{ for all periods.} \end{cases} \quad (6)$$

Step 3: Construction of scenarios and counterfactuals

We estimate counterfactual trade costs by adding ad valorem tariff-equivalent to unilateral EUDR compliance costs on the tariffs for the exports to the EU countries in equation (6):

$$[\tilde{t_{ij}^{1-\sigma}}]^{CFL} = \begin{cases} \exp(\tilde{\gamma}_{ij}) \exp(\tilde{\gamma}_1 \log(1+\tau_{ij}^{CFL})) \\ \tilde{\exp}(\tilde{\gamma}_{ij}) \exp(\tilde{\gamma}_1 \log(1+\tau_{ij}^{CFL})). \end{cases} \quad (7)$$

where $\tau_{ij}^{CFL} = \tau_{ij} + EUDR\_AVE_{ij}$. Under the baseline condition of the year 2022, the $EUDR\_AVE_{ij}$ is zero, meaning there is no effect of the EUDR trade restriction. We model EUDR as an ad valorem compliance wedge on EU-bound imports, consistent with structural gravity practice of representing policy change as ad valorem trade-cost changes (Larch, Tan and Yotov 2021). We assign $EUDR\_AVE_{i,EU}$ from external estimates on scenario-specific price-wedge at the EU border, in the spirit of price-wedge/tariff-equivalent AVE discussed by Kravchenko et al. (2022) and Bellora and Fontagné (2023).

We simulate two scenarios for the implementation of the EUDR. In the first scenario, all countries comply with the regulation, which we will refer to as the "compliance" scenario hereafter. We assume that compliance costs impose trade frictions to enter the EU market. According to the EU impact assessment paper (European Commission 2021), the estimated compliance costs for soy range from 32.3 to 478.7 million euros. Adding these compliance costs to the EU's imports, the rough estimate of the increase in expenditure lies between 0.29% and 4.29% (Rabobank 2023). Additionally, the European Feed Manufacturers' Federation (FEFAC) projects that procurement costs for EUDR-compliant soy meal will rise by 5–10%, potentially leading to a similar increase in the price index of the soybean cake in the EU (European Feed Manufacturers' Federation (FEFAC) 2024). Further, the suppliers may incur additional costs to demonstrate and transition to deforestation-free production. We model this as an increase in trade costs of a magnitude equivalent to the estimated increase in price or expenditure. We choose a conservative middle value trade cost increase of 6%, equivalent to an increase in a 6% ad valorem tariff, to simulate the compliance scenario as shown below:

$$EUDR\_AVE_{ij}^{comp} = \begin{cases} 0.06, & \text{if } j \in EU \text{ and } i \notin EU \\ 0, & \text{otherwise} \end{cases} \tag{8}$$

In the second scenario, termed "non-compliance" scenario hereafter, the EU market is closed to selected deforestation-risk tropical countries- Brazil, Argentina, and Paraguay. These countries are chosen because they are the largest suppliers of soy to the EU, accounting for 39.05%, 11.53%, and 1.14% of total EU soy imports, respectively (see appendix table A4.1), and are also major contributors to deforestation. An analysis conducted by Singh and Persson (2024) using a four-year attribution window for deforestation measurement, identifies Brazil as the largest contributor, with 59.3% of global soybean-related deforestation, followed by Bolivia (15.5%), Argentina (6.0%), and Paraguay (4.4%) in 2020. However, the EU's share in the exports of Brazil, Argentina, and Paraguay is only 8.06%. If these countries expect that compliance costs outweigh their benefits from compliance, it is possible that exporters may shift to alternative markets. This economic logic is consistent with the analytical model proposed by Gilbert (2024), which illustrates that producers will invest in the EUDR compliance only when the European premium exceeds their compliance costs plus the logistic costs of selling to non-EU markets. We model the second scenario for an increase in trade costs to a prohibitive level, effectively shutting down exports to the EU market as shown below:

$$EUDR\_AVE_{ij}^{ncomp} = \begin{cases} H_s, & \text{if } i \in \{BRA, ARG, PRY\},\ j \in EU \\ 0.06, & \text{if } i \notin \{BRA, ARG, PRY, EU\},\ j \in EU \\ 0, & \text{otherwise} \end{cases} \tag{9}$$

where H_s is a product-specific prohibitive wedge. In our counterfactual gravity estimation, a 5000% AVE shuts down the export of soybeans to the EU market, while a lower AVE (~700%) shuts down the export of soybean oil and cake. This is reasonable because the trade elasticity of soybeans is lower than that of soybean oil and cake.

Step 4: Estimate conditional gravity

Using counterfactual bilateral trade costs from equation (7), we estimate counterfactual fixed effects with the constrained regression in equation (10), holding trade costs fixed and allowing fixed effects to adjust for changes in multilateral resistance due to compliance costs.

$$X_{ij} = \exp[\gamma_i^{CFL} + \gamma_j^{CFL} + \theta \log \widetilde{[t_{ij}^{1-\sigma}]}^{CFL}]\varepsilon_{ij}^{CFL}, s.t. \theta = 1 \quad (10)$$

With the estimated counterfactual fixed effects and trade cost, the counterfactual trade flows are predicted as:

$$\tilde{X}_{ij}^{CFL} = \widetilde{[t_{ij}^{1-\sigma}]}^{CFL} \exp[\tilde{\gamma}_i^{CFL} + \tilde{\gamma}_j^{CFL}]. \quad (11)$$

Step 5: Estimate and report effects

We measure compliance-induced change in export from country i to country j in percent as: $(\frac{\tilde{X}_{ij}^{CFL}}{\tilde{X}_{ij}^{BLN}} - 1) * 100\%$. A positive value - when i is the non-EU country and j is an EU country- indicates an increase in exports from i to j while a negative value indicates a decrease in exports.

As suggested by Anderson et al. (2018), welfare change in the conditional scenario is equivalent to change in price index, as calculated below:

$$\hat{W}_i = \left(\frac{\tilde{Y}_i^{CFL}}{\tilde{P}_i^{CFL}}\right)\left(\frac{\tilde{Y}_i^{BLN}}{\tilde{P}_i^{BLN}}\right)^{-1} = \frac{\tilde{P}_i^{BLN}}{\tilde{P}_i^{CFL}}, \forall i, \quad (12)$$

where, the output is kept exogenous in the 'conditional' scenario, i.e. $Y_i^{\tilde{CFL}} = Y_i^{\tilde{BLN}}$. $P_i^{\tilde{BLN}}$ is estimated using equation (4), while $\tilde{P}_i^{CFL}$ is estimated analogously using the corresponding counterfactuals. However, it is possible only after obtaining the power transformation of the IMRs. We estimate the elasticity of substitution (σ) from the tariff elasticity $(\tilde{\gamma}_1)$ as $\sigma = 1 - \tilde{\gamma}_1$.

Further, as discussed in Anderson et al. (2018), this procedure allows the estimation of the changes in producer prices p_{it} between the baseline and counterfactual scenarios. These are derived from the change in outward MRTs implied by the estimates $\tilde{\gamma}_i^{CFL}$ and $\tilde{\gamma}_i^{BLN}$. Within the structural gravity framework, these price changes and terms of trade can be calculated as:

$$\hat{p}_i = \frac{\tilde{p}_i^{[CFL]}}{\tilde{p}_i^{[BLN]}} = \left[\frac{\exp(\tilde{\gamma}_i^{CFL})}{\exp(\tilde{\gamma}_i^{BLN})}\right]^{\frac{1}{1-\sigma}} \quad (13)$$

$$T\hat{O}T_i = \frac{\hat{p}_i}{\hat{P}_i} \quad (14)$$

1.4 Results

1.4.1 Tariffs represent a significant trade cost in soy market

Table 1.2 reports the estimated effects of tariffs on the soy product trade flows for the period 2007–2017. We exclude post-2018 trade flows from the trade elasticity estimation to avoid endogeneity arising from China's retaliatory tariffs on the US soybean export to China. This would also represent normal market responses. Our results reveal trade elasticities of -1.883, -6.394, and -6.227 for soybean, soybean oil, and soybean cake, respectively. Our soybean tariff elasticity (-1.883) is comparable to Fontagné et al. (2022) 's estimate of -1.254. The estimate is lower than Dhoubhadel, Ridley and Devadoss (2023)'s estimate of -5.83, but higher than the estimates reported by Ridley and Shirin (2024) (-0.879). For soybean oil, our estimate (-6.394) is slightly higher than Ridley and Shirin (2024)'s finding of -5.338. However, our soybean cake elasticity (-6.227) is somewhat lower than Fontagné et al. (2022)'s estimate of -11.92. Using these estimates, we recover Armington elasticities, shown in appendix 3. The elasticity of substitution is lower for soybeans than for processed soy products. A plausible explanation could be that processed products (oil and cake) have many substitutes and available across countries, but soybeans are relatively homogeneous that limits rapid reallocation across sources. Therefore, countries respond with more substitution in processed products despite smaller changes in trade costs relative to soybeans.

Table 1.2: Effects of import tariffs on soy products using PPML estimates

	Soybean	Soybean Oil	Soybean Cake
Log(1 + Tariff)	-1.883	-6.394*	-6.227*
	(1.253)	(2.667)	(2.993)
Observations	26619	26651	20748
R-squared	0.995	0.991	0.990
Exporter-Year FE	X	X	X
Importer-Year FE	X	X	X
Pair FE	X	X	X

+ p < 0.1, * p < 0.05, ** p < 0.01, *** p < 0.001

Note: The dependent variables are the unidirectional value (1000 USD) of exports. Standard errors clustered at the country-pairs level. All estimations include exporter-year, importer-year, and pair fixed effects. Inclusion of country-pair fixed effects drop large number of observations due to persistent zero trade flows between country-pairs.

1.4.2 China, including the rest of the world, absorbs trade restriction imposed on BAP

The trade reallocation effects, as shown in Figure 2.5, Figure 2.5 and Figure 2.6.2, are higher for non-compliance. Under compliance, the trade relationship could possibly remain the same as it is. Under non-compliance, soybean exports to China increase substantially: Brazil by 12% and Paraguay by 16.7%. The soybean oil exports to China from Brazil, Argentina, and Paraguay increased by 2.9%, 0.8%, and 22.5%, respectively. The largest changes appear in soybean cake exports. Brazil's soybean cake exports to China surge by 1184.3%, Argentina's increase by 679.5%, and Paraguay's increase by 562.5%. Further, all three countries also experience an increase in their exports to the rest of the world.

1.4.3 The US and Canada export increase substantially to the EU if restrictions target BAP

In the non-compliance scenario, there is a significant shift of exports to the EU market from the US and Canada. US soybean exports to the EU rise by 198.2%, while Canadian exports increase by 118.2%. Soybean oil exports from both countries grow by about 22-23%. The most dramatic changes are seen in soybean cake exports, with US exports soaring by 968.5% and Canadian exports by 549.1%. This surge is driven by the EU's large share of the global import market (32.16%, or USD 10,989.3 million), with Brazil and Argentina the top suppliers of soybean cake to the EU with around 65% share of the EU imports.

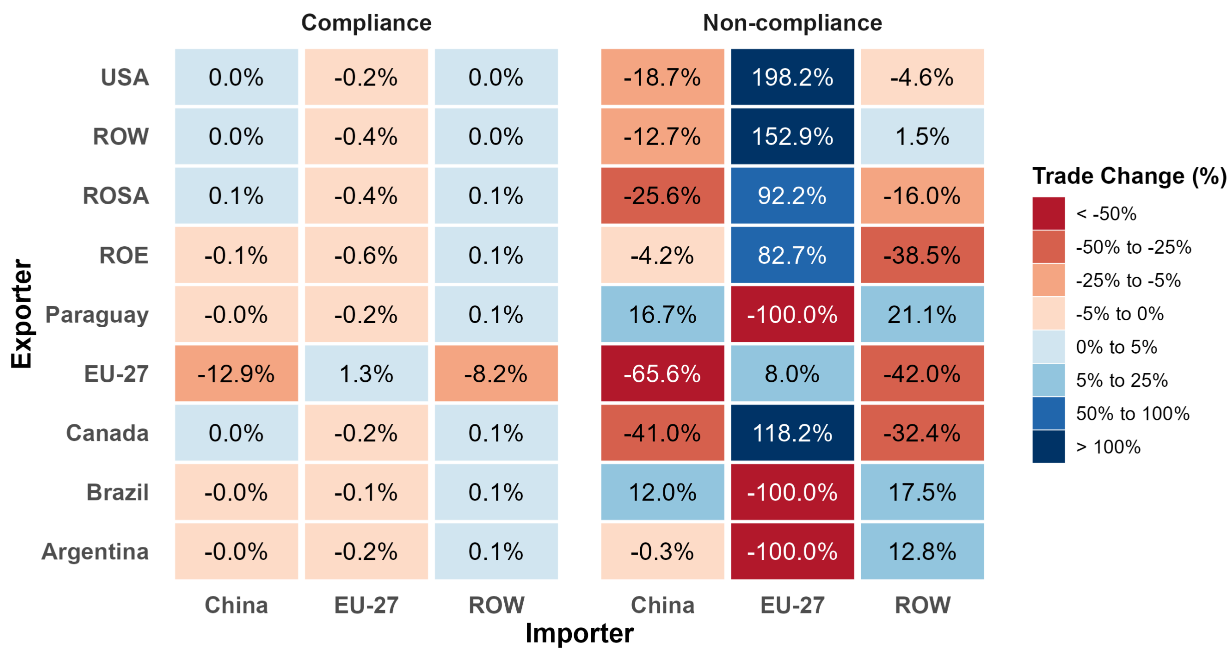

Figure 1.3: Trade reallocation effect of the EUDR in soybean trade.

Notes. The figure shows the percentage change in exports under compliance and non-compliance scenarios, from the countries and regions in the rows to China, the EU, and the rest of the world (ROW), relative to a baseline without the EUDR. Red denotes a reduction in exports; blue denotes an increase. ROSA: Rest of South America, ROE: Rest of Europe.

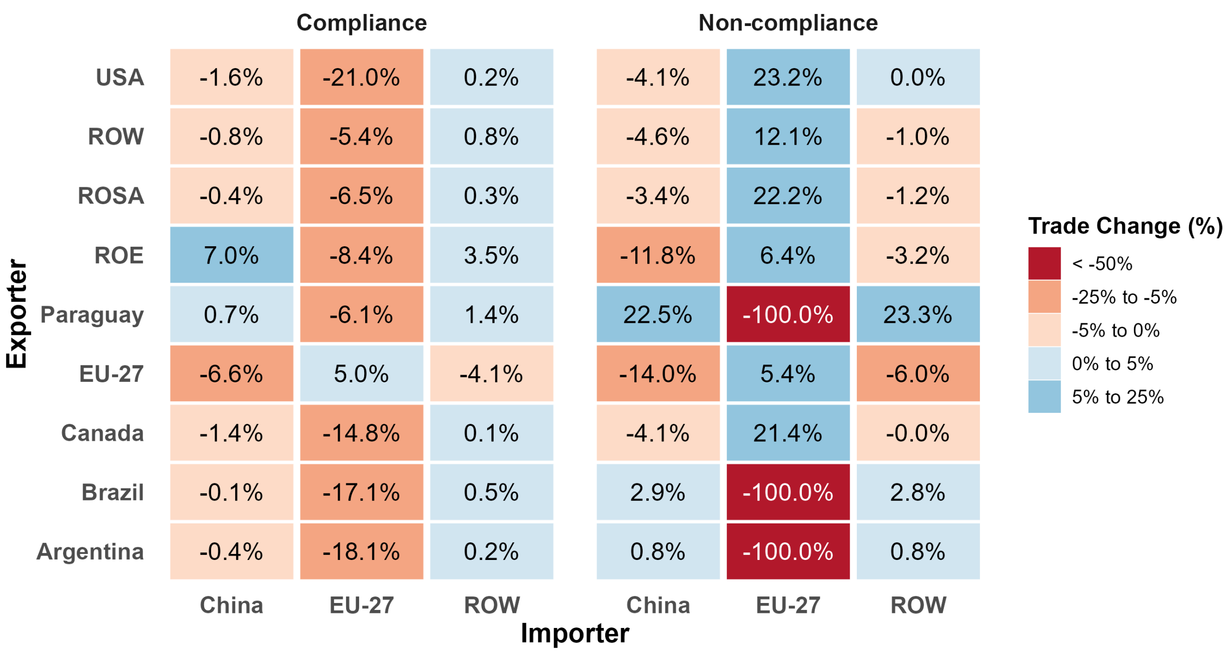

Figure 1.4: Trade reallocation effect of the EUDR in soybean oil trade.

Notes. The figure shows the percentage change in exports under compliance and non-compliance scenarios, from the countries and regions in the rows to China, the EU, and the rest of the world (ROW), relative to a baseline without the EUDR. Red denotes a reduction in exports; blue denotes an increase. ROSA: Rest of South America, ROE: Rest of Europe.

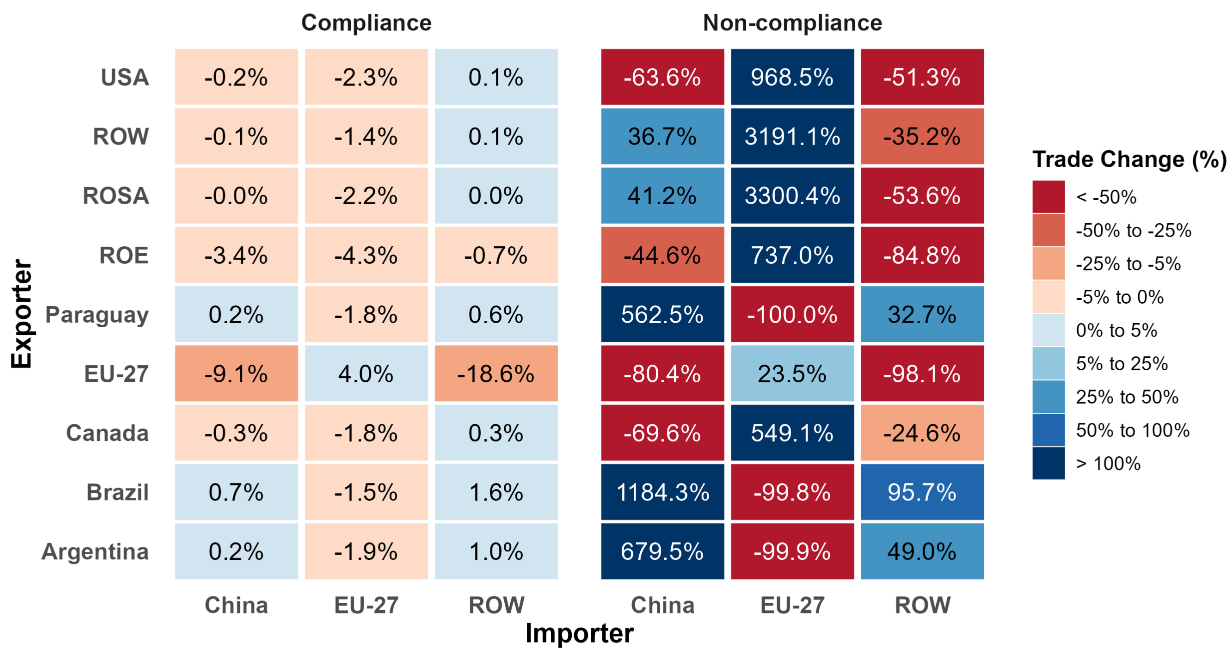

Figure 1.5: Trade reallocation effect of the EUDR in soybean oilcake trade.

Notes. The figure shows the percentage change in exports under compliance and non-compliance scenarios, from the countries and regions in the rows to China, the EU, and the rest of the world (ROW), relative to a baseline without the EUDR. Red denotes a reduction in exports; blue denotes an increase. ROSA: Rest of South America, ROE: Rest of Europe.

1.4.4 The EU faces rising prices and declining terms of trade

As illustrated in Figure 1.6, the EU would bear substantial expenditure loss if BAP do not comply with the EUDR. Among the three products, the EU experiences the highest welfare losses in soybeans, followed by soybean cake and soybean oil. In the soybean trade, EU expenditure losses can reach \$18,179.84 million, accompanied by average price increases of 60.26%. The EU could face expenditure losses to \$1357.54 million for soybean oil and from \$16481.93 million for soybean cake. The economic burden is disproportionately concentrated among major European importers, which have larger relative shares of imports (see appendix figure A4.2). Spain, the Netherlands, Italy, and Germany face the most significant expenditure losses in soybeans. Similarly, these countries, along with Poland, France, Denmark, and Belgium, experience the highest expenditure losses in soybean cake and soybean oil. Most EU countries experience expenditure losses, increases in producer prices, and increases in price indices but experience decreases in terms of trade (see appendix A5.1(d)). This indicates that the EU lacks sufficient market leverage to benefit from import restrictions, as it remains heavily dependent on imports.

1.4.5 Import restrictions could boost demand for soy products from target countries

Our analysis reveals no significant change in total exports from target countries under either scenario (see figure A5.4). This results reflects the short-run nature of our simulation, which holds total output and expenditures constant and assumes zero supply elasticity. Notably, the decline in producer prices for Brazil, Argentina and Paraguay points to increased export competitiveness driven by lower prices. We further confirm this by keeping supply constant for each country but allowing expenditures to change. Under these conditions, we find significant export growth (see figure A5.3). Soybean exports increased by 7.4% for Brazil, 3.1% for Argentina, and 4.8% for Paraguay, directly resulting from lower producer prices in these countries. The effects emerged pronounced in soybean cake exports, with increases of 69.6% for Argentina, 106.3% for Brazil, and a surge of 93.2% for Paraguay. Moreover, soybean oil exports showed minimal growth across these countries, increasing by less than 0.5%.

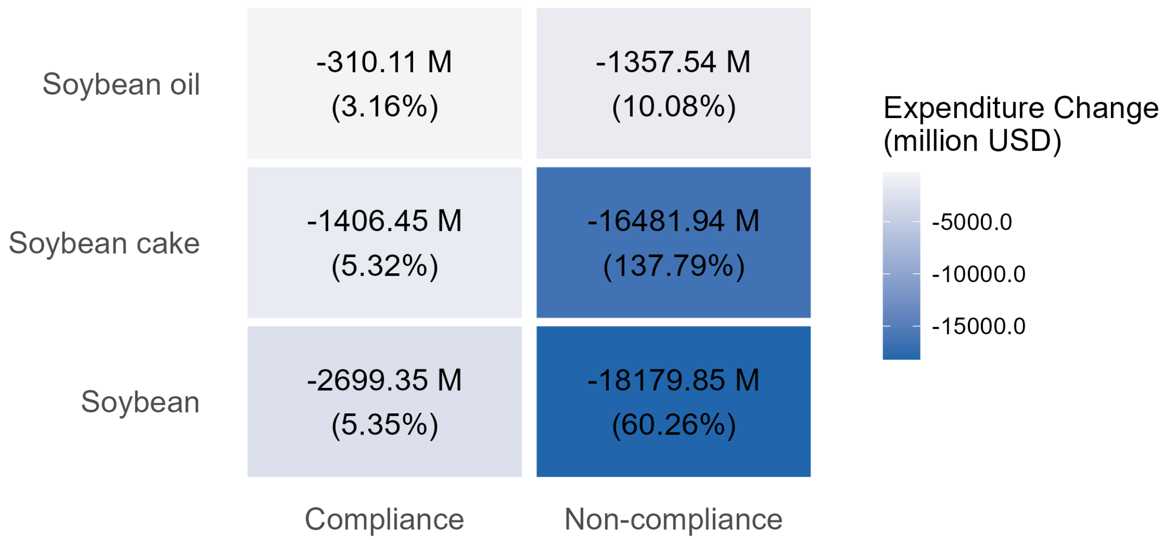

Figure 1.6: Expenditure loss faced by EU27 under the EUDR simulation.
Notes. Expenditure loss is reported in million USD, measured relative to the baseline without the EUDR. The percents in parenthesis denote average of change in price index in the EU countries. The expenditure loss is measured as $[\frac{\widetilde{E_i^{CFL}}}{\widetilde{P_i^{CFL}}} - \frac{\widetilde{E_i^{BLN}}}{\widetilde{P_i^{BLN}}}]$.

1.4.6 BAP face decrease in price index of soybean, but some declines in terms of trade

Figure 1.7 illustrates the effects of the EUDR on exporting countries. In the soybean and soybean oil, BAP experiences declines in price indexes and producer prices, however they see little to no change in terms of trade. However, for soybean cake, BAP see increase in price index and decrease in terms of trade illustrates the effects of the EUDR on major soy traders. In soybeans and soybean oil, BAP experiences a decline in price indexes and producer prices; however, it sees little to no change in terms of trade. In soybean cake, Paraguay and Argentina see an increase in price index and producer price, while Brazil sees a decrease in both prices.

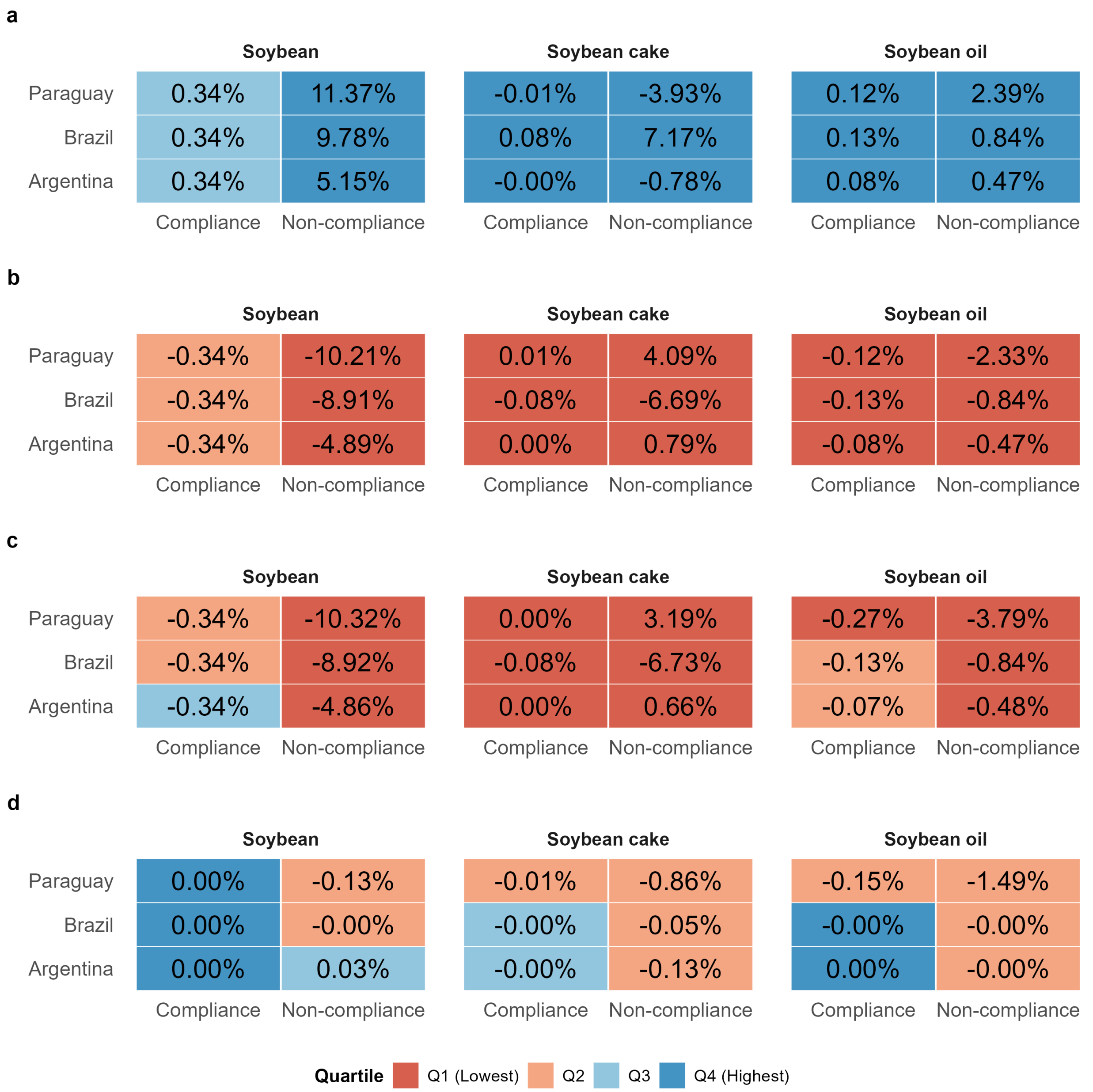

Figure 1.7: Changes in indices under compliance and non-compliance scenarios.

Notes. Changes are measured relative to a baseline without the EUDR. Quartile is measured at the scenario-product level for each index. (a) percentage change in welfare. (b) percentage change in producer price. (c) percentage change in price index. (d) percentage change in terms of trade.

1.5 Sensitivity checks

Our exercise is purely an ex-ante assessment of the regulation based on the 2022 base year. For credibility and robustness, we (i) check the effects of compliance AVEs. For example, in the compliance case, we impose a 6% AVE compliance cost, which yields a tentatively similar increase in the EUDR price index (see figure A5.1(b)). This verifies that our compliance scenario represents what we simulate. For the non-compliance scenario, our chosen AVE estimates effectively shut down exports from BAP to the EU, as evidenced by Figures 2.5, 2.5, and 2.6.2. (ii) We report sensitivity over plausible lower and upper bounds of 2% and 10% AVE and Armington elasticities at the lower and upper bounds of the 95% confidence intervals. Across these ranges, the qualitative results are stable (see appendix A6): EU substitution toward compliant suppliers and diversion of displaced South American volumes to non-EU destinations. Higher AVEs predictably amplify EU price index increases and welfare losses, but do not overturn the direction of reallocation.

1.6 Discussions

Our analysis indicates that the EUDR faces notable limitations in reducing exports that drive tropical deforestation linked to the soy sector. The direct competitors to South American soy exporters are the US and Canada, which are largely deforestation-free producers and redirect their exports to the EU under the EUDR implementation. As a result, the soy supply restricted from BAP is reallocated to China. These patterns align with the well-documented effects of the NTMs: trade reduction between compliant and non-compliant pairs, while facilitating trade among compliant origins (Fontagné et al. 2005; Santeramo and Lamonaca 2019; Santeramo et al. 2025). Particularly, the trade reallocation we observe is a canonical response to unilateral NTMs implemented by importers that are not the dominant buyer for targeted exporters: restricted supply absorbed by third markets, while the import market under the compliance turns to compliant suppliers.

With the EUDR in place, the trade pattern indicates two segregated supply chains: first, the EU can import verifiable deforestation-free soy from North America and, to a limited extent, from South

America, where supplies are already deforestation-free.[1] Actually, this partial compliance of South America represents the distributional consequences. Smallholders and smaller firms would lose access to the EU market. Nevertheless, this compliance supply chain represents a small fraction of the total supply chain (~15%). Consequently, with the changed composition of the destination market, the pressure on deforestation in South America does not necessarily decrease. Even with full compliance of South American soy targeted at the EU market, particularly from Brazil, it does not guarantee a reduction in deforestation, as long as the demand pressure for soy from the non-EU market remains constant. Evidence of substantial domestic leakage within Brazil, on the order of 43–50%, suggests that reductions in deforestation in some locations can be offset by increases elsewhere (Villoria et al. 2022).

Second, a conventional supply chain serving the non-EU market (notably China) without compliance requirements. The increasing reliance of South America on the Chinese market may further erode the EU's leverage in promoting environmental compliance in the future. Understanding the long-term consequences of these trade reallocation patterns is therefore important. In our baseline EUDR simulation, producer prices in BAP fall, and constrained volumes are reallocated toward China. Over longer horizons, the net effect on production and land use in high-risk areas depends on the magnitude and persistence of the price signal, supply elasticities, and how fully China/ROW) absorb displaced flows. Because the EU accounts for a relatively small share of BAP exports, an EU-only signal may be too weak to induce contraction; if China's demand expansion keeps producer prices near baseline, output could be sustained, and deforestation pressures may persist or even rise, raising the prospect of a fragmented global soy market less responsive to EU regulations.

The economic implications for the EU are substantial. Certain EU members, such as the Netherlands, Poland, Spain, Germany, France, and Italy, bear disproportionate burdens, reflecting differences in import dependency, processing capacity, and supply chain integration. Gilbert (2024) discusses that this creates a "European premium" over world prices, with compliance costs directly

[1] Brazil's soy sector has long-running zero-deforestation efforts. In the Amazon, the Soy Moratorium- implemented by firms handling ~90–95% of exports- was associated with a 57% reduction in direct soy-deforestation in treated municipalities; in the Cerrado, several traders have adopted ZDCs but implementation and coverage remain incomplete (Gollnow et al. 2022).

passed to EU consumers. Further, the loss is also pronounced in soybean cake, despite its lower share in global soy trade, which is due to the higher elasticity of substitution for soybean cake. This result is consistent with the studies by Branger and Quirion (2014) and Böhringer, Rosendahl and Storrøsten (2017), which show that higher trade elasticities increase trade reallocations. According to Noordwijk et al. (2025), the EUDR may cause "collateral damage" to unintended stakeholders. For example, in our analysis, restrictions on BAP increase welfare losses in the US and Canada due to an increase in the price index.

The EUDR, similar to non-tariff measures, appears as both a trade catalyst and a barrier. For forest-risk countries, it functions as a trade barrier, as these countries will be under higher scrutiny and compliance costs could rise. However, the EUDR can catalyse trade within the EU; this provides an opportunity for soy producers and producers of substitute products, such as other vegetable oils and cake, from EU countries. This is evidenced by increased producer prices for soy products in EU countries (see appendix figure A5.1). Trade between compliers (most likely North American exporters) and the EU also rises. This finding is in line with Santeramo et al. (2025), which highlights that the EU TBT has the capacity to redirect imports towards compliant origins.

Our findings on the consequences of the EUDR simulation underscore the limitations of a purely demand-side regulatory. A more effective approach would combine demand-side and supply-side measures, including direct forest conservation incentives, carbon payments, and Contingent Trade Agreements (CTAs) that penalize exporters based on changes in forest cover. Muradian et al. (2025) argue that territorial approaches, such as Brazil's Amazon Soy Moratorium and the Action Plan for the Prevention and Control of Deforestation in the Legal Amazon (PPCDAm), have been more effective in reducing deforestation by aligning with local public governance. In contrast, the EUDR's focus on value chain interventions fails to address underlying drivers of deforestation, such as weak governance and land speculation. Harstad (2024b) also emphasizes the importance of balancing depth and breadth in environmental agreements. The EUDR, as a "deep-but-narrow" policy, imposes strict deforestation-free requirements on imports but applies only to the EU market. A "broader-but-shallow" agreement involving multiple major importers with less ambitious regulations could reduce leakage and achieve greater global impact. For instance, a CTA between the

EU and the US could potentially reduce agricultural expansion in Brazil by up to 27% compared to unrestricted free trade scenarios (Harstad 2024a; Harstad 2024c).

1.7 Conclusion

The EUDR is the EU's first regulatory initiative to curb tropical deforestation through trade restrictions on the soy sector. We fitted the gravity model, taking the base year 2022, and assessed the effects of the EUDR under two scenarios: one in which exporters comply with the regulation and another in which BAP do not export soy to the EU. We chose these three countries for the non-compliance scenario because they have faced significant forest loss directly attributable to soybean expansion, are characterized by weak environmental governance, and hold a substantial share of global soy production. Our results show that restrictions on South American exports redirect soy flows toward China, while EU imports are substituted by US and Canadian suppliers. The EU experiences expenditure losses due to increased prices arising from compliance costs, leading to deteriorated terms of trade. The expenditure losses are even more severe when South American countries do not comply with the EUDR. Conversely, South American countries face declining soy price indices and producer prices with no change in terms-of-trade effects. These findings suggest that the EU lacks sufficient market leverage to incentivize pro-forest land use decisions in major South American soy producers.

We acknowledge some limitations in our study. Our results are under "conditional" equilibrium in the sense of Anderson et al. (2018), which captures short-run and static trade reallocation and price index effects of the EUDR. This model falls short in offering a discussion on long-run environmental impacts, including endogenous output responses in major producing countries, EU domestic supply responses, and cross-commodity substitution in the vegetable oils complex (e.g., palm, sunflower, rapeseed). Importantly, the model also abstracts from substitution from soybeans toward other oilseeds, which could, for example, shift deforestation from tropical soy production areas to oil palm regions such as Indonesia. If Chinese demand contracts in the future and does not fully absorb the restricted supply, production by South American producers could contract, leading to increased avoided deforestation relative to our short-run benchmarks. Modeling these channels requires a multi-sectoral equilibrium framework with endogenous supply responses, which is beyond the scope of this paper. Finally, we do not model heterogeneous compliance capacity (e.g., partial compliance by larger firms with exclusion of smaller producers) or subnational leakage dynamics within Brazil; as a result, country-level "avoided deforestation" inferences should be interpreted cautiously. A subregional trade–land-use model linking destination-specific demand to producing meso-regions would be better suited to assess how EUDR-induced demand shifts affect frontier expansion versus consolidated, low-forest areas.

While our study focuses on the soy sector, future research should also examine the trade reallocation and the possible deforestation leakage for commodities covered by the EUDR, such as palm oil, rubber, cattle, cocoa, coffee, and wood products. Further evidence and robust measurements of environmental effectiveness are warranted, particularly in measuring deforestation leakage and indirect land use changes. Furthermore, governance and implementation challenges, such as traceability and interactions with local governance, deserve research attention to ensure the regulation's success.

Chapter 2

Exports and Deforestation: A Commodity-Level Analysis

2.1 Introduction

Agricultural expansion is a leading driver of tropical deforestation (Curtis et al. 2018; Hosonuma et al. 2012; Pendrill et al. 2022). Agricultural deforestation matters because of its ecological, climatic, and public-health consequences (Giam 2017; Snyder 2010; Chaves et al. 2020). Specifically, a large share of global biodiversity resides in tropical forest, and the loss of these forests' loss accelerates biodiversity decline (Giam 2017; Alroy 2017). Regarding climate, deforestation intensifies warming and drying of local weather (e.g., Lee and Lo 2021; Werth and Avissar 2005; Lawrence and Vandecar 2015) and also disrupts rainfall patterns, which can directly reduce agricultural productivity (Lawrence and Vandecar 2015). These climatic impacts extend beyond deforested areas and alter distant climate, which is also known as eco-climatic teleconnections (e.g., Snyder 2010; Garcia et al. 2016; Serrão et al. 2025). Deforestation is further linked to respiratory and cardiovascular diseases in populations near burning or clearing sites—documented in the Brazilian Amazon and Indonesian Borneo, where fire-season smoke dramatically raises hospital admissions for respiratory illness among communities within hundreds of kilometers of active clearing (Damm et al. 2024; Du, Li and Zou 2024). Deforestation is also linked to higher malaria incidence in nearby communities (Chaves et al. 2020; Arisco et al. 2024; Berazneva and Byker 2017). These externalities make it important to understand the economic forces that convert forests into agricultural land.

International demand for agricultural commodities is one such force. International agricultural trade is associated with approximately one-quarter to one-third of tropical deforestation and related emissions linked to agriculture and forestry (Pendrill, Persson, Godar, Kastner, Moran, et al. 2019; Pendrill, Persson, Godar and Kastner 2019; Persson, Henders and Kastner 2014; Henders, Persson and Kastner 2015). Cattle, soy, oil palm, cocoa, coffee, and rubber account for much of the deforestation embodied in trade, with hotspots in South America, Southeast Asia, and parts of Africa (Zu Ermgassen et al. 2020; Pendrill, Persson, Godar and Kastner 2019; Singh and Persson 2024; Goldman et al. 2020).

Three strands of research have shaped our understanding on how trade and markets affect forests, and our contribution builds directly on them. The first uses spatially explicit accounting and tele-coupling frameworks to trace the deforestation and emissions embodied in the production and trade of forest-risk commodities (Pendrill, Persson, Godar, Kastner, Moran, et al. 2019; Persson et al. 2014; Henders et al. 2015; Zu Ermgassen et al. 2020). This literature identifies the commodities and supply chains with the largest forest footprints and shows how consumption in one region is linked to forest loss in another. By construction, however, it documents physical flows and associations rather than the causal response of forest loss to a change in trade. A second strand estimates the causal effect of aggregate trade exposure—through trade liberalization, regional trade agreements, or world prices in structural models—on land use and forest loss (Abman and Lundberg 2020; Farrokhi et al. 2025; Jeddi and DePaula 2026). This work shows that trade openness raises forest pressure where countries hold a comparative advantage in agriculture, and that higher world prices for land-intensive sectors reallocate land toward those sectors and toward land-abundant exporters (Farrokhi et al. 2025). These studies, however, operate at the level of aggregate trade or modeled equilibria and do not recover how forest loss responds to realized exports of individual commodities. A third strand identifies the causal effect of commodity prices on clearing, particularly for a single country or crop (Berman et al. 2023; Lundberg and Abman 2021; Harding, Herzberg and Kuralbayeva 2021; Bragança 2018; Wilcox, Just and Ortiz-Bobea 2025). This literature has established that higher output prices increase deforestation and that the response is shaped by agro-climatic suitability, governance, and credit conditions; prices, however, move for many reasons other than foreign demand, and the evidence remains largely confined to specific hotspots in Brazil, Indonesia, Southeast Asia, and parts of Africa, reflecting data and identification challenges (e.g., Burgess et al. 2012; Du et al. 2024; Carreira, Costa and Pessoa 2024; Bragança 2018; Wilcox et al. 2025; Abman and Lundberg 2020; Balboni et al. 2022; Richards and Arima 2026).

This literature lacks a commodity-specific elasticities of deforestation with respect to export demand, that is comparable across commodities and regions at a global scale. To our knowledge, no previous study has recovered commodity- and region-specific elasticities of deforestation with respect to exports. Framing the question at the commodity level is deliberate as demand-side forest regulation, the European Union Deforestation Regulation (EUDR), imposes due-diligence obligations on a defined list of forest-risk commodities (cattle, cocoa, coffee, oil palm, rubber, soy, and wood) rather than on trade in general (European Parliament and of the Council 2023). A regulation that is commodity specific requires evidence that on an estimate of how much deforestation a marginal unit of export demand carries for each commodity and region. The estimates can also inform the EUDR's risk-benchmarking of commodity-region pairs.

To estimate the elasticities, we assemble data on 18 agricultural commodity groups for 138 countries from 2001 to 2022. Deforestation data come from the DeDuCE model (Singh and Persson 2024), which spatially allocates tree-cover loss to specific commodities. Bilateral trade flows of 493 products, categorized into 18 commodity groups, are sourced from the CEPII-BACI database. Exports and deforestation are jointly determined and driven by common domestic policies. To aid identification, we instrument exports with a measure of foreign demand that is uncorrelated with supply conditions in the exporting country. Specifically, we estimate the import-demand component that captures how much each destination increases its imports of a product for reasons internal to that destination (income growth, policy changes, or preferences), using a gravity model that controls for exporter-product-year and country-pair fixed effects. We treat this component as a residual import-demand shock. For each exporter and commodity, we then construct a shift-share measure of foreign demand (Borusyak, Hull and Jaravel 2022; Goldsmith-Pinkham, Sorkin and Swift 2020; Adão, Kolesár and Morales 2019) by weighing the importer demand shocks by the exporter's average export shares in each destination. We use this shift-share foreign-demand measure as an instrument for exports in a control-function Poisson pseudo-maximum likelihood (PPML) framework. The PPML accommodates the many zeros in commodity-specific deforestation and allows coefficient estimates to be interpreted as elasticities (Silva and Tenreyro 2006; Mullahy and Norton 2024), while the control function corrects endogeneity in the nonlinear specification (Wooldridge 2015). We include country–year fixed effects to absorb time-varying national policies and conditions, and commodity–year fixed effects to control for global price and technology trends.

We find that a 10% increase in export value raises deforestation by about 2.96% on average across commodities. The effects are highly heterogeneous across commodities and regions. The elasticity of deforestation with respect to export value is largest for perennial and frontier commodities (stimulants and spices, rubber, oil palm, cocoa, nuts, coffee), as well as for cattle, soybeans, and sugar crops. Staples and horticultural crops generally show weaker responses. Using our estimated elasticities, we estimate avoided deforestation that would have occurred had export demand remained at their 2001 baseline. We keep exports constant at their 2001 level while leaving the fixed effects and the control-function residual unchanged, so the comparison isolates the portion of observed deforestation attributable to post-2001 export growth driven by export demand, rather than to domestic conditions or unobserved supply shocks (see appendix A13 for the derivation). These calculations indicate that growth in international demand can account for roughly 53 million hectares of agricultural expansion into forests between 2001 and 2022, corresponding to about 49% of the observed forest-to-agriculture conversion.

Our contribution is to show where, across commodities and regions, foreign demand drives deforestation. The export–deforestation response is uneven: it is concentrated in perennial and tree crops and in extensive livestock and feedstock sectors, and within humid-tropical frontiers, while staple and horticultural crops respond weakly. This advances the existing trade–deforestation literature, which has documented the forest footprints embodied in trade (Pendrill, Persson, Godar and Kastner 2019; Zu Ermgassen et al. 2020), the aggregate effects of trade and world prices on land use (Farrokhi et al. 2025; Harstad 2024), and the price responsiveness of clearing in particular hotspots (Berman et al. 2023; Du et al. 2024). Relative to that work, our results show how much of the demand-driven forest response is attributable to each commodity and region, rather than to aggregate trade or price exposure, on a globally comparable basis.

This heterogeneity matters for the design of trade-linked forest regulation, such as the European Union Deforestation Regulation (EUDR) (European Parliament and of the Council 2023). Because the Regulation requires due diligence only for a defined list of forest-risk commodities, the deforestation risk carried per unit of export is the quantity needed to prioritize enforcement. Our estimates identify which commodity–region pairs carry the highest risk—for example, palm oil from Indonesia or cattle from Brazil—relative to low-risk flows such as cereals from temperate exporters. By the same logic, they indicate where blanket commodity-neutral restrictions would impose due-diligence costs with little forest benefit.

2.2 Conceptual framework: The effects of foreign demand and export sales on deforestation

In a competitive world market, an increase in foreign demand for agricultural commodities raises international prices and reallocates production of the commodities across countries according to comparative advantage. At forest frontiers, higher expected returns to the cultivation of export-oriented commodities can increase land rents and incentives for agricultural expansion, pushing the agricultural margins into forests (Du et al. 2024; Jeddi and DePaula 2026; Richards and Arima 2026). As illustrated in figure 1, land allocation follows a von Thünen–Ricardo logic in which producers expand land use until the marginal value product of land, $MVPL$, equals its opportunity cost or rental value, R (Angelsen and Kaimowitz 1999). The rental value is drawn horizontal, which corresponds to a perfectly elastic supply of convertible land under the assumption that forest land can be brought into cultivation without surpassing its opportunity cost. The assumption is reasonable for open frontiers where forest land is abundant and weakly priced, but it is an upper bound on the land-use response. A foreign-demand-induced price increase shifts the $MVPL$ schedule outward, raising the profit-maximizing land allocation from L_1 to L_2. When the relevant margin is forest, this adjustment takes the form of additional deforestation and higher export volumes. The allocation of land across activities is governed by relative $MVPL$s. In many tropical settings, marginal returns to export-oriented agriculture (e.g., beef, soy, palm oil) exceed those from forestry, which helps explain high deforestation rates in these regions (Benhin 2006; Angelsen and Kaimowitz 1999). While privately optimal, these choices need not be socially efficient because markets typically fail to price the public-good services of forests—carbon storage, biodiversity, hydrological regulation—so that the private opportunity cost of forest conservation understates its social value (Angelsen and Kaimowitz 1999). Expectations further amplify these responses: if land users anticipate persistently high future export prices or tighter future land-use regulation, they may clear speculatively to secure land rights or future rents, even before demand fully materializes (Angelsen and Kaimowitz 1999; Benhin 2006).

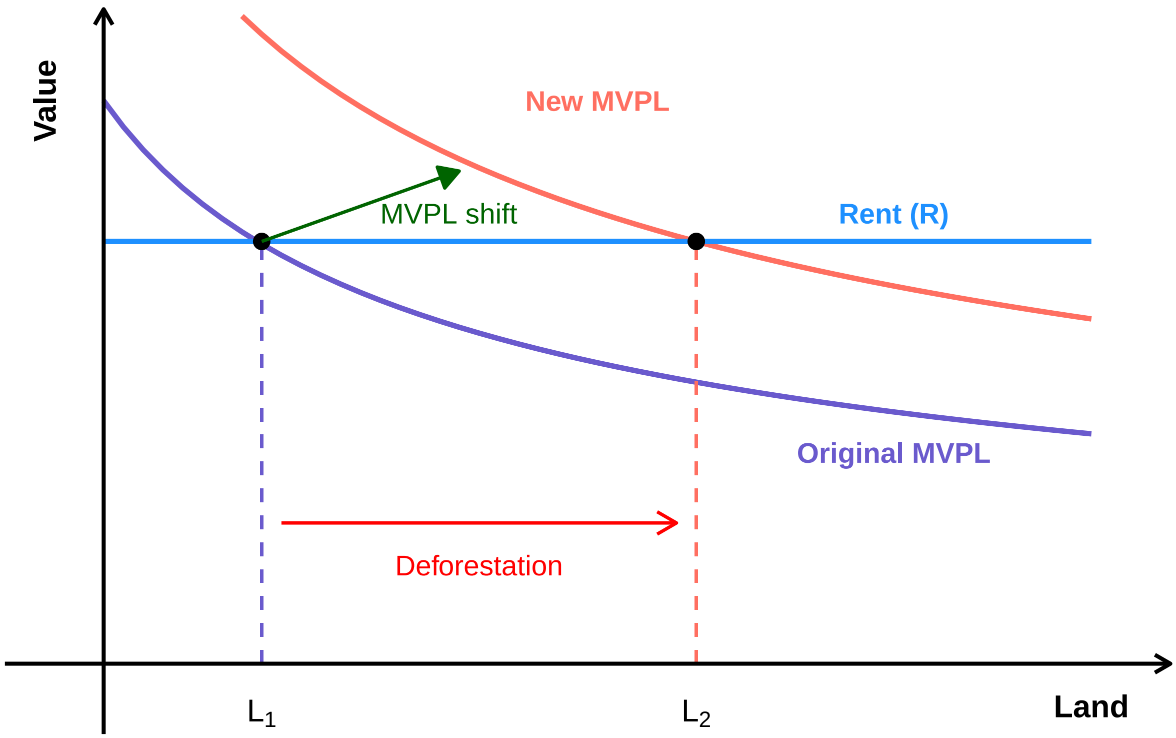

Figure 1: Shift in the marginal product value of land resulting from an increase in price due to higher foreign demand

Source: Own illustration

Berman et al. (2023) shows that increases in a global crop-price index, interacted with local agro-climatic suitability, are associated with disproportionately higher deforestation in cells with abundant suitable forest and good market access. Bragança (2018) finds that increases in the relative price of soy versus beef shift land into soy production in the Brazilian Amazon, with important implications for forest and pasture dynamics. Wilcox et al. (2025) document that rice price spikes in Cambodia raise deforestation, particularly outside formal concessions, and Lundberg and Abman (2021) show that cocoa- and staple-price dynamics shape forest conversion in West Africa. Structural trade models with land as a factor similarly predict that increases in world prices for land-intensive export sectors reallocate land toward those sectors and toward land-abundant exporters (Farrokhi et al. 2025). Beyond prices, institutional and supply-chain conditions—weak land rights, pro-cyclical enforcement, credit access, and concentrated buyer power—govern how strongly a given demand shock is translated into clearing (Burgess et al. 2012; Cisneros, Kis-Katos and Nuryartono 2021; Assunção, Gandour and Rocha 2015; Harding et al. 2021; Nedoncelle, Delacote and Crepin 2025; Abman and Lundberg 2020).

Moreover, international prices move for reasons beyond foreign demand, such as oil prices and exchange-rate fluctuations (De Gorter, Drabik and Just 2013; Roberts and Schlenker 2013; Headey and Fan 2008). Foreign demand is one driver of the international commodity price. Global markets also feature feedback. Large-scale deforestation increases export supply, which can feed back into world prices and, ultimately, foreign demand. In our empirical design, we therefore use foreign-demand-driven variation as an instrument for exports and control separately for other international price movements and domestic supply shocks.

2.3 Empirical Strategy

Our objective is to estimate how changes in international demand affect deforestation at the country–commodity level. Let i index countries, k commodities, and t years. We denote C_{ikt} for commodity-specific deforestation in country i and year t, and X_{ikt} for the export value of commodity k from country i in year t.

We regress deforestation on exports while controlling for time-varying confounders using country–year (α_{it}) and commodity–year (α_{kt}) fixed effects. Specifically, we model

$$\mathbb{E}[C_{ikt} \mid X_{ikt}, \alpha_{it}, \alpha_{kt}] = \exp\left(\gamma \ln X_{ikt} + \alpha_{it} + \alpha_{kt}\right), \qquad (1)$$

The country–year effects absorb shocks common to all commodities within a country–year (e.g., macroeconomic conditions, broad policy changes, domestic supply-side disruptions such as weather). The commodity–year effects absorb global commodity-specific shocks common across countries in year t, in particular changes in world market conditions (including prices) for commodity k.

We estimate (1) by Poisson pseudo–maximum likelihood (PPML). This estimator is appropriate because C_{ikt} contains 19.5% zeros (see Table 2.1), naturally accommodates zeros, and remains consistent under heteroskedasticity (Silva and Tenreyro 2006). In a log-link mean model with $\ln X_{ikt}$ as a regressor, γ can be interpreted as an elasticity of deforestation with respect to exports,

$$\frac{\partial \ln \mathbb{E}[C_{ikt} \mid \cdot]}{\partial \ln X_{ikt}} = \gamma, \qquad (2)$$

so that a 1 percent increase in export value is associated with an approximate γ percent change in expected deforestation (Mullahy and Norton 2024).

2.3.1 Endogeneity and shift–share instrument

The identification of the effect of export sales on deforestation faces two main challenges. First, expanding agricultural land and clearing forests can directly raise production capacity and thus exports (Carreira et al. 2024; Bragança 2018; Du et al. 2024). In addition, unobserved shocks—such as infrastructure expansion, subsidy or credit programs, or changes in enforcement—may affect both deforestation and export performance (Balboni et al. 2022; Assunção et al. 2015; Burgess et al. 2012; Cisneros et al. 2021). Second, international price shocks that do not primarily originate from international demand changes—for example, exchange-rate movements or changes in international supply-chain governance—can also incentivize deforestation (Harding et al. 2021). We address the first challenge by using a shift-share instrument, namely foreign demand instrument, for endogenous exports. In addition, we address second challenge by including commodity–year fixed effects, which control for global price and technology trends that affect all exporters of a commodity in a given year.

The instrument isolates variation in export value driven by destination-side demand conditions by combining time-invariant exposure weights that capture each country–commodity pair's average export shares across destination–product markets, and time-varying import-demand shifters at the destination–product level that are purged of exporter-side supply shocks. This is consistent with shift–share guidelines developed by Borusyak, Hull and Jaravel (2024).

Let j index the countries that import commodities from the countries in which deforestation is occurring. Further, let s index products, with $s \in k$ indicating that product s belongs to commodity k. We first estimate a product-level multiplicative gravity equation:

$$X_{ijst} = \exp\left(\phi_{ist} + \psi_{jst} + \mu_{ijs}\right)\varepsilon_{ijst}, \qquad (3)$$

where X_{ijst} is the export value of product s from exporter i to importer j in year t. The exporter–product–year fixed effects ϕ_{ist} absorb exporter-side supply conditions for product s in year t that accounts for the outward multilateral resistances and for production (Anderson, Larch and Yotov 2018). The importer–product–year fixed effects ψ_{jst} summarize importer-side conditions, which accounts for inward multilateral resistances and expenditures (Anderson et al. 2018). The exporter–importer–product fixed effects μ_{ijs} capture time-invariant bilateral trade costs and policies, such as long-standing trade agreements, distance, contiguity, and colonial or language.

We measure the exposure of each country–commodity pair to destination markets using average export shares over 2001–2022:

$$\omega_{ijs}^{k} = \frac{X_{ijs}^{k,\,2001\text{–}2022}}{\sum_{j'}\sum_{s'\in k} X_{ij's'}^{k,\,2001\text{–}2022}}, \qquad \sum_{j}\sum_{s\in k}\omega_{ijs}^{k} = 1, \qquad (4)$$

where $X_{ijs}^{k,\,2001\text{–}2022}$ is cumulative export value of product $s \in k$ from country i to destination j over 2001–2022, and the denominator is total export value of commodity k from country i over the same period. These long-run averages capture persistent trade orientation—reflecting comparative advantage, geography, agro-ecological suitability, and stable trade relationships—rather than short-run shocks.

Our foreign-demand instrument aggregates the one-year lagged importer–product–year fixed effect $\hat{\psi}_{jst}$ from equation (3) with the exposure weights from (4), as follows:

$$\widehat{FD}_{ikt} = \sum_{j}\sum_{s\in k}\omega_{ijs}^{k}\,\hat{\psi}_{js,t-1}. \qquad (5)$$

Following Fally (2015), $\hat{\psi}_{js,t-1}$ equals $\log\left(\hat{P}^{\theta}_{js,t-1}\, E_{js,t-1}/E_0 s\right)$, where $\hat{P}_{js,t-1}$ is the CES price index of destination j for product s in year $t-1$[1], $E_{js,t-1}$ is total imports of product s at destination j in year $t-1$, and E_{0s} is a normalization constant. Thus $\widehat{FD}_{ikt}$ measures how much exporter i's commodity-k exports are exposed to shifts in destination price indexes and import demand. We use a one-year lag in (5), which limits simultaneity between current deforestation C_{ikt} and destination-side import demand. The instrument is plausibly exogenous as it captures variation in importer-side conditions that is uncontaminated with exporter supply.

Exclusion restriction. Identification requires that $\widehat{FD}_{ikt}$ affect deforestation in country i only through its effect on that country's exports of commodity k, and through no other channel correlated with deforestation. Conditional on the country–year and commodity–year fixed effects, the lagged destination-side import-demand shifters $\hat{\psi}_{js,t-1}$ that drive the instrument must be uncorrelated with exporter-side commodity-specific shocks to land clearing such as domestic credit, enforcement, zoning, or weather. The design makes this plausible in two ways. First, the shifters are uncontaminated with exporter-side supply conditions by the exporter–product–year fixed effects ϕ_{ist} in the gravity model (3), so $\hat{\psi}_{js,t-1}$ reflects destination income, preferences, and policy rather than conditions in the exporter country. Second, the country–year and commodity–year fixed effects in the estimating equation absorb, respectively, all national shocks common across commodities and all global commodity-specific shocks (including world prices), so the instrument is identified from the interaction of destination demand with each exporter's predetermined market exposure. The restriction would fail if a destination's import demand responded to anticipated supply and hence clearing—in origin i. To break this anticipation effect, the one-year lag of shifter is used.

2.3.2 First stage and PPML IV estimation

We estimate the first-stage regression:

$$\ln X_{ikt} = \pi \widehat{FD}_{ikt} + \alpha_{it} + \alpha_{kt} + \nu_{ikt}, \qquad (6)$$

[1] $P^{-\theta}_{js,t-1}$ is the inward multilateral resistance, measuring the average trade cost that destination j faces when sourcing product s from all origins. The exponent $-\theta$ captures the trade elasticity, therefore θ is positive by construction in Fally (2015).

The expected sign of coefficient $\hat{\pi}$ on $\widehat{FD}_{ikt}$ is positive by construction. Because $\widehat{FD}_{ikt}$ rises when destination j faces higher import demand and price index, that should increase the export value of commodity k from country i if it is exposed to that destination.

To estimate the causal effect of exports on deforestation in the PPML framework, we use a control-function estimator (CF-PPML). In nonlinear models, simply replacing an endogenous regressor by its first-stage fitted value does not deliver consistent partial effects, however residual inclusion restores consistency (Papke and Wooldridge 2008; Wooldridge 2015). We estimate (6) by fixed-effects OLS and obtain residuals $\hat{\nu}_{ikt}$. We then estimate the second-stage PPML:

$$\mathbb{E}[C_{ikt} \mid \ln X_{ikt}, \alpha_{it}, \alpha_{kt}, \hat{\nu}_{ikt}] = \exp\left(\gamma \ln X_{ikt} + \alpha_{it} + \alpha_{kt} + \delta\hat{\nu}_{ikt}\right), \qquad (7)$$

where γ identifies the effect of export value on deforestation. The strength and significance of $\delta = 0$ provides a formal test of whether residual inclusion effectively controls endogenous supply shocks. Because the second stage includes generated regressors ($\hat{\nu}_{ikt}$), we base inference on a nonparametric block bootstrap that resamples at the country–commodity level and re-estimates both stages within each replication (see appendix 9 for details). We estimate heterogeneity by commodity group, by continent, and by continent-commodity pairs using the same CF-PPML estimator but replacing $\ln X_{ikt}$ with the interaction of $\ln X_{ikt}$ and the relevant subgroup indicator in the second stage. The full estimating equations for the pooled and heterogeneous (commodity, continent, and continent–commodity) specifications are written out in appendix A11.

2.4 Data

Our dataset covers 138 countries (listed in appendix 1) and 18 commodity groups comprising 493 HS products over 2001-2022. We select only countries that experienced agricultural-driven deforestation in all 22 years. The correspondence between HS codes and 18 commodity groups is shown in appendix 2. The unit of observation is a country-commodity-year triplet. The panel is unbalanced because agro-climatic conditions exclude many country-commodity combinations from production. For example, European countries are excluded from tropical commodities such as rubber, coffee, cocoa and cassava, since these crops require tropical conditions that European climates cannot support. We drop 483 agroclimatically infeasible country-commodity pairs out of 2,484 possible pairs (138×18), leaving 2001 country-commodity pairs.

Deforestation. We obtain commodity-specific deforestation from the DeDuce model developed by Singh and Persson (2024), which attributes observed tree-cover loss to the most likely proximate commodity driver by combining remote-sensing layers (i.e. spatial attribution) where available and, otherwise, a land-balance method using agricultural land-use and harvested area statistics (i.e statistical attribution). The model reports the ex-post unamortized and amortized deforestation based on land-cover and land use dynamics (see appendix 3 for model details). Unamortized deforestation assigns the full forest loss to the year it occurs, whereas amortized deforestation distributes impacts (especially carbon emissions) over a 5-year period to better capture short- to medium-run policy relevance. We use unamortized deforestation data in the main analysis. Figure A3.1 illustrates the cumulative deforestation by country over the sample period. We aggregate FAOSTAT commodity-level deforestation into 18 groups: cassava, cocoa, coffee, fibre crops, fruits, maize, nuts, other cereals, other oilseeds, cattle (pasture), pulses and legumes, rice, rubber, soybeans, stimulants/spices/aromatics, sugar crops, and vegetables. The correspondence of FAOSTAT items to these 18 groups is shown in appendix 4.

Trade: We use the CEPII-BACI trade matrix, which reports bilateral export values (in USD) by HS product and reconciles mirror figures to address measurement error relative to Comtrade data (Gaulier and Zignago 2010). We match HS codes to our 18 commodity groups to construct country–commodity–year export values.

The analysis sample includes 37,948 country-commodity-year observations with non-missing exports and instrument. Table 2.1 reports the descriptive statistics of deforestation (ha), exports (thousands USD), and the shift-share foreign demand instrument. Deforestation is highly skewed, with a mean of 2,490 hectares, a median of 4.85 hectares, and a standard deviation of 36,596 hectares. A total of 9,164 country-commodity-year observations record zero deforestation. Export sales are similarly skewed, with a mean of 430,647 thousand USD, a median of 22,015 thousand USD, and a maximum of approximately 62.6 billion USD. The foreign demand instrument has a mean of

0.94 (median 0.99) and ranges from -9.41 to 8.76, reflecting variation in destination-market demand conditions across commodities and years. Descriptive statistics for exposure shares and the underlying shifts are reported in appendix 5 and appendix 6, respectively.

Table 2.1: Descriptive statistics of variables under study

Statistic	Export ('000 USD)	Deforestation (ha)	Foreign Demand ($\widehat{FD}_{ikt}$)
Count of Zero	0	9164	0
Minimum	0.00	0.00	-9.41
Mean	430646.56	2490.24	0.94
Maximum	62635824.56	2467977.22	8.76
1st Quartile	1790.45	0.00	0.48
Median	22014.76	4.85	0.99
3rd Quartile	160538.46	155.42	1.44
Standard Deviation	1695259.13	36595.86	0.88

Notes: Export is total bilateral export value in thousands of USD. Deforestation is unamortized commodity-attributed forest loss in hectares. Foreign demand is the lagged shift-share instrument constructed from the gravity model.

Figure 2 illustrates the relationship between deforestation, foreign demand, and exports. Panel (a) indicates that commodities with higher export growth tend to have higher cumulative deforestation. Commodities with notably higher export growth include other oilseeds (1,139%), palm (1,137%), cassava (1,028%)[2], soybeans (557%), and maize (493%). However, cattle have a very high cumu-

[2] Cassava's very high percentage export growth reflects an extremely small initial export base. Cassava is predominantly a non-traded subsistence staple, so even modest absolute increases in trade translate into large proportional changes. This also leads to higher deforestation intensity.

lative deforestation footprint with moderate export growth (394%). Panel (b) indicates that commodities have a disproportionate deforestation share relative to export share. Commodities such as cattle, cassava, palm, rubber, rice, pulses, cocoa, and maize have a higher deforestation share relative to export share. Conversely, fruits, other cereals, vegetables, sugar, stimulants, coffee, other oilseeds, nuts, and soybeans have a lower deforestation share in relation to their export share. Panel (c) shows that commodities vary starkly in deforestation intensity, measured as hectares per $1 billion of export sales. Intensity is highest for cassava (~69 ha per $1 billion), followed by cattle (~32), palm (~19), and rubber (~15). A middle tier includes pulses (~12), rice (~11), cocoa (~10), and maize (~9). Other oilseeds and soybeans both record ~4 ha per $1 billion, and coffee, stimulants, nuts, sugar, and vegetables each record 2–3 ha per $1 billion. Fruits, fiber, and other cereals have the lowest intensity (~1 ha per $1 billion). Panel (d) presents the Pearson correlation matrix. The correlations are 0.19 between deforestation and exports, 0.04 between deforestation and foreign demand, and 0.27 between foreign demand and exports. The deforestation–foreign demand and deforestation–exports correlations are weak, while the foreign demand–exports correlation is moderate and positive, consistent with the instrument's relevance condition.

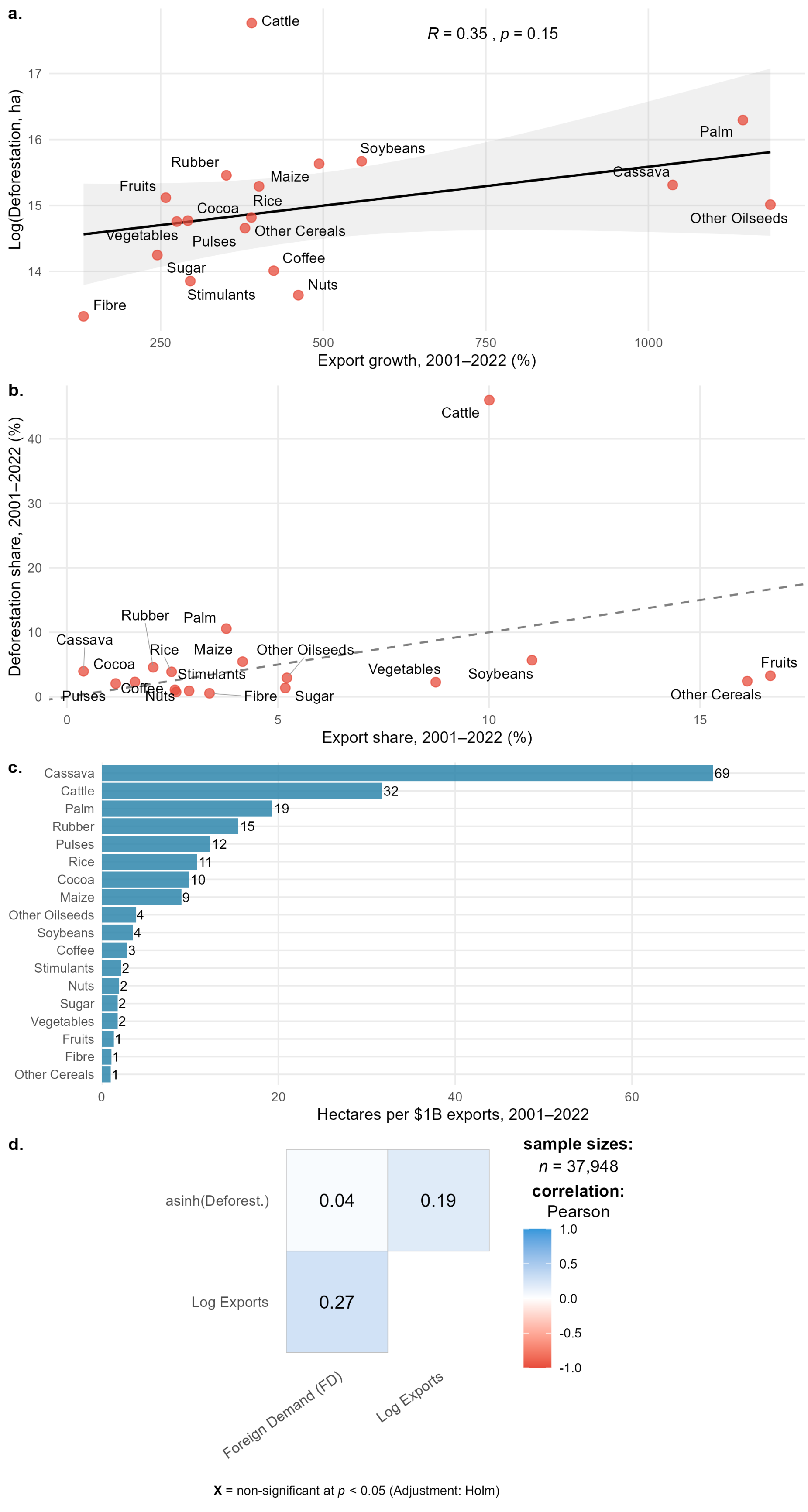
a.
Cattle
R = 0.35 , p = 0.15
Palm
Soybeans
Rubber
Maize
Fruits
Rice
Cocoa
Cassava
Other Cereals
Other Oilseeds
Vegetables
Pulses
Coffee
Sugar
Nuts
Stimulants
Fibre
Log(Deforestation, ha)
17
16
15
14
250
500
750
1000
Export growth, 2001–2022 (%)
b.
Cattle
Deforestation share, 2001–2022 (%)
40
30
20
10
0
Rubber
Palm
Cassava
Rice
Maize
Other Oilseeds
Cocoa
Stimulants
Vegetables
Soybeans
Fruits
Pulses
Coffee
Nuts
Fibre
Sugar
Other Cereals
5
15
Export share, 2001–2022 (%)
c.
Cassava 69
Cattle 32
Palm 19
Rubber 15
Pulses 12
Rice 11
Cocoa 10
Maize 9
Other Oilseeds 4
Soybeans 4
Coffee 3
Stimulants 2
Nuts 2
Sugar 2
Vegetables 2
Fruits 1
Fibre 1
Other Cereals 1
0
20
40
60
Hectares per $1B exports, 2001–2022
d.
asinh(Deforest.)
0.04
0.19
Log Exports
0.27
Foreign Demand (FD)
Log Exports
sample sizes:
n = 37,948
correlation:
Pearson
1.0
0.5
0.0
-0.5
-1.0
X = non-significant at p < 0.05 (Adjustment: Holm)

Figure 2. Relationship between foreign demand, exports, and deforestation. Panel (a) shows the log of cumulative deforestation (hectares) against the export growth over 2001 to 2022 by commodity group. The black solid line represents the OLS fitted line, and the shaded regions denote 95% confidence interval. Panel (b) compares deforestation shares against export share by commodity group. The dashed line is a 45-degree line indicating equal shares of deforestation and exports. Panel (c) shows bar plots of deforestation intensity, measured as hectares per \$1 billion of export sales. Panel (d) presents the Pearson correlation matrix between deforestation, foreign demand, and exports. Panels (a)-(c) use commodity-level aggregates. Panel (d) uses country-commodity-year data.

2.5 Results

Table 2.2 reports the first-stage estimates, where log X_{ikt} is regressed on $\widehat{FD}_{ikt}$ conditional on country–year and commodity–year fixed effects. The coefficient on $\widehat{FD}_{ikt}$ is positive and statistically significant. The positive sign reflects the construction of the instrument. $\widehat{FD}_{ikt}$ rises when destination markets have higher total import demand and price index, which raises bilateral import demand from exporter i and increases X_{ikt}. The F-statistic is above the conventional rule-of-thumb threshold of 10 (Staiger and Stock 1997), suggesting that the instrument is strong. The subsample first-stage regressions by commodity groups and continents (see appendix table A7) show that the instrument is strong for most commodity groups and continents, with F-statistic above 10 for most of them. Further, following Borusyak et al. (2022), we check that this strength does not rest on a few dominant destination–product markets by computing the effective number of shifters (the inverse Herfindahl–Hirschman index of the exposure weights) for each country–commodity pair (see appendix 5). The large effective number of shifters indicates that the instrument draws on sufficiently diversified exposure patterns rather than a handful of markets.

Table 2.2: First-stage regression: effect of foreign demand instrument on log exports

	Log Exports
$\widehat{FD}_{ikt}$	0.9080***
	(0.0623)
Observations	37,948
F-statistic	38.91
R^2	0.649
Country × Year FE	Yes
Commodity × Year FE	Yes

Notes: Standard errors clustered by country–commodity and year in parentheses. Country–year and commodity–year fixed effects included. * $p < 0.10$, ** $p < 0.05$, *** $p < 0.01$.

Table 2.3 reports the pooled estimate of the elasticity of deforestation with respect to export sales, instrumented with $\widehat{FD}_{ikt}$. The export elasticity coefficient is 0.31, implying that a 10% increase in export sales raises deforestation by 2.96%. The control-function residual $\hat{\nu}_{ikt}$ is positive but not statistically significant, suggesting that after controlling for country–year and commodity–year fixed effects, the remaining variation in exports is approximately exogenous to deforestation. $\widehat{FD}_{ikt}$ removes exporter-specific and bilateral shocks that move both export shares and deforestation, isolating variation in destination–product demand and inward multilateral resistance common to all origins.

Table 2.3: Effect of export sales on deforestation

	Deforestation
Log(Exports)	0.306***
	(0.138)
	[0.073, 0.606]
Residual	0.135
	(0.156)
	[-0.238, 0.359]
Observations	37,405
Pseudo R-squared	0.862
Country × Year FE	Yes
Commodity × Year FE	Yes
Instrument	$\widehat{FD}_{ikt}$

Notes: Bootstrap standard errors (1,000 replications) in parentheses. 95% bootstrap percentile CIs in brackets. Fixed effects: country×year, commodity×year. * p<0.10, ** p<0.05, *** p<0.01.

Figure 3 illustrates the heterogeneous effects of export sales on deforestation by commodities and continents. At the commodity level, the largest elasticities are for tree and perennial crops: stimulants (0.92), rubber (0.84), palm (0.82), cocoa (0.76) and nuts (0.68). Substantial elasticities also appear for soybeans (0.60), other cereals (0.59), cattle (0.54), sugar (0.49), coffee (0.48), and fibre (0.46). Smaller but statistically significant elasticities appear for other oilseeds (0.36), vegetables (0.32), pulses (0.31), fruits (0.26), maize (0.23), and rice (0.21). Cassava (0.03) has a small and statistically insignificant elasticity.[3] At the continent level, export elasticities are highest in South America (0.65), Southeast Asia (0.52), and Europe (0.50), all significant at the 1% level. North and Central America (0.34) and Rest of Asia (0.31) show moderate significant responses, while Africa (0.12), Oceania (0.11), and North Asia (0.20) have statistically insignificant elasticities.

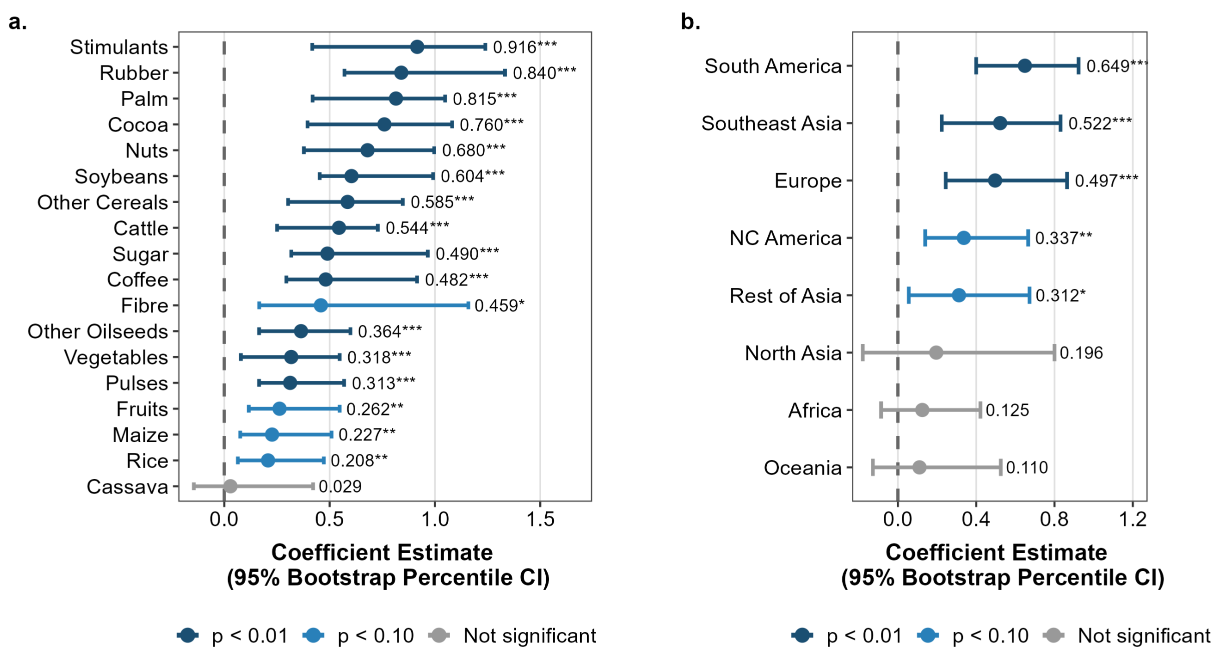

Figure 3: Heterogeneous deforestation elasticities with respect to exports. Panel (a) shows estimates by commodity; Panel (b) shows estimates by continent. All specifications include country-year and commodity-year fixed effects and are estimated by control-function PPML, instrumenting exports with $\widehat{FD}_{ikt}$. The bootstrap standard errors of 1000 replications are reported in parenthesis. Significance levels: *** p<0.01, ** p<0.05, * p<0.1.

Figure 4 disaggregates the export–deforestation elasticities by continent–commodity pair. Ex-

[3] The near-zero cassava elasticity, despite its large measured export growth, is consistent with cassava being a largely non-traded subsistence staple whose export growth comes off a very small base, so foreign demand exerts little leverage on cassava-related clearing.

port-driven deforestation is again concentrated in humid-tropical frontiers in South America, Southeast Asia, and Africa, where suitable agro-climatic conditions for palm oil, cocoa, rubber, coffee, nuts, and stimulants overlap strongly with remaining forests. In South America, almost all export commodities exhibit large positive elasticities. Cocoa (0.97), coffee (0.89), stimulants (0.89), palm (0.88), nuts (0.86), rubber (0.79), soybeans (0.77), fibre (0.72), other cereals (0.68), cattle (0.65), sugar (0.59), pulses (0.59), other oilseeds (0.59), vegetables (0.48), maize (0.46), fruits (0.45), cassava (0.41), and rice (0.38) all show statistically significant responses. In Southeast Asia, export elasticities are large for tree crops: stimulants (0.72), cocoa (0.69), nuts (0.68), coffee (0.65), palm (0.64), and rubber (0.53) are strongly positive. Soybeans (0.46), fibre (0.43), other oilseeds (0.35), other cereals (0.33), sugar (0.33), pulses (0.30), cattle (0.27), vegetables (0.26), and fruits (0.23) are positive and significant. Maize (0.21) and rice (0.17) are positive but insignificant; cassava (0.03) is near zero.

In Africa, tree and perennial crops dominate. Nuts (0.73), coffee (0.70), cocoa (0.69), stimulants (0.63), palm (0.54), fibre (0.50), soybeans (0.46), rubber (0.35), other cereals (0.33), pulses (0.30), other oilseeds (0.29), cattle (0.28), and vegetables (0.19) are positive and significant. Sugar, maize, fruits, cassava, and rice have small and statistically insignificant elasticities. In the Rest of Asia, nuts (0.68), stimulants (0.65), fibre (0.56), cocoa (0.55), coffee (0.54), soybeans (0.49), other cereals (0.41), rubber (0.41), pulses (0.37), palm (0.37), other oilseeds (0.35), cattle (0.33), sugar (0.28), and vegetables (0.26) show positive and significant responses. Fruits, maize, and rice are positive but insignificant; cassava records a negative and significant elasticity (−0.21). In Europe, elasticities are large across a wide range of crops: nuts (0.96), stimulants (0.78), fibre (0.73), soybeans (0.72), other cereals (0.65), pulses (0.59), other oilseeds (0.58), cattle (0.52), sugar (0.48), maize (0.44), vegetables (0.42), and fruits (0.37) are positive and significant, while rice (0.27) is significant at the 10% level.

Results are mixed in other regions. In North and Central America, coffee (0.80), nuts (0.77), stimulants (0.71), cocoa (0.71), palm (0.69), fibre (0.66), soybeans (0.60), and rubber (0.55) have the largest responses. Other cereals (0.47), pulses (0.46), other oilseeds (0.42), cattle (0.41), sugar (0.40), maize (0.31), fruits (0.29), and vegetables (0.28) are also positive and significant. Rice

(0.15) and cassava (0.03) are statistically insignificant. In Oceania, cocoa (0.63), coffee (0.56), nuts (0.53), stimulants (0.47), and fibre (0.39) are positive and significant. Palm (0.47), other cereals (0.28), other oilseeds (0.25), rubber (0.23), and soybeans (0.19) are positive but insignificant; rice (−0.39) and cassava (−0.89) are negative and insignificant. North Asia is generally muted: stimulants (0.56), nuts (0.53), and rubber (0.52) are marginally significant at the 10% level, while all other commodities are statistically insignificant. Cassava (−0.25) and rice (−0.04) are negative but insignificant.

	Africa	Europe	North and Central America	North Asia	Oceania	Rest of Asia	South America	Southeast Asia
Vegetables	0.19* (0.11)	0.42*** (0.14)	0.28** (0.13)	0.17 (0.27)	0.11 (0.16)	0.26* (0.13)	0.48*** (0.13)	0.26** (0.13)
Sugar	0.17 (0.16)	0.48*** (0.17)	0.40*** (0.16)	0.16 (0.26)	0.09 (0.18)	0.28* (0.16)	0.59*** (0.14)	0.33** (0.15)
Stimulants	0.63*** (0.16)	0.78*** (0.18)	0.71*** (0.18)	0.56* (0.29)	0.47** (0.21)	0.65*** (0.16)	0.89*** (0.16)	0.72*** (0.16)
Soybeans	0.46*** (0.16)	0.72*** (0.16)	0.60*** (0.16)	0.38 (0.26)	0.19 (0.19)	0.49*** (0.16)	0.77*** (0.13)	0.46*** (0.16)
Rubber	0.35* (0.19)		0.55** (0.23)	0.52* (0.31)	0.23 (0.22)	0.41* (0.21)	0.79*** (0.23)	0.53*** (0.18)
Rice	0.02 (0.10)	0.27* (0.15)	0.15 (0.15)	-0.04 (0.28)	-0.39 (0.27)	0.12 (0.13)	0.38*** (0.12)	0.17 (0.11)
Pulses	0.30*** (0.10)	0.59*** (0.15)	0.46*** (0.13)	0.16 (0.42)	0.14 (0.21)	0.37*** (0.14)	0.59*** (0.13)	0.30** (0.15)
Palm	0.54*** (0.17)		0.69*** (0.18)	0.16 (0.32)	0.47 (0.34)	0.37* (0.19)	0.88*** (0.18)	0.64*** (0.17)
Other Oilseeds	0.29** (0.11)	0.58*** (0.13)	0.42*** (0.14)	0.24 (0.24)	0.25 (0.17)	0.35*** (0.13)	0.59*** (0.13)	0.35*** (0.12)
Other Cereals	0.33* (0.19)	0.65*** (0.18)	0.47*** (0.18)	0.31 (0.27)	0.28 (0.25)	0.41** (0.19)	0.68*** (0.18)	0.33* (0.20)
Nuts	0.73*** (0.17)	0.96*** (0.18)	0.77*** (0.17)	0.53* (0.30)	0.53** (0.22)	0.68*** (0.17)	0.86*** (0.18)	0.68*** (0.17)
Maize	0.16 (0.10)	0.44*** (0.13)	0.31** (0.13)	0.13 (0.26)	-0.01 (3.62)	0.16 (0.14)	0.46*** (0.12)	0.21 (0.13)
Fruits	0.15 (0.10)	0.37** (0.14)	0.29** (0.13)	0.11 (0.27)	0.06 (0.16)	0.19 (0.13)	0.45*** (0.12)	0.23* (0.12)
Fibre	0.50*** (0.18)	0.73*** (0.19)	0.66*** (0.20)	0.41 (0.31)	0.39* (0.23)	0.56*** (0.19)	0.72*** (0.22)	0.43** (0.19)
Coffee	0.70*** (0.20)		0.80*** (0.20)	0.41 (0.31)	0.56** (0.24)	0.54** (0.22)	0.89*** (0.18)	0.65*** (0.19)
Cocoa	0.69** (0.19)		0.71** (0.23)		0.63** (0.23)	0.55** (0.23)	0.97*** (0.20)	0.69** (0.21)
Cattle	0.28** (0.11)	0.52*** (0.13)	0.41*** (0.13)	0.25 (0.24)	0.14 (0.15)	0.33*** (0.13)	0.65*** (0.12)	0.27** (0.13)
Cassava	0.10 (0.22)		0.03 (0.27)	-0.25 (0.36)	-0.89 (0.85)	-0.21 (0.25)	0.41* (0.25)	0.03 (0.21)

Estimate
0.5
0.0
-0.5

Figure 4: Deforestation elasticities of commodities with respect to exports for each continent. The estimates are based on control-function PPML estimation. The fixed effects include country–year and commodity–year fixed effects. Bootstrap standard errors based on 1,000 replications are reported in parentheses. Red color indicates positive elasticities and green indicates negative elasticities. Significance levels: *** p<0.01, ** p<0.05, * p<0.1.

2.6 Robustness checks

2.6.1 Alternative specifications checks

To assess robustness to functional form, we estimate the effect of international demand using four alternative outcome transformations, which are log(Deforestation), log(1+Deforestation), asinh(Deforestation) and level. Across these specifications, we keep the same fixed effects and clustering. Qualitatively, the results are similar across all outcomes (see appendix A12). Signs and statistical significance are preserved in the pooled sample. The pattern of heterogeneous responses by commodity (stronger for land-intensive frontier commodities such as cocoa, palm, rubber, soybeans, and pasture) and by region (larger in South America and Southeast Asia) remains consistent with main results. Magnitudes adjust as expected with the transformation. PPML tends to give greater weight to observations with larger conditional means. Log-based models emphasize proportional changes among positive observations. Inverse hyperbolic sine sits between these two.

2.6.2 Placebo test

The consistency of the estimates from our shift-share design relies on the exogeneity of demand at product-destination-year, (s, j, t), for each country-commodity-year, (i, k, t). We treat the shares as fixed and test whether the geographic pattern of importer-side demand shocks matters for identification. Within each commodity–exporter–year cell (k, i, t), we keep the shares ω^k_{isj} unchanged but randomly reassign the importer fixed effects $\hat{\psi}_{jkt}$ across destination countries j, thereby breaking the link between the actual destination-specific shocks and each exporter's trade partners. We repeat this 1,000 times and re-estimate the effect of foreign demand on deforestation. Figure 5 presents the resulting placebo distributions. The estimated coefficient and t-statistic from the actual data fall outside the placebo distribution, confirming that identification stems from the actual geographic pattern of importer-side demand shocks and not from a mechanical correlation in the instrument construction.

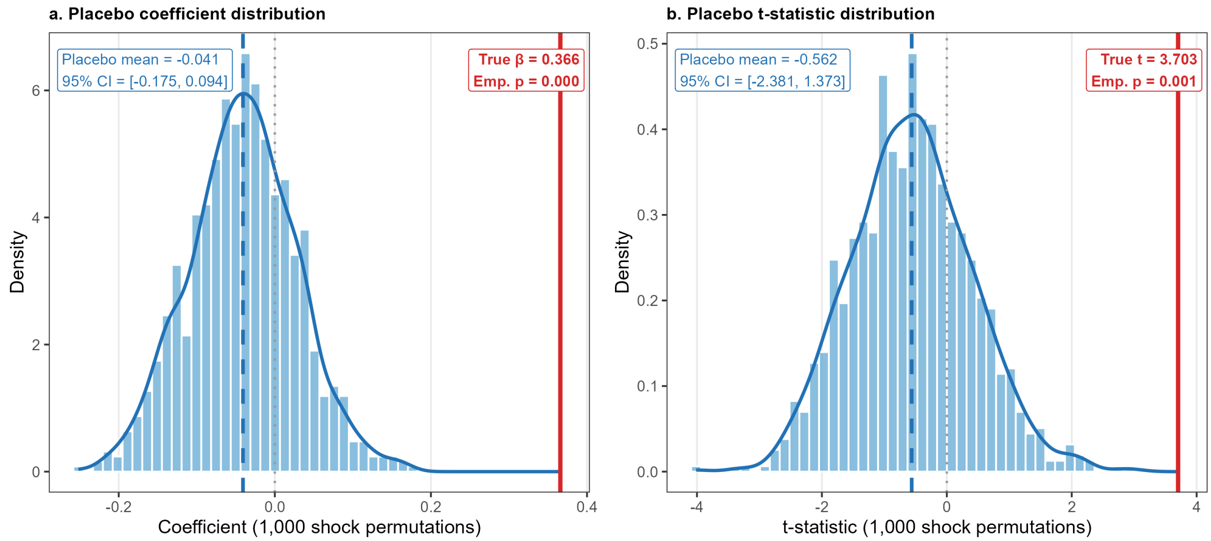

Figure 5: Distributions of estimated coefficients and t-statistics from shock permutation samples. Note: The density plots are based on 1,000 iterations in which importer fixed effects $\hat{\psi}_{jkt}$ are randomly shuffled across destination countries within each commodity–exporter–year cell, keeping export shares fixed. The 95% confidence intervals are constructed using percentile confidence intervals at the 2.5th and 97.5th percentiles of the placebo distribution. The red vertical solid lines represent the coefficient and t-statistic estimated from the actual data.

2.6.3 Alternative shares

A potential concern with our shift-share instrument is that the export shares ω^k_{ijs} are computed over the analysis period (2001–2022) and could themselves reflect deforestation-driven component in trade composition. If, say, clearing additional land enabled country i to expand exports of commodity k to destination j during the study period, the increased shares would represent supply-side responses, violating the exogeneity condition (Goldsmith-Pinkham et al. 2020; Borusyak et al. 2022).

We test this concern by reconstructing the instrument using pre-sample shares computed from the 1996–2000 trade data, five years before the analysis period begins. Formally, we replace ω_{ijs}^{k} with $\omega_{ijs}^{k,pre}$, the average bilateral export share for each country–product pair over 1996–2000, while retaining the same importer-side demand shocks $\hat{\psi}_{jkt-1}$ from the gravity model estimated on the full panel:

$$\widehat{FD}_{ikt}^{pre} = \sum_{j} \sum_{s \in k} \omega_{ijs}^{k,pre} \, \hat{\psi}_{js,t-1}. \qquad (8)$$

Pre-sample shares are predetermined relative to all deforestation and trade adjustments in the analysis period, so this specification is not the endogenous-shares by design. The downside is that pre-sample shares may imprecisely measure each exporter's true market exposure by the mid-2010s, as trade networks evolve. This measurement error in the shares would attenuate the first stage and potentially reduce precision.

Appendix A17 reports the pooled and heterogeneous results under $\widehat{FD}_{ikt}^{pre}$. The pooled export elasticity of deforestation is similar in magnitude to the main estimate, and statistically significant at the 1% level. The pattern of heterogeneous responses is qualitatively preserved: perennial and frontier commodities (stimulants, rubber, palm, cocoa, nuts) and the cattle and soybean sectors carry the largest commodity-level elasticities, while staples show small or insignificant responses. By continent, South America and Southeast Asia retain the highest elasticities. These results indicate that the main findings are not an artifact of endogenous base-period shares.

2.6.4 Alternative instrument check

We construct a second instrument, $\widehat{FD2}_{ikt}$, that replaces bilateral pair fixed effects in the gravity equation (3) with observable trade-cost controls. We estimate the gravity equation as shown below:

$$X_{ijst} = \exp\big(\beta_1 \ln d_{ij} + \beta_2 COL_{ij} + \beta_3 LANG_{ij} + \beta_4 CONTG_{ij} + \phi_{ist} + \psi_{jst}\big)\varepsilon_{ijst}, \qquad (9)$$

where d_{ij} is bilateral distance, COL_{ij} indicates ever-colonial ties, $LANG_{ij}$ a common official language, and $CONTG_{ij}$ a shared land border. Exporter–commodity–year (ϕ_{ist}) and importer–commodity–year (ψ_{jst}) fixed effects are retained. We construct the instrument aggregating destination fixed effects and effects of arguably exogenous bilateral variables.

$$\widehat{FD2_{ikt}} = \sum_j \exp\big(\hat{\beta}_1 \ln d_{ij} + \hat{\beta}_2 COL_{ij} + \hat{\beta}_3 LANG_{ij} + \hat{\beta}_4 CONTG_{ij} + \hat{\psi}_{jkt-1}\big), \tag{10}$$

Unlike $\widehat{FD}_{ikt}$, which weights destination shocks by observed export shares, $\widehat{FD2_{ikt}}$ aggregates gravity-predicted demand using time-invariant bilateral trade costs which is an alternative way to isolate exporter-specific foreign market exposure from supply-side variation.

Appendix table A16.1 reports the pooled result. The pooled export elasticity of deforestation under $\widehat{FD2_{ikt-1}}$ is 0.514, which is larger in magnitude than the 0.31 estimate from the main specification. However, heterogeneous effects by commodity group and continent, shown in appendix figures A16.1–A16.2, are qualitatively consistent with the main results. Perennial and tree crops (stimulants, rubber, palm, cocoa, nuts) carry the largest elasticities, and South America and Southeast Asia account for the highest continent-level responses.

2.7 Discussion

Our control-function PPML estimates indicate that a 10% increase in exports raises commodity-specific deforestation by 2.96%. Berman et al. (2023) estimates that a 10% increase in their suitability-weighted crop price index increases tropical deforestation by a little over 10% (an elasticity on the order of one). This price elasticity is plausible given that they focus on total tree-cover loss, whereas our focus is on forest loss explicitly linked to agricultural expansion.

A key contribution of our analysis is to reveal heterogeneity behind this aggregate effect. Export-mediated deforestation elasticities are concentrated in perennial tree crops (stimulants, rubber, oil palm, cocoa, coffee, nuts) and extensive livestock/feed sectors (cattle, soy), and are largest in South America, Southeast Asia and Europe. This pattern closely mirrors pan-tropical footprint and tele-coupling studies, which attribute most export-embodied deforestation to beef/cattle, soy, palm oil, rubber, cocoa and coffee (Pendrill, Persson, Godar, Kastner, Moran, et al. 2019; Pendrill, Persson, Godar and Kastner 2019; Pacheco et al. 2021; Meyfroidt et al. 2020). The magnitudes are broadly consistent with country-level causal evidence linking export or price shocks to substantial forest loss in Brazil, Indonesia, and other tropical frontiers (e.g., Du et al. 2024; Carreira et al. 2024; Abman et al. 2020). Noticeably, the variation in export-deforestation elasticities is larger across commodities than across regions.

We interpret three mechanisms behind the larger elasticities of the perennial tree crops. First, the agro-climatic niches of these crops overlap closely with tropical and humid forests in the Amazon/Cerrado, Indonesia–Malaysia and West Africa (Pendrill, Persson, Godar, Kastner, Moran, et al. 2019; Pendrill, Persson, Godar and Kastner 2019; Curtis et al. 2018; Pacheco et al. 2021), so expansion margins in these sectors are likely to be forest. Second, these are high-value, export-oriented crops providing higher incentives to expansion. This fits with evidence that a small set of high-value commodities accounts for a disproportionate share of trade-embodied deforestation (Pendrill, Persson, Godar, Kastner, Moran, et al. 2019; Pendrill, Persson, Godar and Kastner 2019; Meyfroidt et al. 2020). Third, perennial tree crops involve high establishment costs and long gestation lags but, once established, are relatively hard to reconfigure (Leijten et al. 2023; Gockowski and Sonwa 2011; Sassen et al. 2022). So, demand shocks are often met by expansion rather than intensifying or rejuvenating existing stands (e.g., Angelsen 2010; Lambin and Meyfroidt 2011; Ahrends et al. 2015).

In contrast, staple cereals and horticultural crops shows comparatively weaker export-deforestation elasticities. One plausible explanation is displacement and intensification mechanisms. As high-value export crops expand, staple and horticultural production can reallocate onto already cleared land, and additional demand may be met through yield gains rather than expansion (García et al. 2020; Meyfroidt, Rudel and Lambin 2010). This interpretation is reasonable in land-scarce or post-transition regions, where agricultural growth occurs through intensification, imports and spatial reorganization than through low-value clearing (García et al. 2020; Meyfroidt et al. 2010). Global and regional studies likewise document land-sparing patterns (e.g., Lambin and Meyfroidt 2011;

Meyfroidt et al. 2020; Zabel et al. 2019; Byerlee, Stevenson and Villoria 2014; Villoria, Byerlee and Stevenson 2014).

The relatively larger elasticities estimated for Europe should be interpreted with caution. They reflect high proportional sensitivity, but not high absolute scale. Europe accounts for only a small share of global commodity-attributed deforestation—for instance, around 0.1% for stimulants (about 530 ha), 4.7% for other cereals (127.7 thousand ha), and 0.4% for cattle (196.8 thousand ha)—far below the corresponding shares in the major tropical frontier regions (appendix A15). Thus, even moderate changes in land conversion can generate comparatively large elasticities when measured against a small initial deforestation base. This denominator effect is reinforced by the fact that export growth in Europe is generally smaller than in other regions (appendix A8), while percentage changes in deforestation can still appear large because baseline deforestation levels are low (see appendix A14). One plausible interpretation is that European export expansion operates through land-use adjustment within post-forest-transition landscapes, such as re-cultivation of fallow land or conversion of secondary and semi-natural woody cover, rather than through large-scale tropical frontier clearing (e.g., Meyfroidt et al. 2020). This is also consistent with Europe's role as a major importer, rather than exporter, of tropical forest-risk commodities such as oil palm, cocoa, coffee, and rubber. On this reading, the European coefficients indicate that export growth can induce measurable land conversion even in mature agricultural systems, while remaining globally much less important than tropical export-frontier dynamics.

Our estimates should be interpreted with several caveats. Because identification comes from shift–share instruments, they capture the effects of differential destination–product demand shocks while absorbing common global price movements and national shocks. However, even with time-varying country controls, we cannot fully exclude the influence of time-varying, commodity-specific domestic policies, such as credit expansion, zoning changes, or shifts in enforcement. In addition, our framework is reduced-form and largely static, so it does not explicitly model dynamic land-use adjustment and may understate or mis-time responses where deforestation occurs with lags, particularly for perennial crops. Finally, although commodity–year fixed effects absorb common international price movements, this effectively treats global price shocks as common across producers. In practice, price pass-through may be incomplete and heterogeneous across countries and sub-national regions.

A further limitation concerns indirect and cross-border leakage. For example, when higher soy demand displaces pasture, the resulting pasture expansion may clear forest, so part of the soy-driven deforestation is realized as pasture clearing. So our commodity-specific elasticity is thus a direct own-commodity conversion response in own country. For a land-displacing crop such as soy, the estimated elasticity is a lower bound on its full demand-driven deforestation, since some of the clearing it induces is counted under the absorbing activity, may be as cattle-driven deforestation.

2.8 Conclusion

We provide evidence that international demand is an important driver of deforestation linked to agricultural expansion. Using a shift–share identification strategy in a panel of 138 countries and 18 commodity groups over 2001–2022, we find that a 10% increase in export sales raises commodity-attributed deforestation by approximately 2.96%. This average effect, however, masks heterogeneity across commodities and regions. Export-driven deforestation is concentrated in a relatively small set of forest-risk commodities, especially perennial and tree crops such as stimulants and spices, rubber, oil palm, cocoa, coffee, and nuts, together with livestock and feed/feedstock commodities such as cattle, soybeans, and sugar crops, while staple and horticultural crops exhibit much smaller or statistically insignificant responses.

These findings speak directly to current debates on trade-linked forest regulation. They support the emphasis of emerging policies on a relatively small set of high-risk commodities, consistent with broader evidence that a limited number of forest-risk exports account for a disproportionate share of deforestation embodied in trade. Because our estimates provide globally comparable elasticities, they can complement simulation-based assessments of demand-side measures, trade policy, and market-mediated leakage (for example, Taheripour, Hertel and Ramankutty 2019; Arima et al. 2021). Conversely, the small or negative elasticities estimated for staple and horticultural crops suggest that blanket zero-deforestation requirements across all agricultural trade may be poorly targeted. In these sectors, sustainable intensification and domestic land-use governance may be more effective than stringent trade restrictions.

Chapter 3

Domestic Market Access and Cropland Expansion in Brazil

3.1 Introduction

Domestic logistics is a constraint on the competitiveness of Brazilian agriculture (Fliehr, Zimmer and Smith 2019; Oliveira and Alvim 2017; Branco et al. 2022). The main reason is grain production remains concentrated in the interior of Brazil. In 2024, the Center-West alone produced 144.5 million tonnes, or 48.5% of Brazil's cereals, legumes, and oilseeds (USDA Agricultural Marketing Service 2024; Companhia Nacional de Abastecimento (Conab) 2025). This carries a large cost to transport from one location to another. For example: the route from North Mato Grosso to the port of Santos, total transportation costs in 2024 amounted to roughly one-third of the reported soy farm-gate price (USDA Agricultural Marketing Service 2024).

Transport infrastructure is therefore central to agricultural growth in Brazil. Long-distance grain flows have historically depended on road transport (Correa and Ramos 2010; Fliehr et al. 2019; Costa, Soares-Filho and Nóbrega 2022), in contrast to the United States, where long-distance grain transport relies on rail and barge movements (Friend and Lima 2011). Recent studies show that rail expansion and intermodal corridor investment can reduce freight costs, reorganize port hinterlands, and shift soybean and corn flows toward northern export routes (Branco et al. 2022; Branco et al. 2021; Wang et al. 2024; Costa et al. 2022). Yet the transport network system remains road dominant and infrastructure is poor. The official statistics indicate that only 12.4% of Brazil's road network is paved and that rail carries 17.7% of the national freight matrix (Confederação Nacional do Transporte 2024; Ministério dos Transportes 2024a). The policy response has accelerated in recent years. The Malha Paulista rail concession was renewed in May 2020 (Governo Federal do Brasil 2020). The BR-163/230 corridor linking Sinop to Miritituba was conceded in 2022, after full paving of the Pará segment reduced trip times from more than ten days to roughly three (Agência Nacional de Transportes Terrestres 2022). At the national level, the current planning framework is organized around PNL 2035, launched in 2021, while a new Integrated Transport Planning cycle was instituted in 2024 to guide subsequent logistics priorities (Governo Federal do Brasil 2021; Ministério dos Transportes 2024b). This reorganization is already visible in shipment patterns, with soy and corn flows through Northern Arc ports rising from 36.7 million tonnes in 2020 to 57.6 million tonnes in 2024 (USDA Agricultural Marketing Service 2024; Companhia Nacional de Abastecimento 2025). These investments amount to a reorganization of Brazil's grain transport system, motivated in part by the expectation that lower logistics costs will raise competitiveness and reshape the geography of agricultural production (Branco et al. 2022; Branco et al. 2021; Wang et al. 2024).

What transport investments do in theory is straightforward. Lower freight costs raise the farm-gate price of output and lower the delivered price of inputs, so they change both the revenue and the cost side of the farm budget (Chomitz and Gray 1996). This makes it cheaper to sell crops, buy inputs, and adopt yield-enhancing technologies, so better connectivity can raise output on land already in cultivation (Shamdasani 2021; Jacoby and Minten 2009; Aggarwal et al. 2024). But that intensive-margin response is itself ambiguous. Yield per hectare can rise simply because cheaper fertilizer and chemicals lead farmers to apply more inputs per hectare or because of technical change that raises output for a given bundle of inputs. Yield alone cannot separate the two, and therefore can be a misleading proxy for productivity in the sense of technical change (Villoria, Byerlee and Stevenson 2014). Lower freight costs also expand the set of locations in which cultivation is profitable. In frontier regions, improved access can induce an extensive-margin response, drawing new and lower-quality land into production rather than raising output on existent farmland (Frey et al. 2018; Schielein et al. 2021; Weinhold and Reis 2008; Vera-Diaz, Kaufmann and Nepstad 2009). The aggregate effect depends on which margin dominates. If improved transport network mainly draws marginal land into cultivation, output rises while output per hectare stays negligible or falls as lower-quality land dilutes the municipal average.

This paper estimates the effect of domestic market access on production value, harvested area, and land productivity of temporary crops across Brazilian municipalities from 2015 to 2023. Using the structural gravity framework of Donaldson and Hornbeck (2016) and Eaton and Kortum (2002), we construct municipality-period market access measures from Dijkstra least-cost bilateral routing on IBGE's multimodal transport network across five survey periods, combining roads, rail, waterways, and transshipment margins into a common cost object. The identifying variation comes from within-municipality changes in market access generated by observed changes in Brazil's network between period, after controlling time-invariant spatial endowments, state-by-period shocks, and smooth spatial trends interacted with time. We do not claim a causal effect, as infrastructure investment is partly directed by anticipated agricultural growth, and the fixed-effects design cannot absorb municipality-specific differential trends in agricultural potential that may be correlated with paving and concession decisions. We therefore treat each effect as a within-municipality conditional association. A 10% improvement in domestic market access raises production value by 0.6 to 0.8% and expands the area under temporary crops by about 0.5%. Our measure of land productivity, value per harvested hectare, shows no robust long-run change. The extensive margin dominates, and improved connectivity in Brazil expands the area under cultivation rather than raising output per hectare.

This aggregate result masks regional heterogeneity. North municipalities show a decline in value per hectare (-0.061 to -0.150), alongside positive area expansion (0.065). This is consistent with cultivation moving onto marginal land. The Cerrado, which accounts for the bulk of Brazilian soy and maize production, drives the aggregate results, with significant effect on value and area. In the semi-arid Caatinga, connectivity raises production value without the accompanying area expansion, with a first-difference value elasticity of 0.62, pointing to market integration rather than frontier advance as the operative mechanism.

The paper fits within a literature on how transport infrastructure reshapes economic activity through market access. Donaldson (2018) shows that Indian colonial railways raised real agricultural income by 16% and compressed interregional price gaps, with planned-but-never-built lines as a placebo; the mechanism is trade expansion, not productivity. Donaldson and Hornbeck (2016) derive market access as the empirical object that summarises railroad welfare effects in the nineteenth-century United States, and find that removing all railroads in 1890 would have reduced agricultural land values by 64%. That is the framework we adapt here. Storeygard (2016) links lower transport costs to higher urban income near Sub-Saharan African ports, and Jedwab and Storeygard (2022) documents that road-induced market access gains raised city populations over 1960 to 2010 with an elasticity of 0.08 to 0.13. These papers establish market access as a tractable summary of network effects for many welfare questions, but they leave less well understood how those gains decompose across value, land, and productivity in a contemporary developing-country agricultural setting.

Two papers, Souza-Rodrigues (2019) and Araujo, Assunção and Bragança (2025), are most closely related to our paper. Souza-Rodrigues (2019) develops a revealed-preference framework for Amazon deforestation and identifies deforestation demand from regional variation in transportation costs; it is foundational for the extensive margin but is cross-sectional and centered on forest loss rather than agricultural production. Araujo et al. (2025) measures market access for the Legal Amazon using Dijkstra shortest paths on roads, railways, rivers, and ports, and finds that a 1% gain in market access raises deforestation by 0.5%, with indirect network spillovers accounting for one-quarter of the total. This literature establishes that better access pushes the agricultural frontier outward; what it does not do is decompose the agricultural adjustment on the cultivated side into how much arrives as higher value, how much as more land, and how much as higher output per hectare.

Our paper makes two contributions. First, where the roads-and-deforestation literature measures the land-use externality of access, we measure the agricultural response that generates it, decomposing it into production value, harvested area, and value per hectare for the whole of Brazil rather than the Amazon alone. This decomposition is what tells transport planners whether a corridor delivers its returns by lifting output per hectare on existing farmland — the food-security and land-sparing case — or by drawing new and often marginal land into cultivation, the case that carries the environmental cost emphasised by Chomitz and Gray (1996) and Gollin and Wolfersberger (2025). Our central finding is that, on average, the response is expansion rather than intensification. Second, we show that this margin is not uniform across space: the frontier expansion visible in the North and Amazônia coexists with a market-integration response in the Cerrado and Caatinga, where better access raises value with little or no area dilution. The same trade-cost reduction therefore implies frontier expansion in one biome and market deepening in another, which matters directly for where and how transport investment is evaluated.

3.2 Theoretical framework

3.2.1 Trade costs and market access

The theoretical framework follows the Ricardian trade model of Eaton and Kortum (2002) and the market-access interpretation of transport networks in Donaldson and Hornbeck (2016). Suppose each municipality i can supply agricultural varieties to every destination municipality j. Under perfect competition, the delivered price from origin i to destination j depends on origin costs, bilateral trade costs, and productivity. In this setting, the share of destination j's expenditure allocated to origin i is

$$\lambda_{ij} = \frac{T_i(\tau_{ij}c_i)^{-\theta}}{\sum_k T_k(\tau_{kj}c_k)^{-\theta}}, \qquad (1)$$

where T_i indexes municipality i's productivity distribution, c_i is its unit cost, $\tau_{ij} \geq 1$ is the iceberg trade cost from i to j, and θ is the trade elasticity. Lower transport costs reduce τ_{ij}, thereby increasing the expenditure share captured by origins that become more accessible to destination markets.

If destination j spends E_j on agricultural goods, then sales from municipality i to municipality j are

$$X_{ij} = \lambda_{ij} E_j. \qquad (2)$$

Total agricultural sales from municipality i are therefore

$$X_i = \sum_j X_{ij}. \qquad (3)$$

Following Donaldson and Hornbeck (2016), these network-wide demand opportunities can be summarised by domestic market access. For municipality i in period t, let

$$\mathrm{MA}_{it} = \sum_j E_{jt} \frac{\tau_{ijt}^{-\theta}}{\Phi_{jt}}, \qquad (4)$$

where

$$\Phi_{jt} = \sum_k T_k (\tau_{kjt} c_k)^{-\theta}, \qquad (5)$$

is the destination-specific price-index term. Municipal sales can then be written as

$$X_{it} = T_i \, c_i^{-\theta} \, \mathrm{MA}_{it}. \qquad (6)$$

This expression links transport networks to agricultural outcomes. Improvements in roads, railways, and waterways reduce bilateral trade costs, increase market access, and thereby raise the demand faced by a municipality's agricultural sector.

3.2.2 Predictions for agricultural outcomes

The trade framework delivers clear predictions for agricultural adjustment, but not a single unambiguous prediction for land productivity. The reason is that an increase in market access raises agricultural demand and profitability through the same channel that increases municipal sales, but the resulting response may occur through either intensification on existing land or expansion onto new land.

Let cultivated land in municipality i consist of plots $h \in H_i$, with plot-specific agricultural productivity a_{ih}. Suppose the operating profit from cultivating plot h in period t is

$$\Pi_{iht} = a_{ih} \, T_i \, c_i^{-\theta} \, \mathrm{MA}_{it} - \kappa_{ih}, \qquad (7)$$

where κ_{ih} is the fixed cost of bringing plot h into production. A plot is cultivated if profits are non-negative, $\Pi_{iht} \geq 0$. Harvested area is therefore

$$A_{it} = \int_{H_i} \mathbf{1}\{\Pi_{iht} \geq 0\}\, dh. \qquad (8)$$

Because Π_{iht} is increasing in MA_{it}, better connectivity expands the set of plots for which cultivation is profitable. The model therefore implies

$$\frac{\partial A_{it}}{\partial \mathrm{MA}_{it}} \geq 0. \qquad (9)$$

This is the extensive-margin prediction: improvements in market access should weakly increase harvested area.

Aggregate agricultural production value can be written as

$$Y_{it} = \int_{H_i} a_{ih}\, T_i\, c_i^{-\theta}\, \mathrm{MA}_{it}\, \mathbf{1}\{\Pi_{iht} \geq 0\}\, dh. \qquad (10)$$

Since higher market access raises returns on already-cultivated plots and also expands the cultivated set, the framework predicts

$$\frac{\partial V_{it}}{\partial \mathrm{MA}_{it}} > 0. \qquad (11)$$

Improvements in market access should therefore increase total agricultural production value.

Land productivity is defined as value per harvested hectare:

$$P_{it} = \frac{V_{it}}{A_{it}}. \qquad (12)$$

Unlike value and area, the sign of the effect of market access on value per hectare is theoretically ambiguous. If higher market access mainly raises returns on land already under cultivation, then the intensive margin dominates and value per hectare rises. If instead higher market access mainly induces cultivation of new and lower-quality plots, then the extensive margin dominates and average value per hectare may remain unchanged or decline (Weinhold and Reis 2008; Vera-Diaz et al. 2009; Souza-Rodrigues 2019; Schielein et al. 2021; Frey et al. 2018).

Which margin dominates depends on how elastic a supply response the municipality has, and this is what makes the ambiguity sharpest in frontier settings. Two features distinguish the frontier. First, frontier municipalities produce highly tradable commodities, for example soybeans and maize bound for exports, and an individual municipality is small relative to those markets, so it faces a near-perfectly-elastic demand, which means the output are sold at given prices, and any gain in profitability translates into the incentive to expand rather than into a falling local price (Hertel, Ramankutty and Baldos 2014). Second, the frontier holds large stocks of convertible land, so the area supply responds strongly to that incentive. Where both conditions hold, a profitability gain is taken out on the extensive margin, and because the marginal land can be lower quality, average value per hectare can fall even as total value rises, which is the mechanism behind documented Jevons-type expansion in the Cerrado and Amazon (Byerlee, Stevenson and Villoria 2014; Bustos, Caprettini and Ponticelli 2016). In consolidated landscapes the opposite holds. A little convertible land remains and producers are closer to land-constrained, so a comparable gain in access is absorbed on the intensive margin with no productivity dilution. The empirical sections show exactly this contrast between the North and Amazônia on one side and the Cerrado, Caatinga, and South on the other.

The framework therefore yields three empirical predictions. First, a rise in domestic market access should increase total agricultural production value. Second, a rise in market access should weakly increase harvested area by expanding the set of profitable plots. Third, the effect of market access on value per hectare is ambiguous: it should be positive if the intensive margin dominates, close to zero if intensive and extensive responses offset, and negative if expansion onto marginal land dominates. We emphasize that this third prediction concerns value per harvested hectare, not total factor productivity; the data cannot adjudicate whether any intensive-margin gain reflects heavier input use or technical change.

3.3 Data

3.3.1 Agricultural outcomes

Agricultural outcomes come from IBGE's Municipal Agricultural Production (PAM) (Instituto Brasileiro de Geografia e Estatística 2024b). For each municipality-year, total production value and total harvested area are constructed by aggregating across temporary crops. Land productivity is defined as value per harvested hectare:

$$\text{Productivity}_{it} = \frac{\sum_c \text{Value}_{cit}}{\sum_c \text{Area}_{cit}}. \qquad (13)$$

3.3.2 Population

Population is drawn from the 2014 IBGE municipal estimates (Instituto Brasileiro de Geografia e Estatística 2024a). This data is used to construct the market access measure as a proxy for destination demand.

3.3.3 Multimodal network data

The transport networks are built from the IBGE BC250 cartographic database (Instituto Brasileiro de Geografia e Estatística 2022), which provides shape files for roads, railways, and navigable waterways. Five survey periods are available: 2015, 2017, 2019, 2021, and 2023. Between 2015 and 2023 the paved road network expanded by about 18%, total road coverage grew by 28%, and the operational rail network grew by 6%. Figure 3.1 compares the network in 2015 and 2023.

3.3.4 Descriptive statistics

Table 1 reports descriptive statistics for the analysis panel. Three features of temporary-crop outcomes stand out. First, the outcomes have right-skewed distributions in levels. Mean production value is R$78,374 thousand and mean harvested area is 14,352 ha, but the medians are R$9,340 thousand and 2,340 ha respectively, with the 75th percentile already below the mean: a hand-

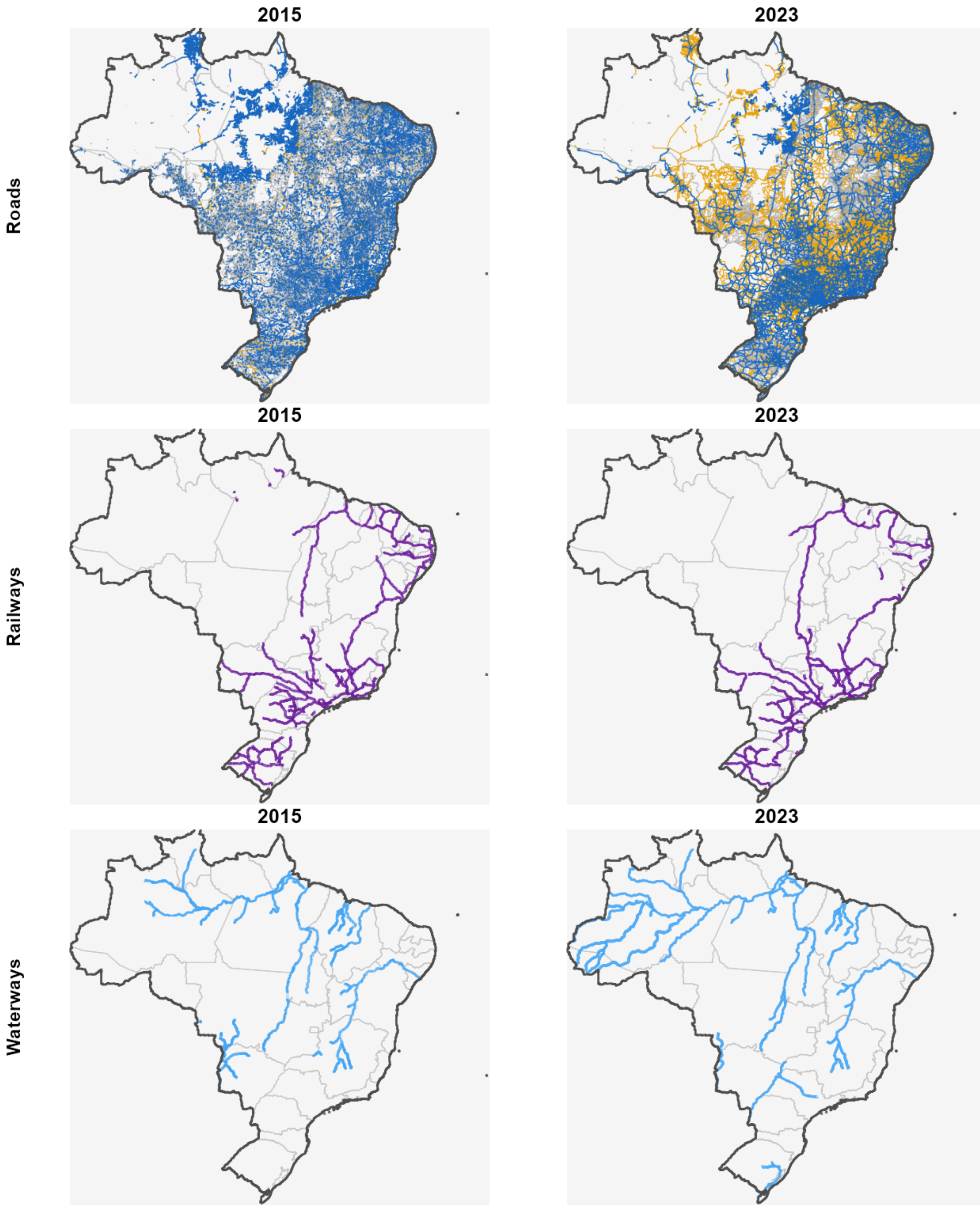

Figure 3.1: Multimodal transportation network: roads, railways, and waterways for 2015 (left) and 2023 (right). Each row shows one mode. Road panels distinguish three surface classes, which are paved (blue), gravel or primary surfacing (orange), and dirt or natural bed (grey). Segments with an unrecorded surface are omitted. Waterway panels distinguish navigable reaches by maximum draught.

ful of large agricultural municipalities, mostly in the Center-West, dominate national totals. The log transformations compress this skew. The log of production value has standard deviation 2.32 against a mean of 9.11, and the log of harvested area has standard deviation 2.09 against a mean of 7.73. Second, productivity (value per harvested hectare) has a tighter distribution, with mean R$6.29 thousand/ha and an interquartile range of R$2.57–7.47 thousand/ha. The log productivity standard deviation of 1.00 is roughly half that of value and area, which reflects that variation across municipalities is dominated by extensive-margin differences in area rather than intensive-margin differences in yield per hectare. Third, the panel is unbalanced: production value and harvested area are non-missing for 26,976 municipality-years (out of a possible 5,527 × 5 = 27,635), so 660 observations are missing from IBGE PAM. These missing observations are concentrated in municipalities that did not cultivate temporary crops in the relevant year.

Table 3.1: Descriptive statistics for the analysis panel (municipality-period observations, 2015–2023).

Variable	N	Mean	SD	Min	P25	Median	P75	Max
Production value (R$ 1,000)	26,976	78,374	297,222	1	1,701	9,340	53,653	9,967,562
Harvested area (ha)	26,979	14,352	47,589	1	555	2,340	10,284	1,218,591
Productivity (R$ 1,000 / ha)	26,976	6.29	9.87	0.00	2.57	4.32	7.47	428.71
log Production value	26,976	9.11	2.32	0.00	7.44	9.14	10.89	16.11
log Harvested area	26,979	7.73	2.09	0.00	6.32	7.76	9.24	14.01
log Productivity	26,976	1.38	1.00	-5.90	0.94	1.46	2.01	6.06

Notes. The panel covers 5,527 Brazilian municipalities observed across five survey periods. The upper three rows present variables in levels: production value (R$1,000), harvested area (hectares), and productivity defined as total value divided by total harvested area (R$1,000 per hectare). The lower three rows present the natural-logarithm transformations of the same three variables that enter the regressions. Domestic market access MA_{it}^{D} is reported separately in the Market Access Measurement section and is not included here. The panel is unbalanced; columns report the sample size, mean, standard deviation, minimum, 25th, 50th, and 75th percentiles, and maximum for each variable.

3.4 Market access measurement

3.4.1 Least-cost multimodal routing

For each survey period, roads, railways, and waterways are combined into a multimodal graph. Municipality administrative centers are connected to the road network, and bilateral transport costs are computed as least-cost routes using Dijkstra's algorithm. The routing problem therefore allows flows to switch across modes when doing so lowers total shipment cost, while also accounting for transshipment penalties at transfer points.

Let cost_{ijt} denote the minimum shipment cost from municipality i to municipality j in period t, measured in reais per tonne. Total route cost is:

$$\text{cost}_{ijt} = \min_{\text{path}} \left[\sum_{e \in \text{path}} \beta_e \, d_e + \sum_{m \in \text{transfers}} c_m^{\text{trans}} \right], \qquad (14)$$

where β_e is the mode-specific freight rate on edge e, d_e is edge length, and c_m^{trans} is the transfer cost incurred when a shipment changes mode. Freight rates are taken from ESALQ-LOG and SIFRECA market information together with public planning benchmarks (ESALQ-LOG / SIFRECA 2024; Empresa de Planejamento e Logística (EPL) 2021). Using observed shipper costs rather than engineering costs follows the applied logic in Donaldson and Hornbeck (2016) and Araujo et al. (2025). The full schedule of mode-specific rates appears in Table 3.2.

Table 3.2: Mode-specific freight rates used in least-cost routing.

Mode	Rate (R$/TKU)	Notes
Highway, paved (reference)	0.425	EPL/PNL benchmark
Highway, gravel	0.691	Speed-adjusted: $0.425 \times 65/40$
Highway, dirt	0.921	Speed-adjusted: $0.425 \times 65/30$
Motorway, paved	0.346	Speed-adjusted: $0.425 \times 65/80$
Rail	0.066	Rumo / VLI bulk-grain average
Waterway, large vessel ($>$ 3 m draught)	0.100	Amazon, Madeira, Paraguay
Waterway, medium (1–3 m draught)	0.140	Tocantins, São Francisco
Waterway, shallow ($<$ 1 m draught)	0.168	Paraná, Tietê systems
Port/terminal transshipment	5.0 R$/tonne	Per modal transfer

Rail transport is 6.4 times cheaper per tonne-kilometre than a paved highway; large-vessel waterways are 4.3 times cheaper. The transshipment fee deters implausible all-river routing by capturing handling costs at Northern Arc terminals.

3.4.2 From route costs to market access

To map route costs into bilateral trade resistance, we convert the least-cost route cost into a road-equivalent effective distance. The road-equivalent distance is

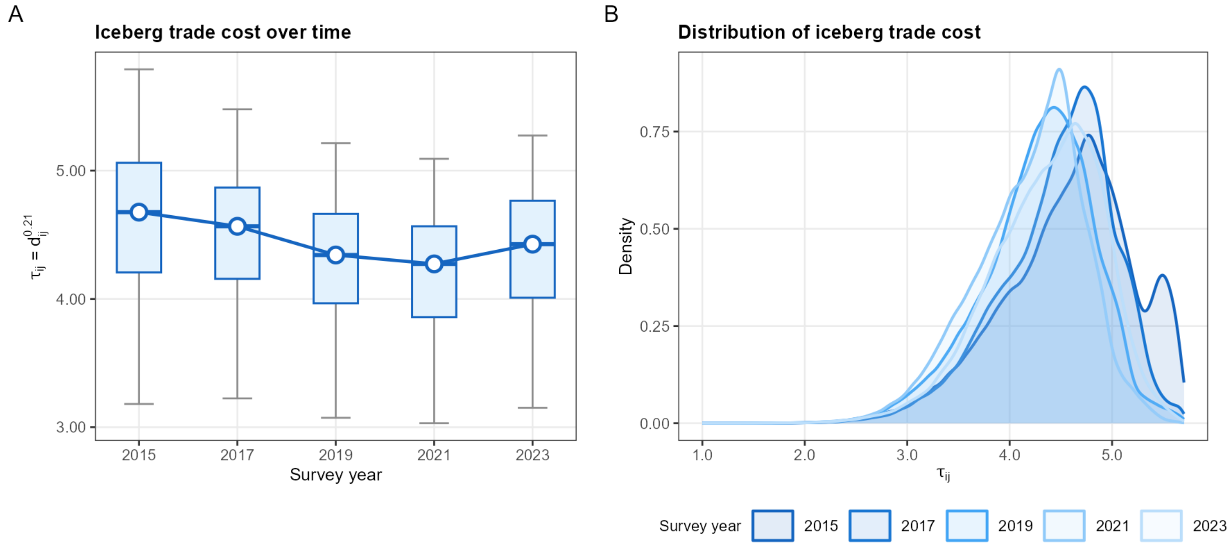

Figure 3.2: Distribution of bilateral iceberg trade costs $\tau_{ijt} = d_{ijt}^{0.21}$ across municipality pairs and IBGE transportation network survey periods (2015–2023), where $d_{ijt} = \text{cost}_{ijt}/\beta_{\text{road}}$ is the road-equivalent effective distance. Panel A shows the period-by-period boxplot; panel B shows the kernel density. Lower values indicate cheaper bilateral trade resistance; shifts in the distribution between periods reflect network improvements (and, in 2021, the drought-driven contraction of the waterway network).

$$d_{ijt} = \frac{\text{cost}_{ijt}}{\beta_{\text{road}}}, \qquad (15)$$

with $\beta_{\text{road}} = 0.425$ R$/TKU, the paved-highway reference freight rate. Dividing route cost by the road rate converts reais-per-tonne back into kilometres of equivalent paved-road travel, which makes the bilateral resistance easier to interpret. The iceberg trade cost then follows Limão and Venables (2001) (Table 2, column 3),

$$\tau_{ijt} = d_{ijt}^{\alpha_{LV}}, \qquad (16)$$

with $\alpha_{LV} = 0.21$, i.e. $\ln \tau = 0.21 \ln d$. Combining this with the trade elasticity $\theta = 8.22$ from Donaldson and Hornbeck (2016) yields a market-access decay parameter of $\theta\alpha_{LV} = 1.726$. Figure 3.2 shows the empirical distribution of τ_{ijt} across municipality pairs and survey periods.

Panel A reports the year-by-year distribution of τ_{ijt}. The median falls from 4.68 in 2015 to 4.27

in 2021, then rises to 4.43 in 2023 as the waterway network partially recovers from the drought. The interquartile range narrows from 0.85 in 2015 to 0.69 in 2019 and 0.71 in 2021, indicating that bilateral trade resistance is both lower and more homogeneous across municipality pairs over the period. Panel B shows the corresponding kernel densities. The year-on-year shift is a leftward translation of the entire distribution, not a movement confined to the upper tail.

Domestic market access for municipality i in period t is then constructed as

$$\mathrm{MA}_{it}^{D} = \sum_{j \neq i} d_{ijt}^{-1.726} \cdot \mathrm{Pop}_{j,2014} + \mathrm{Pop}_{i,2014}, \qquad (17)$$

where d_{ijt} is the road-equivalent effective distance defined in equation (15), and the own-population term is a normalisation for the internal market with $d_{ii} \equiv 1$. Because the own term is time-invariant, the identifying variation in market access comes from changes in bilateral route costs to other municipalities.

This market-access variable is a theory-guided summary of network connectivity rather than a directly observed economic variable. In our study, MA_{it}^{D} in levels has a median of 42.1 million, a mean of 43.9 million, and a maximum of 100.6 million. Log market access has a mean of 17.45 and standard deviation of 0.66 across the pooled panel. The cross-sectional dispersion within a given survey period (standard deviation 0.47–0.89 by year) is the dominant source of variation in the data, but the within-municipality variation that the regressions use comes from changes between survey periods. The mean $\log \mathrm{MA}^{D}$ rises from 17.09 in 2015 to a peak of 17.76 in 2021, then dips to 17.46 in 2023 as the waterway-driven 2021 gain partially reverses with the post-drought network. The mean log change from 2015 to 2023 differs across regions: South (+1.10), North (+0.66), Center-West (+0.58), Southeast (+0.27), and Northeast (–0.02). The South gains the most in proportional terms because much of its incremental connectivity comes from densification of an already-dense road and rail network and the Northeast moves little because its baseline connectivity is high relative to the scale of incremental investment over this period.

Figure 3.3 compares domestic market access in the first and last survey periods, 2015 and 2023, and

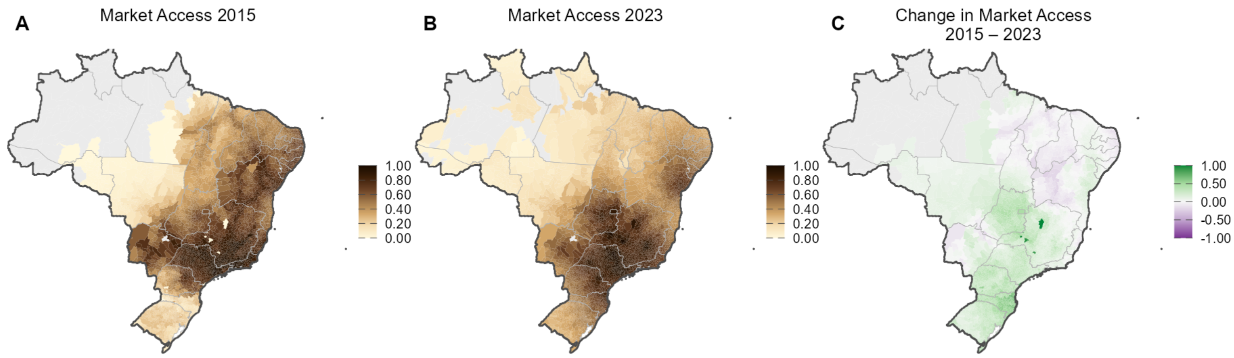

Figure 3.3: Domestic market access (MA^D_{it}) for Brazilian municipalities in the first and last survey periods. Panel A shows 2015 and panel B shows 2023; in each, every municipality's MA^D_{it} is divided by the largest value across municipalities in that same year, so the scale runs from 0 to 1 and 1.0 marks the best-connected municipality of the year. The two level panels are each normalized to their own year and so show within-year relative position rather than directly comparable absolute levels. Panel C maps the raw change $\text{MA}^D_{i,2023} - \text{MA}^D_{i,2015}$ divided by the largest absolute change across municipalities, so it runs from -1 to 1; green denotes gains in market access and purple denotes losses. Isolated municipalities are excluded and shown in grey.

maps the change between them. In both years, market access is highest in the densely connected Southeast and South — the single best-connected municipality is in Rio de Janeiro state in 2015 and in São Paulo state in 2023 — and lowest in remote Amazon municipalities. Connectivity rose broadly over the period: 78.6% of municipalities gained market access and only 21.4% lost it, and the highest municipal value rose by 36% between the two years. Because each level panel is normalized by its own year's maximum, two municipalities with the same shade in panels A and B are not equally connected in absolute terms; the 2023 panel is scaled against a benchmark 36% larger, so it understates the true gain. The change panel, built from the raw difference $\text{MA}^D_{i,2023} - \text{MA}^D_{i,2015}$, is what isolates where connectivity actually improved. Its scale is set by a single Minas Gerais municipality that moved from near-isolation to full connection over the period, which compresses the remaining gains toward the lighter end of the green range.

3.5 Empirical strategy

3.5.1 Baseline panel specification

The main specification relates agricultural outcomes to within-municipality changes in domestic market access:

$$\ln Y_{it} = \beta \ln \mathrm{MA}_{it}^{D} + \sum_{k=1}^{9} \varphi_k \left[g_k(x_i, y_i) \times \mathrm{period}_t \right] + \delta_i + \gamma_{st} + \varepsilon_{it}, \qquad (18)$$

where Y_{it} is production value, harvested area, or land productivity; δ_i are municipality fixed effects; γ_{st} are state-by-period fixed effects; and $g_k(x_i, y_i)$ denotes a cubic polynomial in municipal coordinates interacted with period dummies. Municipality fixed effects absorb time-invariant local characteristics such as soil quality, long-run climate, and historically inherited market access. State-by-period fixed effects absorb common shocks at the state level, including policy shifts and commodity-price conditions. The interacted geographic polynomial removes smooth spatial trends that may be correlated with infrastructure change, following the empirical strategy in Donaldson and Hornbeck (2016).

3.5.2 First differences

The second specification uses consecutive first differences across adjacent survey periods:

$$\Delta \ln Y_{it} = \beta\, \Delta \ln \mathrm{MA}_{it}^{D} + \sum_{k=1}^{9} \varphi_k \left[g_k(x_i, y_i) \times \mathrm{period}_t \right] + \gamma_{st} + \Delta\varepsilon_{it}, \qquad (19)$$

This transformation removes municipality-specific time-invariant components and places more weight on shorter-run changes in connectivity. It checks whether the panel results are driven by slow-moving level differences rather than by changes in the network.

3.5.3 Long difference

The third specification reduces the panel to the total change between 2015 and 2023:

$$\Delta_{15,23} \ln Y_i = \beta\, \Delta_{15,23} \ln \mathrm{MA}_i^D + \sum_{k=1}^{9} \varphi_k\, g_k(x_i, y_i) + \delta_s + \varepsilon_i. \qquad (20)$$

This long-difference design emphasises cumulative network change over the full study period and reduces the influence of short-term noise in outcomes or connectivity.

3.5.4 Identification

A threat to causal estimation is that infrastructure improvements are directed toward places with stronger expected agricultural growth. The empirical design narrows but does not eliminate that concern. Municipality fixed effects absorb time-invariant determinants of productivity and land-use potential; state-by-period fixed effects absorb common shocks at the state level, including policy shifts and commodity-price conditions; the cubic geographic polynomial interacted with period absorbs smooth spatial trends that may be correlated with infrastructure change. What these controls cannot absorb is a municipality-specific differential trend in agricultural potential that is also correlated with prioritisation of paving or concession decisions — for example, the BR-163 paving north of Sinop was prioritised in part because Mato Grosso soy producers were anticipating expansion. The first-difference and long-difference specifications check that the panel pattern is not driven solely by slow-moving level differences, but they do not by themselves provide an exclusion restriction. The paper therefore does not claim a causal estimate, and we treat β throughout as a within-municipality conditional association – a partial correlation that nets out the controls above – rather than an exogenous causal elasticity.

One route to an exclusion restriction, which we leave to future work, exploits the structure of our own measure. Because MA_{it}^D is built from Dijkstra least-cost routes over the observed network, it already embeds endogenous network choices. A complementary design would compute market access over an engineering-ideal or planned network — least-cost routing on links that were planned but not necessarily built — and use it as an instrument for realised connectivity, in the spirit of the planned-but-unbuilt railroad lines used as a placebo by Donaldson (2018).

Two further scope conditions follow from the data. First, the regression sample retains municipality-years with positive harvested area (see Section 3.1), so the estimated area elasticity describes the intensive-area response among municipalities already cultivating temporary crops; entries from zero harvested area to positive cultivation are not in the sample. Second, the productivity outcome is value per harvested hectare, not total factor productivity. Production value combines physical yield with farm-gate price, and connectivity improvements can mechanically raise the farm-gate component without any change in yield. A coefficient on log value per hectare therefore reflects the sum of a price pass-through and a yield response; and the yield response itself blends input intensification with technical change, as discussed in Section 2. We read this coefficient as evidence on the intensive margin broadly, and we are deliberately cautious in attributing it to technical change; we return to this distinction in the interpretation of regional heterogeneity in Section 6.

Estimated separately for production value, harvested area, and value per hectare reveals whether transport improvements are associated mainly with the intensive margin, the extensive margin, or both. That decomposition is the central empirical contribution of the paper.

3.6 Results

3.6.1 Production value and cropland area expand but long-run productivity does not

Table 3.3 reports the effects of transport improvements from equations (18)–(20) for each of the three outcomes. Across all three specifications, the same pattern emerges: better market access raises production value and harvested area.

Table 3.3: Effect of domestic market access on agricultural outcomes.

	Prod.	Value	Area
Panel A: Long Panel OLS			
log MA^{D}	0.018	0.065**	0.047**
	(0.015)	(0.028)	(0.022)
Observations	26,967		
Panel B: First Difference OLS			
log MA^{D}	0.034**	0.080**	0.046*
	(0.014)	(0.033)	(0.025)
Observations	21,451		
Panel C: Long Difference OLS			
log MA^{D}	0.010	0.060**	0.050*
	(0.021)	(0.027)	(0.026)
Observations	5,289		

Notes. The dependent variables are log productivity, log production value, and log harvested area. The regressor in Panel A is $\log \mathrm{MA}_{it}^{D}$ as defined in equation (17); in Panel B it is the first difference of $\log \mathrm{MA}_{it}^{D}$ between consecutive survey periods; in Panel C it is the long difference between 2015 and 2023. Panel A reports the within-municipality long-panel specification (equation (18)) with municipality fixed effects, state-by-period fixed effects, and a cubic polynomial in municipal coordinates interacted with period. Panel B reports the consecutive first-difference specification (equation (19)) on stacked 2-year gaps with the same fixed-effect and polynomial controls. Panel C reports the long-difference specification (equation (20)) on the 2015-to-2023 cross-section with state fixed effects and a cubic geographic polynomial. The standard errors are in parentheses, which are clustered at the state level. *** $p < 0.01$; ** $p < 0.05$; * $p < 0.10$.

First, production value rises significantly across all three specifications. The elasticity of production value with respect to market access ranges between 0.060 and 0.080. These magnitudes imply that a 10% gain in domestic market access raises production value by 0.6 to 0.8%. Second, cropland area increases alongside production value. The elasticity of land use with respect to domestic market access is 0.047 to 0.050. For the median municipality, which harvests 4,800 ha of temporary crops, a 10% market access gain implies an additional 230 to 240 ha under cultivation. Third, land productivity shows different responses across time horizons. The long-panel and long-difference productivity elasticities in Panels A and C of Table 3 are 0.018 and 0.010 respectively, and neither is statistically significant. The consecutive first-difference productivity elasticity in Panel B is 0.034 and is significant at the 5% level. One interpretation is that reduced trade cost can generate short-run gains in value per hectare through lower transport costs, cheaper input access, or better market integration, as in evidence from developing country agriculture (Aggarwal et al. 2024; Jacoby and Minten 2009; Shamdasani 2021).

The three outcomes point to a clear mechanism. Better market access increases agricultural production value, and it does so in part by increasing harvested area. But because value per hectare shows no robust long-run response, the aggregate output effect is not driven by sustained gains in output per hectare. Instead, the estimates point to an extensive-margin adjustment in which lower trade costs draw additional land into cultivation. That interpretation is consistent with the frontier evidence in Weinhold and Reis (2008) and Vera-Diaz et al. (2009). The link from improved access to deforestation in the Amazon is documented in Souza-Rodrigues (2019) and Araujo et al. (2025).

This interpretation is consistent with the literature. Araujo et al. (2025) shows that improved multimodal market access in the Amazon raises deforestation, which is one mechanism through which previously uncultivated or lower-quality land enters production. Donaldson (2018) likewise finds that railroads in colonial India raised real income through market integration and trade expansion rather than through a farm-level productivity channel.

3.6.2 The North shows the extensive-margin response

Figure 3.4 shows heterogeneity of production across Brazilian regions, with the clearest extensive-margin pattern concentrated in the North.

The North region shows that better connectivity expands cultivation onto marginal land. The elasticity of land productivity with respect to market access is –0.061 in the long panel and –0.150 in the long difference, both statistically significant at the 1% level. However, harvested area rises in the long panel, with an elasticity of 0.065 that is also significant at the 1% level. This combination of falling productivity and expanding area points towards an extensive-margin response. Improved market access draws new cultivation into Amazon municipalities, and the additional land brought into production has below-average productivity, which lowers the municipal average. This finding is consistent with Weinhold and Reis (2008) and Vera-Diaz et al. (2009), which emphasise how lower transport costs can expand cultivation into less developed frontier areas. It is consistent with Araujo et al. (2025), which shows that market access in the Legal Amazon increases deforestation.

The Southeast warrants caution in interpretation. In the long panel, market access is associated with positive effects on both production value (0.080) and harvested area (0.049), each statistically significant at the 1% level. But unlike in the North, these gains are not accompanied by a negative productivity effect. That makes the Southeast result look less like frontier expansion and more like market integration or selective expansion within an established agricultural region. This interpretation differs from the Amazon frontier mechanism emphasized by Weinhold and Reis (2008), Vera-Diaz et al. (2009), and Araujo et al. (2025). If anything, it is consistent with the view that lower trade costs improve commercialization and output value without inducing land-quality dilution (Aggarwal et al. 2024; Jacoby and Minten 2009; Shamdasani 2021).

The Central-West region, which accounts for the largest share of Brazilian soybean and maize production, shows a different pattern. Production value responds positively to market access across specifications, while the productivity response is weaker and limited to the short run. In the first-difference specification, the productivity elasticity is 0.024 and marginally significant at the 10% level. That short-run pattern is consistent with evidence that lower transport costs improve farm performance through cheaper inputs and better market integration (Aggarwal et al. 2024; Jacoby and Minten 2009; Shamdasani 2021). The long-difference area estimate is large, at 0.290, reflecting cross-sectional heterogeneity in agricultural development across Center-West municipalities. The Central-West estimates suggest connectivity raises agricultural activity in the country's main grain-producing region, but the balance between intensification and expansion is less sharply identified than in the North.

The South region shows coefficients close to zero throughout, consistent with diminishing returns to additional connectivity in a dense and mature transport network. The Northeast presents larger point estimates but limited precision. The long-panel production-value elasticity is 0.231 and marginally significant at the 10% level, suggesting that some municipalities in the semi-arid interior are sensitive to connectivity improvements, even if the average regional estimate is noisy. The Southeast shows a stable positive pattern in the long panel, with significant effects on both production value (0.080) and harvested area (0.049), each at the 1% level. These estimates indicate that better market access continues to support agricultural expansion in parts of the Southeast, though without the productivity decline observed in the North.

The regional results support the main interpretation of the paper. Lower transport costs do not generate a uniform agricultural response across Brazil. In frontier regions, especially the North, improved connectivity operates through area expansion onto lower-productivity land. In consolidated agricultural regions, the same connectivity gains are associated with increases in output value and, in some cases, area expansion, but not with the same frontier mechanism. The aggregate estimates thus mask spatial heterogeneity in how transport infrastructure reshapes agricultural adjustment.

Notes. Each box reports the estimate of the elasticity of the outcomes with respect to market access for regions. Regions are represented in rows. The columns are the three specifications: long panel OLS (equation (18)), with municipality and state-by-period fixed effects and a cubic polynomial in coordinates interacted with period; consecutive first-difference OLS (equation (19)), with state-by-period fixed effects and the cubic geographic polynomial interacted with period; and 2015-to-2023

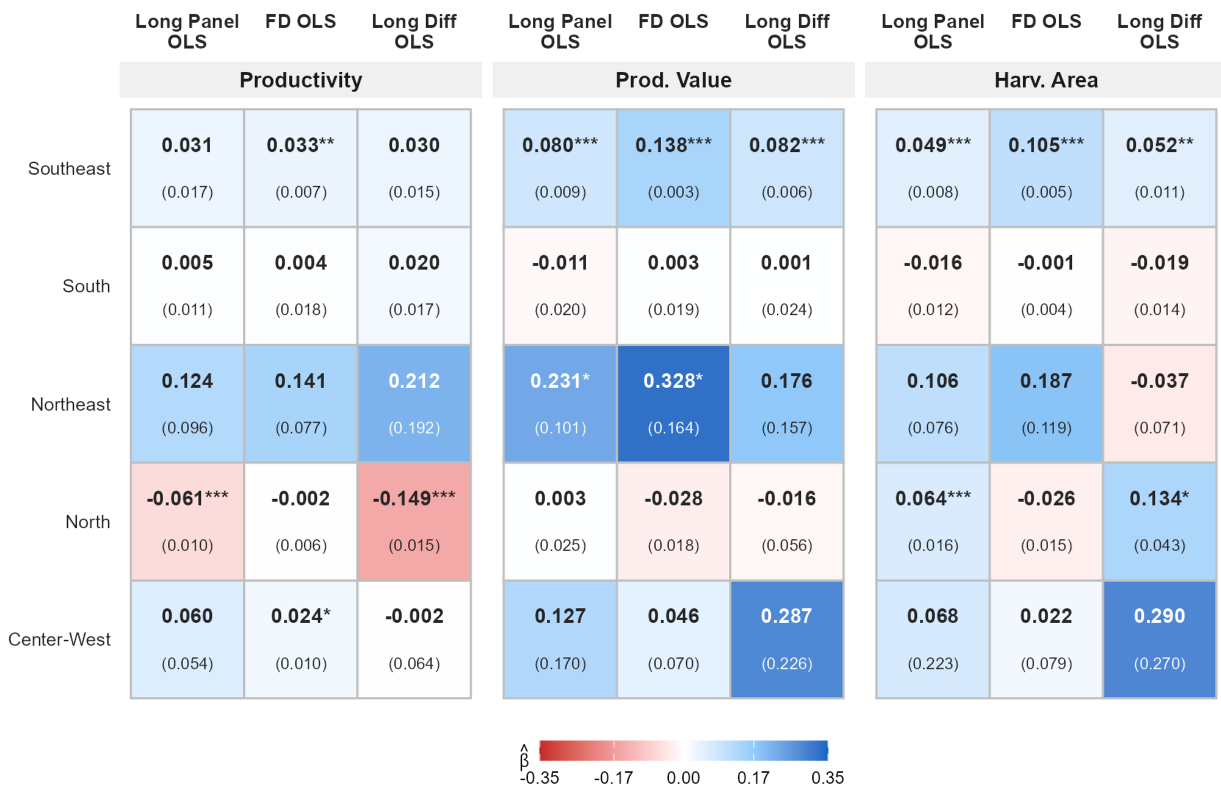

Figure 3.4: Effect of domestic market access on agricultural outcomes by region.

long-difference OLS (equation (20)), a cross-section with a cubic geographic polynomial. The blue color represents the positive elasticity and red represents the negative. Standard errors are in parentheses, and clustered at the state level. *** $p<0.01$, ** $p<0.05$, * $p<0.10$.

3.6.3 Biome estimates distinguish the Amazon frontier from the Cerrado

Figure 3.5 illustrates the biome-level estimates, which contrast Amazônia with the Cerrado.

The Amazônia biome shows the largest negative long-difference productivity coefficient (–0.134), statistically significant and larger in magnitude than the full-sample estimate. One interpretation: improved transportation induced agricultural expansion in the forest frontier, and the newly cultivated land is marginal enough to reduce average productivity (Weinhold and Reis 2008; Vera-Diaz et al. 2009). The link from improved access to frontier expansion and deforestation in the Amazon is consistent with Souza-Rodrigues (2019) and Araujo et al. (2025). By contrast, production-value effects in Amazônia are weak or negative, indicating that the frontier mechanism is not one of efficiency gains.

The Cerrado shows a stable positive response across outcomes. Production value is positive and statistically significant in all three specifications, with elasticities of 0.058 in the long panel, 0.077 in first differences, and 0.057 in the long difference. Harvested area is likewise positive and significant, while productivity is small but weakly positive. This pattern is consistent with improved transportation supporting continued agricultural expansion in Brazil's core grain-producing biome without the productivity penalty seen in the Amazon frontier.

The Caatinga and Mata Atlântica require caution. In the Caatinga, production value responds strongly in the first-difference specification, but area and productivity estimates are less stable across estimators. This suggests that transport improvement in the semi-arid Northeast supports market integration and short-run value gains rather than a land-expansion margin, a pattern closer to the market-integration channel emphasized in Aggarwal et al. (2024), Jacoby and Minten (2009), and Shamdasani (2021) than to a frontier-expansion story. The Mata Atlântica, like the South region, shows coefficients close to zero throughout. In dense and historically integrated transport

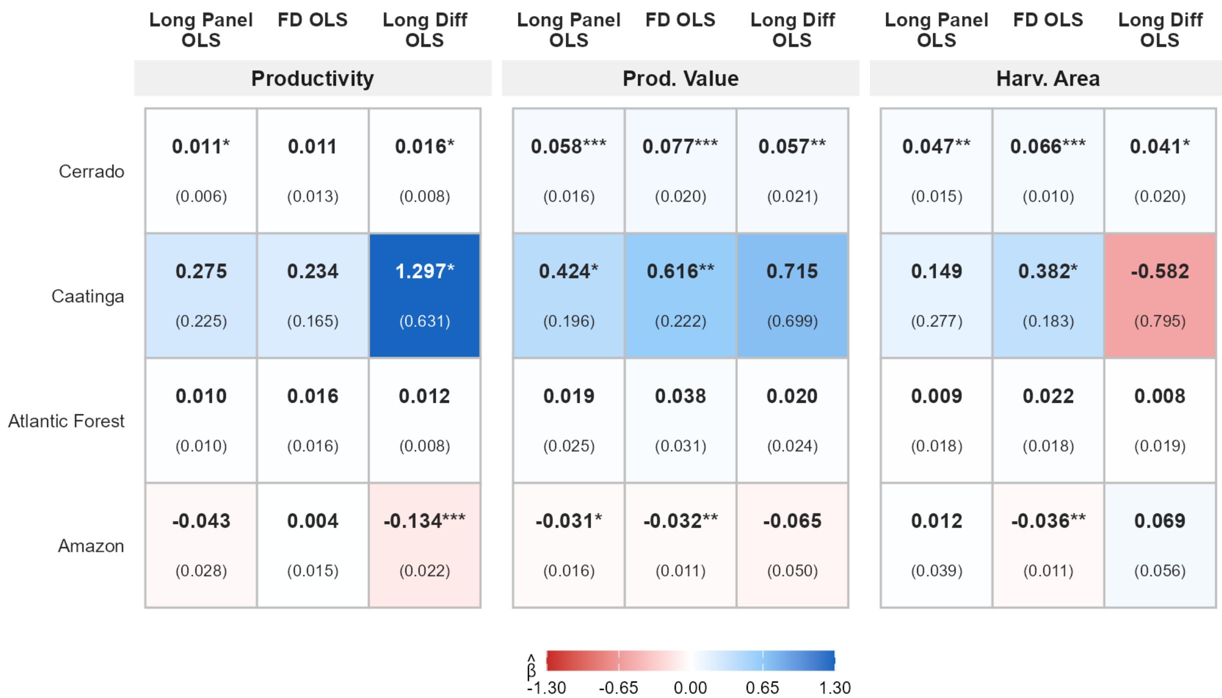

Figure 3.5: Effect of domestic market access on agricultural outcomes by biome.

space, further reductions in domestic trade costs yield limited agricultural adjustment.

The biome estimates complement the regional results by providing an ecological interpretation of the main mechanism. The effect of domestic market access depends not only on the size of the transport shock but also on the type of land into which agriculture expands. In frontier biomes, especially Amazônia, better connectivity is associated with falling average productivity, consistent with cultivation moving onto lower-quality land. In the Cerrado, by contrast, better connectivity raises value and area with little evidence of a comparable productivity decline. The aggregate Brazilian response is therefore an average of distinct regional and biome-specific adjustment processes.

Notes. Each box reports the estimate of the elasticity of the outcomes with respect to market access for each biome. Regions are represented in rows. The columns are the three specifications: long panel OLS (equation (18)), with municipality and state-by-period fixed effects and a cubic polynomial in coordinates interacted with period; consecutive first-difference OLS (equation (19)), with state-by-period fixed effects and the cubic geographic polynomial interacted with period; and 2015-

to-2023 long-difference OLS (equation (20)), a cross-section with a cubic geographic polynomial. The blue color represents the positive elasticity and red represents the negative. Standard errors are in parentheses, and clustered at the state level. *** p<0.01, ** p<0.05, * p<0.10.

3.7 Conclusion

This paper estimates how improvements in domestic market access affect agricultural outcomes across Brazilian municipalities. Using a market-access measure built from least-cost routes on roads, railways, and waterways, it shows that better transportation raises agricultural production value and expands the area under temporary crops, but does not generate a robust long-run gain in value per harvested hectare. Across the three main specifications, the elasticity of production value with respect to domestic market access lies between 0.060 and 0.080, while the elasticity of harvested area lies between 0.047 and 0.050. By contrast, the long-panel and long-difference estimates for value per hectare remain close to zero, even though the consecutive first-difference specification shows a short-run positive effect of 0.034. The broad pattern is expansion of the cultivated area rather than a higher-value intensive margin.

The result fits the market-access framework developed in Donaldson and Hornbeck (2016) and the Brazilian frontier evidence in Weinhold and Reis (2008), Vera-Diaz et al. (2009), Souza-Rodrigues (2019), and Araujo et al. (2025). Lower transport costs raise agricultural demand and profitability, but the resulting increase in output need not come from higher value per hectare. In Brazil, the dominant margin is cropland expansion. The regional and biome results reinforce that conclusion. In the North and in the Amazônia biome, better transportation is associated with falling value per hectare and expanding area, consistent with cultivation moving onto marginal land. In the Cerrado, by contrast, better transportation raises production value and harvested area consistently, with little evidence of a comparable productivity reduction (Branco et al. 2021; Wang et al. 2024). The aggregate Brazilian response is therefore an average of distinct spatial adjustment processes.

Our results suggest two policy implications. First, in frontier regions, transport improvements appear to operate in part through land expansion rather than sustained intensification. If the policy goal is higher long-run output per hectare, transport investment likely needs to be complemented by better access to inputs, storage, extension, and production technology, rather than treated as sufficient on its own (Aggarwal et al. 2024; Shamdasani 2021). Second, in Amazon frontier settings, the land margin made newly profitable by better transport access may overlap with forested areas, as emphasized in Vera-Diaz et al. (2009), Souza-Rodrigues (2019) and Araujo et al. (2025). For that reason, cost-benefit analysis of transport investment should account not only for direct freight-cost savings, but also for environmental externalities associated with induced land conversion (Wang et al. 2024).

Several limitations qualify these conclusions and suggest directions for future research. First, our productivity measure, value per harvested hectare, mixes physical yield with farm-gate prices, so better market access can raise the measure mechanically through higher prices, while even the yield component does not by itself distinguish greater input use from true technical change (Villoria et al. 2014). For that reason, we interpret the no long-run response as evidence of no intensive-margin gain in this measure, rather than as evidence against productivity growth more broadly. A cleaner test would examine margins such as double cropping, which increases output per hectare-year through management changes and has been linked to frontier expansion in Brazil (Jeddi and DePaula 2026), ideally using municipality-level data on input use, double-cropped area, and crop-specific yields to separate price effects, intensification, and technical change. Relatedly, because we do not observe input prices or land prices, we cannot tell how much of the estimated value response reflects price pass-through rather than real quantity adjustment, even though improved access likely affects both (Chomitz and Gray 1996). Second, our design is not causal. Infrastructure development may respond to expected agricultural growth, and fixed effects cannot fully absorb municipality-specific trends in agricultural potential that are correlated with paving and concession decisions, so we interpret the estimates as within-municipality conditional associations rather than exogenous effects. A more credible identification strategy would exploit planned or engineering-ideal transport networks to instrument for realized connectivity, following the logic of planned-but-unbuilt infrastructure used elsewhere (Donaldson 2018).

Bibliography

Abman, R., T. Garg, Y. Pan, and S. Singhal. 2020. "Agriculture and deforestation." Working Paper No. 3692682, SSRN.

Abman, R., and C. Lundberg. 2020. "Does Free Trade Increase Deforestation? The Effects of Regional Trade Agreements." *Journal of the Association of Environmental and Resource Economists* 7:35–72.

Adão, R., M. Kolesár, and E. Morales. 2019. "Shift-Share Designs: Theory and Inference." *The Quarterly Journal of Economics* 134:1949–2010.

Aggarwal, S., B. Giera, D. Jeong, J. Robinson, and A.C. Spearot. 2024. "Market Access, Trade Costs, and Technology Adoption: Evidence from Northern Tanzania." *Review of Economics and Statistics* 106:1511–1528.

AgUnity. 2023. "Unveiling EU's Green Ambitions: The Dual Impact of EU Deforestation Regulations on Global Trade and Developing Economies." Accessed: March 9, 2024.

Agência Nacional de Transportes Terrestres. 2022. "ANTT e Via Brasil assinam contrato de concessão da BR-163/230/MT/PA." Gov.br news release.

Ahrends, A., P.M. Hollingsworth, A.D. Ziegler, J.M. Fox, H. Chen, Y. Su, and J. Xu. 2015. "Current trends of rubber plantation expansion may threaten biodiversity and livelihoods." *Global Environmental Change* 34:48–58.

Aichele, R., and G. Felbermayr. 2015. "Kyoto and Carbon Leakage: An Empirical Analysis of the Carbon Content of Bilateral Trade." *Review of Economics and Statistics* 97:104–115.

Alroy, J. 2017. "Effects of habitat disturbance on tropical forest biodiversity." *Proceedings of the National Academy of Sciences* 114:6056–6061.

Anderson, J.E., M. Larch, and Y.V. Yotov. 2018a. "GEPPML: General equilibrium analysis with PPML." *The World Economy* 41:2750–2782.

—. 2018b. "GEPPML: General equilibrium analysis with PPML." *The World Economy* 41:2750–2782.

Anderson, J.E., and E. Van Wincoop. 2003. "Gravity with gravitas: A solution to the border puzzle." *American Economic Review* 93:170–192.

Angelsen, A. 2010. "Policies for reduced deforestation and their impact on agricultural production." *Proceedings of the National Academy of Sciences* 107:19639–19644.

Angelsen, A., and D. Kaimowitz. 1999. "Rethinking the causes of deforestation: lessons from economic models."

ao, E.A.O.S., R.B.L. Cavalcante, P.R. Zanin, R.G. Tedeschi, T.R. Ferreira, and P.R.M. Pontes. 2025. "The effects of teleconnections on water and carbon fluxes in the two South Americaâ€™s largest biomes." *Scientific Reports* 15:1395.

ao, J.A., C. Gandour, and R. Rocha. 2015. "Deforestation slowdown in the Brazilian Amazon: prices or policies?"

Araujo, R., J. Assunção, and A. Bragança. 2025. "Transportation Infrastructure and Deforestation in the Amazon." *Journal of Development Economics* 177:103559.

Arima, E., P. Barreto, F. Taheripour, and A. Aguiar. 2021. "Dynamic Amazonia: The EU–mercosur trade agreement and deforestation." *Land* 10:1243.

Arisco, N.J., C. Peterka, C. Diniz, B. Singer, and M.C. Castro. 2024. "Ecological change increases malaria risk in the Brazilian Amazon." *Proceedings of the National Academy of Sciences of the United States of America* 121.

Baier, S.L., and J.H. Bergstrand. 2007. "Do free trade agreements actually increase members' international trade?" *Journal of International Economics* 71:72–95.

Balboni, C., A. Berman, R. Burgess, and B.A. Olken. 2022. “The Economics of Tropical Deforestation.” Unpublished, Working Paper.

Bellora, C., and L. Fontagné. 2023. “EU in search of a carbon border adjustment mechanism.” *Energy Economics* 123.

Benhin, J.K. 2006. “Agriculture and deforestation in the tropics: a critical theoretical and empirical review.” *AMBIO: A Journal of the Human Environment* 35:9–16.

Berazneva, J., and T.S. Byker. 2017. “Does Forest Loss Increase Human Disease? Evidence from Nigeria.” *The American economic review* 107 5:516–21.

Berman, N., M. Couttenier, A. Leblois, and R. Soubeyran. 2023. “Crop prices and deforestation in the tropics.” *Journal of Environmental Economics and Management* 119:102819.

Böhringer, C., K.E. Rosendahl, and H.B. Storrøsten. 2017. “Robust policies to mitigate carbon leakage.” *Journal of Public Economics* 149:35–46.

Borusyak, K., P. Hull, and X. Jaravel. 2024. “A Practical Guide to Shift-Share Instruments.” Working Paper No. 33236, National Bureau of Economic Research, December.

—. 2022. “Quasi-experimental shift-share research designs.” *The Review of Economic Studies* 89:181–213.

Bragança, A. 2018. “The effects of crop-to-beef relative prices on deforestation: evidence from the TapajÃ³s Basin.”

Branco, J.E.H., D.B. Bartholomeu, P.N. Alves Junior, and J.V. Caixeta-Filho. 2022. “Evaluation of the Economic and Environmental Impacts from the Addition of New Railways to the Brazilian’s Transportation Network: An Application of a Network Equilibrium Model.” *Transport Policy* 124:61–69.

—. 2021. “Mutual Analyses of Agriculture Land Use and Transportation Networks: The Future Location of Soybean and Corn Production in Brazil.” *Agricultural Systems* 194:103264.

Branger, F., and P. Quirion. 2014. “Would border carbon adjustments prevent carbon leakage and heavy industry competitiveness losses? Insights from a meta-analysis of recent economic studies." *Ecological Economics* 99:29–39.

Burgess, R., M. Hansen, B.A. Olken, P. Potapov, and S. Sieber. 2012. "The Political Economy of Deforestation in the Tropics." *The Quarterly Journal of Economics* 127:1707–1754.

Bürgi, E., and C. Oberlack. 2023. "Breakout Session: Impacts of the EUDR on commodity-producing countries: How to establish partnerships for deforestation-free supply chains?" Summary report, University of Bern.

Bustos, P., B. Caprettini, and J. Ponticelli. 2016. "Agricultural Productivity and Structural Transformation: Evidence from Brazil." *American Economic Review* 106:1320–1365.

Byerlee, D., J. Stevenson, and N. Villoria. 2014a. "Does intensification slow crop land expansion or encourage deforestation?" *Global food security* 3:92–98.

Byerlee, D., J. Stevenson, and N.B. Villoria. 2014b. "Does Intensification Slow Crop Land Expansion or Encourage Deforestation?" *Global Food Security* 3:92–98.

Carreira, I., F. Costa, and J.P. Pessoa. 2024. "The deforestation effects of trade and agricultural productivity in Brazil." *Journal of development economics* 167:103217.

Cassman, K.G., and P. Grassini. 2020. "A global perspective on sustainable intensification research." *Nature Sustainability* 3:262–268.

Cha, Y., and M.G. Koo. 2021. "Who embraces technical barriers to trade? The case of European REACH regulations." *World Trade Review* 20:25–39.

Chaves, L.S.M., J. Fry, A. Malik, A. Geschke, M.A.M. Sallum, and M. Lenzen. 2020. "Global consumption and international trade in deforestation-associated commodities could influence malaria risk." *Nature Communications* 11:1258.

Chomitz, K.M., and D.A. Gray. 1996. "Roads, Land Use, and Deforestation: A Spatial Model Applied to Belize." *The World Bank Economic Review* 10:487–512.

Cisneros, E., K. Kis-Katos, and N. Nuryartono. 2021. "Palm oil and the politics of deforestation in

Indonesia." *Journal of Environmental Economics and Management* 108:102453, Open access, under a Creative Commons license.

Companhia Nacional de Abastecimento. 2025. "Exportações de Milho e Soja pelo Arco Norte Crescem Mais de 50% com Investimentos em Infraestrutura Multimodal." News release.

Companhia Nacional de Abastecimento (Conab). 2025. "Projections for Brazilian Agriculture 2025/2026." Agricultural outlook, Companhia Nacional de Abastecimento.

Comtrade. 2024. "UN Comtrade Database."

Confederação Nacional do Transporte. 2024. "O que é a Pesquisa CNT de Rodovias?" Institutional explainer.

Conte, M., P. Cotterlaz, and T. Mayer. 2023. "The CEPII Gravity Database."

Copeland, B.R., J.S. Shapiro, and M.S. Taylor. 2022. "Globalization and the Environment." In G. Gopinath, E. Helpman, and K. Rogoff, eds. *Handbook of International Economics*. Amsterdam: Elsevier, vol. 5 of *Handbook of International Economics*, pp. 61–146.

Correa, V.H.C., and P. Ramos. 2010. "A Precariedade do Transporte Rodoviário Brasileiro para o Escoamento da Produção de Soja do Centro-Oeste: Situação e Perspectivas." *Revista de Economia e Sociologia Rural* 48:1–26.

Costa, W., B. Soares-Filho, and R. Nóbrega. 2022. "Can the Brazilian National Logistics Plan Induce Port Competitiveness by Reshaping the Port Service Areas?" *Sustainability* 14:14567.

Curtis, P.G., C.M. Slay, N.L. Harris, A. Tyukavina, and M.C. Hansen. 2018. "Classifying Drivers of Global Forest Loss." *Science* 361:1108–1111.

Damm, Y., J. BÃ¶rner, N. Gerber, and B. Soares-Filho. 2024. "Health benefits of reduced deforestation in the Brazilian Amazon." *Communications Earth & Environment* 5:693.

De Gorter, H., D. Drabik, and D.R. Just. 2013. "How biofuels policies affect the level of grains and oilseed prices: theory, models and evidence." *Global Food Security* 2:82–88.

de Oliveira, S.E.C., L. Nakagawa, G.R. Lopes, J.C. Visentin, M. Couto, D.E. Silva, and C. West.

2024. “The European Union and United Kingdom’s deforestation-free supply chains regulations: Implications for Brazil.” *Ecological Economics* 217:108053.

Dhoubhadel, S.P., W. Ridley, and S. Devadoss. 2023. “Brazilian soybean expansion, US–China trade war, and US soybean exports.” *Journal of the Agricultural and Applied Economics Association* 2:446–460.

Donaldson, D. 2018. “Railroads of the Raj: Estimating the Impact of Transportation Infrastructure.” *American Economic Review* 108:899–934.

Donaldson, D., and R. Hornbeck. 2016. “Railroads and American Economic Growth: A “Market Access” Approach.” *Quarterly Journal of Economics* 131:799–858.

Du, X., L. Li, and E. Zou. 2024. “Trade, Trees, and Lives.” NBER Working Paper No. 33143, National Bureau of Economic Research, November.

Eaton, J., and S. Kortum. 2002. “Technology, Geography, and Trade.” *Econometrica* 70:1741–1779.

Empresa de Planejamento e Logística (EPL). 2021. “Plano Nacional de Logística: Relatório de Custos Logísticos do Brasil.” Technical report, Ministério da Infraestrutura, Governo Federal do Brasil.

ESALQ-LOG / SIFRECA. 2024. “Freight Rate Survey for Agricultural Products in Brazil.” Escola Superior de Agricultura Luiz de Queiroz, University of São Paulo.

European Commission. 2021. “Impact Assessment: Minimising the risk of deforestation and forest degradation associated with products placed on the EU market.” Working paper No. SWD(2021) 326 final, Part 1/2, European Commission, Brussels, November.

European Feed Manufacturers’ Federation (FEFAC). 2024. “FEFAC Memo: EUDR Implementation â€“ Economic and Supply Chain Impact Assessment.” Working paper, FEFAC, September.

European Union. 2023. “Regulation (EU) 2023/1115 of the European Parliament and of the Council of 31 May 2023 on the making available on the Union market and the export from the Union of certain commodities and products associated with deforestation and forest degradation and repealing Regulation (EU) No 995/2010 (Text with EEA relevance).” *Official Journal of the European Union* 66:150–206.

Fally, T. 2015. “Structural gravity and fixed effects.” *Journal of International Economics* 97:76–85.

FAOSTAT. 2024. “FAOSTAT- Food Balances.”

Farrokhi, F., E. Kang, H.S. Pellegrina, and S. Sotelo. 2025. “Deforestation: A global and dynamic perspective.” Working paper, National Bureau of Economic Research.

Farrokhi, F., and A. Lashkaripour. 2024. “Can Trade Policy Mitigate Climate Change.”, pp. . Forthcoming.

Feenstra, R.C. 2002. “Border effects and the gravity equation: Consistent methods for estimation.” *Scottish Journal of Political Economy* 49:491–506.

Fehlenberg, V., M. Baumann, N.I. Gasparri, M. Piquer-Rodriguez, G. Gavier-Pizarro, and T. Kuemmerle. 2017. “The role of soybean production as an underlying driver of deforestation in the South American Chaco.” *Global Environmental Change* 45:24–34.

Felbermayr, G., S. Peterson, and J. Wanner. 2024. “Trade and the environment, trade policies and environmental policiesâ€”How do they interact?” *Journal of Economic Surveys*, pp. , Open Access Publications from Kiel Institute for the World Economy (IfW Kiel).

Fisher, M.R., K. Obidzinski, A.M. Alves, and A.D. Ekaputri. 2024. “Commodities and Global Climate Governance: Early Evidence From the EU Deforestation-free Regulation (EUDR).” *Asia Pacific Issues - East West Center* 27.

Fliehr, O., Y. Zimmer, and L.H. Smith. 2019. “Impacts of Transportation and Logistics on Brazilian Soybean Prices and Exports.” *Transportation Journal* 58:65–77.

FontagnÃ©, L., H. Guimbard, and G. Orefice. 2022. “A new dataset on product-level trade elasticities.” *Data in Brief* 45:108668.

Fontagné, L., F. von Kirchbach, and M. Mimouni. 2005. "An assessment of environmentally-related non-tariff measures." *The World Economy* 28:1417–1439.

Frey, G., T.A.P. West, T. Hickler, L. Rausch, H. Gibbs, and J. Börner. 2018. "Simulated Impacts of Soy and Infrastructure Expansion in the Brazilian Amazon: A Maximum Entropy Approach." *Forests* 9:600.

Friend, J.D., and R.d.S. Lima. 2011. "Impact of Transportation Policies on Competitiveness of Brazilian and U.S. Soybeans: From Field to Port." *Transportation Research Record* 2238:61–67.

Gale, F., C. Valdes, and M. Ash. 2019. "Interdependence of China, United States, and Brazil in Soybean Trade." Economic Research Service Report No. OCS-19F-01, United States Department of Agriculture, June.

Garcia, E.S., A.L.S. Swann, J.C. Villegas, D.D. Breshears, D.J. Law, S.R. Saleska, and S.C. Stark. 2016. "Synergistic Ecoclimate Teleconnections from Forest Loss in Different Regions Structure Global Ecological Responses." *PLoS ONE* 11:e0165042.

García, V.R., F. Gaspart, T. Kastner, and P. Meyfroidt. 2020. "Agricultural intensification and land use change: assessing country-level induced intensification, land sparing and rebound effect." *Environmental Research Letters* 15:085007.

Gaulier, G., and S. Zignago. 2010. "BACI: International Trade Database at the Product-Level (the 1994-2007 Version)." *SSRN Electronic Journal*, pp. .

Giam, X. 2017. "Global biodiversity loss from tropical deforestation." *Proceedings of the National Academy of Sciences* 114:5775–5777.

Gilbert, C.L. 2024. "The EU Deforestation Regulation." *EuroChoices* 23:64–70.

Gockowski, J., and D. Sonwa. 2011. "Cocoa intensification scenarios and their predicted impact on CO_2 emissions, biodiversity conservation, and rural livelihoods in the Guinea rain forest of West Africa." *Environmental Management* 48:307–321.

Goldman, E., M. Weisse, N. Harris, and M. Schneider. 2020. “Estimating the role of seven commodities in agriculture-linked deforestation: Oil palm, soy, cattle, wood fiber, cocoa, coffee, and rubber.” *Technical Note, World Resources Institute* 22.

Goldsmith-Pinkham, P., I. Sorkin, and H. Swift. 2020. “Bartik Instruments: What, When, Why, and How.” *American Economic Review* 110:2586–2624.

Gollin, D., and J. Wolfersberger. 2025. “Agricultural Trade and Deforestation: The Role of New Roads.” *The Economic Journal*, pp. , Advance article.

Gollnow, F., F. Cammelli, K.M. Carlson, and R.D. Garrett. 2022. “Gaps in adoption and implementation limit the current and potential effectiveness of zero-deforestation supply chain policies for soy.” *Environmental Research Letters* 17:114003.

Gouveris, T. 2024. “Competition in the Global Agricultural Value Chain: A Review of the Role of ABCD Giants Including Research on Their Public Visibility.” *Open Journal of Business and Management* 12:4401–4412.

Governo Federal do Brasil. 2020. “Novo contrato de concessão ferroviária da Malha Paulista é assinado.” Gov.br news release.

—. 2021. “Plano Nacional de Logística 2035 traça oportunidades e necessidades futuras para a infraestrutura de transportes.” Gov.br news release.

Harding, T., J. Herzberg, and K. Kuralbayeva. 2021. “Commodity prices and robust environmental regulation: Evidence from deforestation in Brazil.”

Harstad, B. 2024a. “Contingent Trade Agreements.” National Bureau of Economic Research, Working Paper 32392.

—. 2024b. “On International Cooperation.” In L. Barrage and S. Hsiang, eds. *Handbook of the Economics of Climate Change*. Elsevier, vol. 1 of *NBER Working Paper Series*, Forthcoming in Handbook of the Economics of Climate Change, Volume 1.

—. 2024c. “Trade and Trees.” *American Economic Review: Insights* 6:155–175.

Headey, D., and S. Fan. 2008. "Anatomy of a crisis: the causes and consequences of surging food prices." *Agricultural Economics* 39:375–391.

Henders, S., U.M. Persson, and T. Kastner. 2015. "Trading forests: land-use change and carbon emissions embodied in production and exports of forest-risk commodities."

Heron, T., P. Prado, and C. West. 2018. "Global Value Chains and the Governance of 'Embedded' Food Commodities: The Case of Soy." *Global Policy* 9:29–37.

Hertel, T.W., N. Ramankutty, and U.L.C. Baldos. 2014. "Global Market Integration Increases Likelihood That a Future African Green Revolution Could Increase Crop Land Use and CO2 Emissions." *Proceedings of the National Academy of Sciences* 111:13799–13804.

Hosonuma, N., M. Herold, V. De Sy, R.S. De Fries, M. Brockhaus, L. Verchot, A. Angelsen, and E. Romijn. 2012. "An assessment of deforestation and forest degradation drivers in developing countries." *Environmental research letters* 7:044009.

Instituto Brasileiro de Geografia e Estatística. 2022. "Bases Cartográficas Contínuas do Brasil (BC250), Versão 2021: Camadas de Transporte." `https://geoftp.ibge.gov.br/cartas_e_mapas/bases_cartograficas_continuas/bc250/`, Spatial layers used: roads (*trecho rodoviário*), railways (*trecho ferroviário*), and navigable waterways (*trecho hidroviarió*). Survey periods: 2015, 2017, 2019, 2021, 2023. Scale 1:250,000; coordinate reference system SIRGAS 2000.

—. 2024a. "Estimativas de População Residentes nos Municípios e para as Unidades da Federação com Data de Referência em 1º de Julho: Tabela 6579." `https://sidra.ibge.gov.br/tabela/6579`, Annual municipality-level population estimates. 2014 estimates used as fixed market-size weights across all survey periods to avoid endogeneity of contemporaneous population. Sistema IBGE de Recuperação Automática (SIDRA). Accessed January 2024.

—. 2024b. "Produção Agrícola Municipal (PAM): Tabela 1612 — Área Plantada ou Destinada à Colheita, Área Colhida, Quantidade Produzida, Rendimento Médio e Valor da Produção das Lavouras Temporárias." `https://sidra.ibge.gov.br/tabela/1612`, Municipal-level annual data on harvested area (ha) and production value (R$1,000) for temporary crops, 2015–2023. Sistema IBGE de Recuperação Automática (SIDRA). Accessed January 2024.

International Trade Centre. 2024. "Market Access Map."

Jacoby, H.G., and B. Minten. 2009. "On Measuring the Benefits of Lower Transport Costs." *Journal of Development Economics* 89:28–38.

Jeddi, B., and G. DePaula. 2026a. "Environmental Impacts of Agricultural Intensification: Evidence from Brazil's Double-Cropping Boom." *Journal of Environmental Economics and Management* 130:103286.

—. 2026b. "Environmental Impacts of Agricultural Intensification: Evidence from Brazil's Double-Cropping Boom." *Journal of Environmental Economics and Management*, pp. 103286.

Jedwab, R., and A. Storeygard. 2022. "The Average and Heterogeneous Effects of Transportation Investments: Evidence from Sub-Saharan Africa 1960–2010." *Journal of the European Economic Association* 20:1–38.

KPMG. 2023. "A high-level introduction to the EU Deforestation-Free Regulation (EUDR) - what it means for international supply chains." Accessed June 18, 2024.

Kravchenko, A., A. Strutt, C. Utoktham, and Y. Duval. 2022. "New Price-based Bilateral Ad-valorem Equivalent Estimates of Non-tariff Measures." *Journal of Global Economic Analysis*, pp. .

Lambin, E.F., and P. Meyfroidt. 2011. "Global Land Use Change, Economic Globalization, and the Looming Land Scarcity." *Proceedings of the National Academy of Sciences* 108:3465–3472.

Larch, M., S. Shikher, and Y.V. Yotov. 2025. "The International Trade and Production Database for Estimation – Release 3 (ITPD-E-R03)." USITC Working Paper No. 2025-06-A, U.S. International Trade Commission, Washington, DC.

Larch, M., S. Tan, and Y. Yotov. 2021. "A Simple Method to Quantify the Ex-Ante Effects of "Deep" Trade Liberalization and "Hard" Trade Protection." *CESifo Working Paper Series*, pp. .

Larch, M., and J. Wanner. 2017. "Carbon tariffs: An analysis of the trade, welfare, and emission effects." *Journal of International Economics* 109:195–213.

Lawrence, D., and K. Vandecar. 2015. "Effects of tropical deforestation on climate and agriculture." *Nature climate change* 5:27–36.

Lee, T.H., and M.H. Lo. 2021. "The role of El NiÃ±o in modulating the effects of deforestation in the Maritime Continent." *Environmental Research Letters* 16:054056.

Leijten, F., U.L.C. Baldos, J.A. Johnson, S. Sim, and P.H. Verburg. 2023. "Projecting global oil palm expansion under zero-deforestation commitments: Direct and indirect land use change impacts." *iScience* 26:106971.

Li, Y., and J.C. Beghin. 2012. "A meta-analysis of estimates of the impact of technical barriers to trade." *Journal of Policy Modeling* 34:497–511.

Limão, N., and A.J. Venables. 2001. "Infrastructure, Geographical Disadvantage, Transport Costs, and Trade." *World Bank Economic Review* 15:451–479.

Lundberg, C., and R. Abman. 2021. "Maize price volatility and deforestation."

Meyfroidt, P., J. Börner, R. Garrett, T. Gardner, J. Godar, K. Kis-Katos, and S. Wunder. 2020. "Focus on Leakage and Spillovers: Informing Land-Use Governance in a Tele-Coupled World." *Environmental Research Letters* 15:090202.

Meyfroidt, P., T.K. Rudel, and E.F. Lambin. 2010. "Forest transitions, trade, and the global displacement of land use." *Proceedings of the National Academy of Sciences* 107:20917–20922.

Ministério dos Transportes. 2024. "Ferrovias Brasileiras." Government webpage.

Ministério dos Transportes. 2024. "Visão de longo prazo: decreto que institui Planejamento Integrado de Transportes fará parte de projetos de investimento até 2055." Gov.br news release.

Mullahy, J., and E.C. Norton. 2024. "Why transform Y? The pitfalls of transformed regressions with a mass at zero." *Oxford Bulletin of Economics and Statistics* 86:417–447.

Muradian, R., R. Cahyafitri, T. Ferrando, C. Grottera, L. Jardim-Wanderley, T. Krause, N.I.

Kurniawan, L. Loft, T. Nurshafira, D. Prabawati-Suwito, D. Prasongko, P.A. Sanchez-Garcia, B. SchrÃ¶ter, and D. Vela-Almeida. 2025. “Will the EU deforestation-free products regulation (EUDR) reduce tropical forest loss? Insights from three producer countries.” *Ecological Economics* 227:108389.

Nedoncelle, C., P. Delacote, and L. Crepin. 2025. “Agricultural Exports, Market Power, and Deforestation.” Unpublished, UniversitÃ© Paris-Saclay, INRAE, AgroParisTech, Paris-Saclay Applied Economics; INRAE, BETA; Climate Economics Chair; Paris School of Economics.

Oliveira, A.L.R., and A.M. Alvim. 2017. “The Supply Chain of Brazilian Maize and Soybeans: The Effects of Segregation on Logistics and Competitiveness.” *International Food and Agribusiness Management Review* 20:45–62.

Pacheco, P., K. Mo, N. Dudley, A. Shapiro, and N. Aguilar-Amuchastegui. 2021. “Deforestation and Forest Degradation Associated with Trade in Forest-Risk Commodities.” *Frontiers in Forests and Global Change* 4:692760.

Papke, L.E., and J.M. Wooldridge. 2008. “Panel data methods for fractional response variables with an application to test pass rates.” *Journal of econometrics* 145:121–133.

Pendrill, F., T.A. Gardner, P. Meyfroidt, U.M. Persson, J. Adams, T. Azevedo, M.G.B. Lima, M. Baumann, P.G. Curtis, C. West, et al. 2022a. “Disentangling the numbers behind agriculture-driven tropical deforestation.” *Science* 377:eabm9267.

Pendrill, F., U.M. Persson, J. Godar, and T. Kastner. 2019a. “Deforestation Displaced: Trade in Forest-Risk Commodities and the Prospects for a Global Forest Transition.” *Environmental Research Letters* 14:055003.

Pendrill, F., U.M. Persson, J. Godar, T. Kastner, D. Moran, S. Schmidt, and R. Wood. 2019b. “Agricultural and Forestry Trade Drives Large Share of Tropical Deforestation Emissions.” *Global Environmental Change* 56:1–10.

Pendrill, F., U.M. Persson, T. Kastner, and R. Wood. 2022b. “Deforestation risk embodied in production and consumption of agricultural and forestry commodities 2005-2018 (Version 1.1) [Dataset].”

Persson, M., C. Singh, O. Pereira, and H. Bellfield. 2024. “DeDuCE: New Data to Inform Action Against Commodity-Driven Deforestation.” A new global dataset on commodity-driven deforestation called DeDuCE is helping governments, companies and civil society assess the deforestation exposure of producer and consumer countries.

Persson, U.M., S. Henders, and T. Kastner. 2014. “Trading Forests: Quantifying the Contribution of Global Commodity Markets to Emissions from Tropical Deforestation.”

Rabobank. 2023. “The EU Deforestation Regulation is a Complex and Costly Undertaking.” Working paper, Rabobank.

Richards, P., and E. Arima. 2026. “High Profits from Soybean-Corn Agriculture Are Associated with Increased Land Prices and Deforestation Rates in Mato Grosso’s Amazon Forests.” *Communications Earth & Environment*, pp. , ahead of print.

Ridley, W., and F. Shirin. 2024. “The effectiveness of development-oriented nonreciprocal trade preferences in promoting agricultural trade.” *American Journal of Agricultural Economics*, pp. , First published: 26 July 2024.

Roberts, M.J., and W. Schlenker. 2013. “Identifying supply and demand elasticities of agricultural commodities: Implications for the US ethanol mandate.” *American Economic Review* 103:2265–2295.

Santeramo, F.G., and E. Lamonaca. 2019. “The effects of non-tariff measures on agri-food trade: A review and meta-analysis of empirical evidence.” *Journal of Agricultural Economics* 70:595–617.

Santeramo, F.G., E. Lamonaca, and C. Emlinger. 2025. “Technical measures, environmental protection, and trade.” *Review of International Economics* 33:537–555.

Sassen, M., and others. 2022. “Patterns of (future) environmental risks from cocoa expansion and intensification in West Africa call for context specific responses.” *Land Use Policy* 120:106142.

Schielein, J., G. Frey, J. Miranda, R. Souza, J. Boerner, and J. Henderson. 2021. "The Role of Accessibility for Land Use and Land Cover Change in the Brazilian Amazon." *Applied Geography* 132:102419.

Shamdasani, Y. 2021. "Rural Road Infrastructure & Agricultural Production: Evidence from India." *Journal of Development Economics* 152:102686.

Shapiro, J.S. 2021. "The Environmental Bias of Trade Policy." *The Quarterly Journal of Economics* 136:831–886.

Silva, J.M.C.S., and S. Tenreyro. 2006. "The log of gravity." *The Review of Economics and Statistics* 88:641–658.

Singh, C., and U.M. Persson. 2024. "DeDuCE: Deforestation and carbon emissions due to agriculture and forestry activities from 2001-2022 (v1.0.1)."

Snyder, P.K. 2010. "The influence of tropical deforestation on the Northern Hemisphere climate by atmospheric teleconnections." *Earth Interactions* 14:1–34.

Song, X.P., M.C. Hansen, P. Potapov, B. Adusei, J. Pickering, M. Adami, A. Lima, V. Zalles, S.V. Stehman, C.M. Di Bella, M.C. Conde, E.J. Copati, L.B. Fernandes, A. Hernandez-Serna, S.M. Jantz, A.H. Pickens, S. Turubanova, and A. Tyukavina. 2021. "Massive soybean expansion in South America since 2000 and implications for conservation." *Nature Sustainability* 4.

Souza-Rodrigues, E. 2019. "Deforestation in the Amazon: A Unified Framework for Estimation and Policy Analysis." *Review of Economic Studies* 86:2713–2744.

Staiger, D., and J.H. Stock. 1997. "Instrumental Variables Regression with Weak Instruments." *Econometrica* 65:557–586.

Storeygard, A. 2016. "Farther on down the Road: Transport Costs, Trade and Urban Growth in Sub-Saharan Africa." *Review of Economic Studies* 83:1263–1295.

Taheripour, F., T.W. Hertel, and N. Ramankutty. 2019. "Market-mediated responses confound policies to limit deforestation from oil palm expansion in Malaysia and Indonesia." *Proceedings of the National Academy of Sciences* 116.

Umburanas, R.C., J. Kawakami, E.A. Ainsworth, J.L. Favarin, L.Z. Anderle, D. Dourado-Neto, and K. Reichardt. 2022. "Changes in soybean cultivars released over the past 50 years in southern Brazil." *Scientific Reports* 12:508.

USDA Agricultural Marketing Service. 2024. "Brazil Soybean Transportation Guide." Transportation report, United States Department of Agriculture.

van Noordwijk, M., B. Leimona, and P.A. Minang. 2025. "The European deforestation-free trade regulation: collateral damage to agroforesters?" *Current Opinion in Environmental Sustainability* 72:101505.

Vasconcelos, A., F. Cerignoni, V. Silgueiro, and T. Reis. 2023. "Soy and legal compliance in Brazil: Risks and opportunities under the EU deforestation regulation." Technical report, Trase.

Vera-Diaz, M.d.C., R.K. Kaufmann, and D.C. Nepstad. 2009. "The Environmental Impacts of Soybean Expansion and Infrastructure Development in Brazil's Amazon Basin." Working Paper No. 09-01, Global Development and Environment Institute, Tufts University.

Villoria, N., R. Garrett, F. Gollnow, and K. Carlson. 2022. "Leakage does not fully offset soy supply-chain efforts to reduce deforestation in Brazil." *Nature Communications* 13:5476, Open access.

Villoria, N.B. 2025. "Trade frictions and domestic food price stability in the presence of large-scale climate shocks." *American Journal of Agricultural Economics*, pp. , First published: 06 February 2025. This work was supported by the USDA National Institute of Food and Agriculture (NIFA) under Hatch project number S1072 and competitive grant number 2022-10683.

Villoria, N.B., D. Byerlee, and J. Stevenson. 2014a. "The Effects of Agricultural Technological Progress on Deforestation: What Do We Really Know?" *Applied Economic Perspectives and Policy* 36:211–237.

—. 2014b. “The Effects of Agricultural Technological Progress on Deforestation: What Do We Really Know?” *Applied Economic Perspectives and Policy* 36:211–237.

Wang, Z., G.B. Martha, J. Liu, C.Z. Lima, and T. Hertel. 2024. “Planned Expansion of Transportation Infrastructure in Brazil Has Implications for the Pattern of Agricultural Production and Carbon Emissions.” *Science of the Total Environment* 928:172434.

Weinhold, D., and E. Reis. 2008. “Transportation Costs and the Spatial Distribution of Land Use in the Brazilian Amazon.” *Global Environmental Change* 18:54–68.

Werth, D., and R. Avissar. 2005. “The local and global effects of Southeast Asian deforestation.” *Geophysical Research Letters* 32.

Wilcox, S.W., D.R. Just, and A. Ortiz-Bobea. 2025. “The Role of Staple Food Prices in Deforestation: Evidence from Cambodia.” *Land Economics* 101:89–118.

Wooldridge, J. 2015. “Control Function Methods in Applied Econometrics.” *The Journal of Human Resources* 50:420 – 445.

World Bank. 2025. “”Pink Sheet” Data: Annual prices.” Annual prices dataset.

Yotov, Y.V., R. Piermartini, J.A. Monteiro, and M. Larch. 2016. *An Advanced Guide to Trade Policy Analysis: The Structural Gravity Model*. Geneva: World Trade Organization.

Zabel, F., R. Delzeit, J.M. Schneider, et al. 2019. “Global Impacts of Future Cropland Expansion and Intensification on Agricultural Markets and Biodiversity.” *Nature Communications* 10:2844.

zu Ermgassen, E.K., B. Ayre, J. Godar, M.G.B. Lima, S. Bauch, R. Garrett, J. Green, M.J. Lathuillière, P. Löfgren, C. MacFarquhar, P. Meyfroidt, C. Suavet, C. West, and T. Gardner. 2020. “Using Supply Chain Data to Monitor Zero Deforestation Commitments: An Assessment of Progress in the Brazilian Soy Sector.” *Environmental Research Letters* 15:035003.

Zu Ermgassen, E.K., J. Godar, M.J. Lathuillière, P. Löfgren, T. Gardner, A. Vasconcelos, and P. Meyfroidt. 2020. “The origin, supply chain, and deforestation risk of Brazilâ€™s beef exports.” *Proceedings of the National Academy of Sciences* 117:31770–31779.

Appendix A

Appendix A: Chapter 1

A.1 Selection of countries

We included 90 countries in the simulation exercise. However, Saudi Arabia (SAU) and Panama (PAN) were removed from the soybean analysis, seven countries (ARE, ISL, KEN, MUS, MNE, OMN, DZA) were removed from the soybean cake analysis, and two countries (ISL, GAB) were removed from the soybean oil analysis. These countries were selected because they are either significant producers or consumers of soy products.

These countries are selected because they are either significant producers or consumers of soy products. The selected countries are: United Arab Emirates (ARE), Argentina (ARG), Australia (AUS), Austria (AUT), Belgium (BEL), Bulgaria (BGR), Bolivia (BOL), Brazil (BRA), Canada (CAN), Switzerland (CHE), Chile (CHL), China (CHN), Colombia (COL), Costa Rica (CRI), Cyprus (CYP), Czech Republic (CZE), Germany (DEU), Denmark (DNK), Algeria (DZA), Egypt (EGY), Spain (ESP), Estonia (EST), Finland (FIN), France (FRA), Gabon (GAB), United Kingdom (GBR), Greece (GRC), Hong Kong (HKG), Croatia (HRV), Hungary (HUN), Indonesia (IDN), India (IND), Ireland (IRL), Iran (IRN), Iceland (ISL), Italy (ITA), Jordan (JOR), Japan (JPN), Kenya (KEN), Cambodia (KHM), South Korea (KOR), Laos (LAO), Lebanon (LBN), Sri Lanka (LKA), Lithuania (LTU), Luxembourg (LUX), Latvia (LVA), Morocco (MAR), Madagascar (MDG), Mexico (MEX), North Macedonia (MKD), Malta (MLT), Myanmar (MMR), Montenegro (MNE), Mozambique (MOZ), Mauritius (MUS), Malaysia (MYS), Nicaragua (NIC), Netherlands (NLD), Norway (NOR), New Zealand (NZL), Oman (OMN), Panama (PAN), Peru (PER), Philippines (PHL), Poland (POL), Portugal (PRT), Paraguay (PRY), Romania (ROU), Russia (RUS), Saudi Arabia (SAU), Singapore (SGP), El Salvador (SLV), Serbia (SRB), Slovakia (SVK), Slovenia (SVN), Sweden (SWE), Thailand (THA), Trinidad and Tobago (TTO), Turkey (TUR), Taiwan (TWN), Ukraine (UKR), Uruguay (URY), United States (USA), Venezuela (VEN), Vietnam (VNM), South Africa (ZAF), Zimbabwe (ZWE), Kazakhstan (KAZ), and Ecuador (ECU).

A.2 Structural Gravity

To analyze the potential effects of the EUDR on global soy trade, we employ the procedure developed by Anderson et al. (2018), which is grounded in the structural gravity framework of Anderson and van Wincoop (Anderson and Van Wincoop 2003). In this framework, the bilateral trade flows (X_{ijt}) of soy products at time t, where i denotes exporters and j denotes importers, are a function of the economic size of the partner countries and the costs associated with trade. The gravity equation is given by:

$$X_{ijt} = \frac{Y_{it}E_{jt}}{Y_t}\left(\frac{t_{ijt}}{\Pi_{it}P_{jt}}\right)^{1-\sigma}, \quad (A1.1)$$

where (Y_{it}) is the total soy supply from the exporter i, (E_{jt}) is the total soy expenditure of importer j, and (Y_t) is total world production/consumption of soy. The parenthetical term captures trade costs, including bilateral trade cost (t_{ijt}) and multilateral resistance terms: outward multilateral resistance (OMR, Π_{it}) and inward multilateral resistance (IMR, P_{jt}). These resistance terms are expressed as follows:

$$\Pi_{it}^{1-\sigma} = \sum_j \left(\frac{t_{ijt}}{P_{jt}}\right)^{1-\sigma}\frac{E_{jt}}{Y_t}, \quad (A1.2)$$

$$P_{jt}^{1-\sigma} = \sum_i \left(\frac{t_{ijt}}{\Pi_{it}}\right)^{1-\sigma}\frac{Y_{it}}{Y_t}. \quad (A1.3)$$

These equations illustrate how global trade patterns are interconnected. For example, when China imposed a 25% retaliatory tariff on US soybeans in 2018, the resulting increase in trade costs between the US and China directly reduced their bilateral trade. At the same time, trade between China and Brazil increased, as the relative trade cost between these two countries fell. Such relationships are captured by the trade cost term t_{ijt} within the OMR and IMR, reflecting how changes in trade costs in one bilateral relationship can affect trade flows across many country pairs.

Following Silva and Tenreyro (2006), equation (A1) can be expressed in multiplicative form as:

$$X_{ijt} = \exp\left(\alpha_{it} + \alpha_{jt} + \alpha_{ij} + \sum_{k=1}^{n} \alpha_k d_{k,ijt}\right)\epsilon_{ijt}, \quad (A1.4)$$

where, bilateral trade cost ($t_{ijt}^{1-\sigma}$) is captured by $\exp\left(\alpha_{ij} + \sum_{k=1}^{n} \alpha_k d_{k,ijt}\right)$, incorporating both time-invariant costs (e.g., geographic distance, contiguity) through $\exp(\alpha_{ij})$ and k number of time-varying costs (e.g., tariffs, trade agreements) through $d_{k,ijt}$. Baier and Bergstrand (2007) emphasize to include country-pair fixed effects (α_{ij}) which captures time-invariant factors sepific to each country pair. These fixed effects also address the potential by accounting for unobserved, long-term factors such as historical trade relationships that might otherwise bias the estimates. The term $\exp(\alpha_{it} + \alpha_{jt})$ represents exporter-time and importer-time fixed effects, corresponding to $\frac{Y_{it}E_{jt}}{Y_t}\left(\frac{1}{\Pi_{it}P_{jt}}\right)^{1-\sigma}$. As Feenstra (2002) suggests, these fixed effects capture OMR, IMR, and market sizes, that vary by exporter-year and importer-year level. Santos Silva and Tenreyro (2006) recommend estimating equation (4) using the pseudo-Poisson maximum likelihood (PPML) approach, which allows including zero trade flows in the dependent variable. In addition, this leads to unbiased and consistent estimation of parameter under heteroskedasticity.

For the conditional counterfactual study, we decompose the equation (A1.1) for the base year 2022 as follows:

$$\Delta X_{ij}^{s} = (1 - \sigma_s)[\Delta t_{ij}^{s} - \Delta \Pi_i^{s} - \Delta P_j^{s}], \quad (A1.4)$$

A.3 Armington elasticities

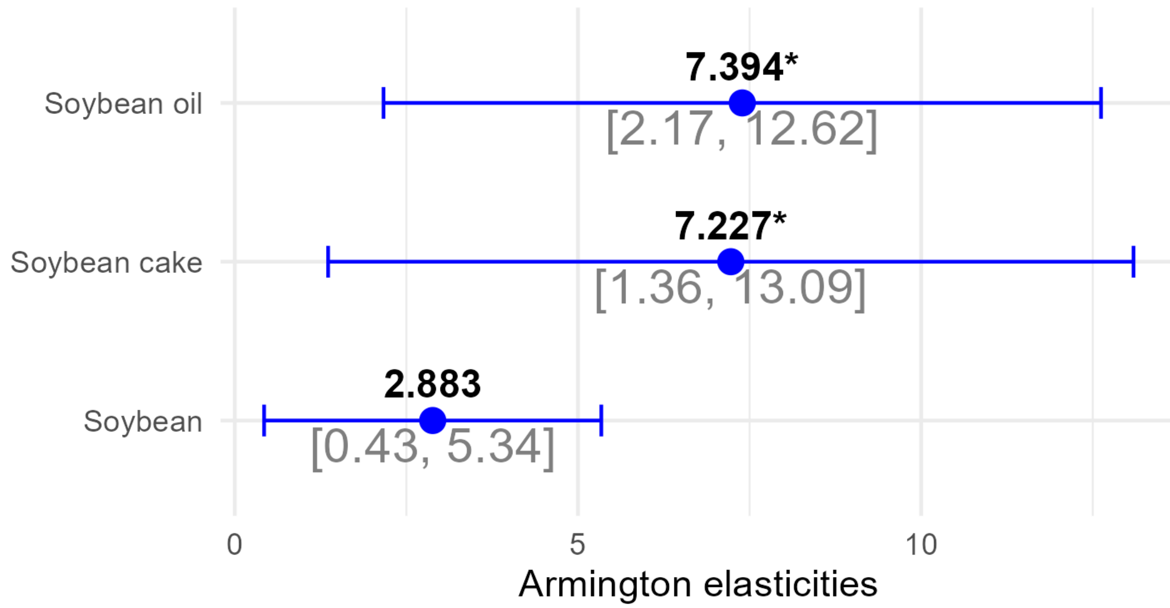

Figure A3.1: Estimates of Armington elasticites with 95% condidence intervals. Note: Armington elasticities are defined as 1 minus tariff elasticities. We estimate tariff elasticities using the pseudo-Poisson maximum likelihood (PPML) estimator. Exporter-year, importer-year, and country-pair fixed effects are included. Standard errors are clustered at the country-pair level. *** p<0.001, ** p<0.01, * p<0.05, . p<0.1

A.4 EU involvement with soy trade

Table A4.1: Import share of EU-27 countries in soy products (2021-2023)

Selected Countries	Import Share of EU-27 (%)	Export Share to EU-27 (%)	Export Share to World (%)
BRA	39.05	14.17	42.99
USA	14.45	8.54	26.39
ARG	11.53	16.51	10.90
UKR	3.67	50.54	1.13
CAN	2.36	16.81	2.19
PRY	1.14	6.34	2.80
RUS	0.90	14.19	0.99
IND	0.80	18.14	0.69
CHN	0.45	13.46	0.53
TUR	0.12	2.79	0.64
BOL	0.02	0.26	1.34

Source: Own estimation based on CEPII-BACI database (Gaulier and Zignago 2010)

	Export			Import		
	Soybean	Soybean Cake	Soybean Oil	Soybean	Soybean Cake	Soybean Oil
Sweden	0.05%	0.00%	0.76%	0.34%	1.28%	2.28%
Spain	0.52%	3.62%	20.26%	24.44%	10.94%	12.30%
Slovenia	1.14%	4.82%	0.30%	0.06%	2.92%	0.80%
Slovakia	2.96%	0.13%	2.29%	0.07%	0.49%	0.80%
Romania	8.08%	2.38%	0.43%	1.30%	2.36%	0.48%
Portugal	0.34%	1.11%	6.56%	5.86%	0.48%	1.25%
Poland	1.29%	1.44%	2.93%	0.47%	10.72%	17.56%
Netherlands	44.77%	42.21%	36.12%	27.54%	12.13%	9.00%
Malta	0.00%	0.00%	0.03%	0.00%	0.08%	0.24%
Luxembourg	0.29%	0.55%	1.51%	0.06%	0.20%	0.22%
Lithuania	0.16%	1.14%	0.25%	0.02%	0.72%	1.33%
Latvia	0.01%	1.05%	0.04%	0.00%	0.72%	0.19%
Italy	1.89%	3.73%	7.45%	11.72%	7.02%	2.27%
Ireland	0.33%	1.38%	0.22%	0.21%	3.12%	4.56%
Hungary	3.63%	1.48%	1.16%	0.77%	1.72%	0.54%
Greece	0.24%	0.67%	0.59%	1.66%	1.49%	1.01%
Germany	6.35%	22.54%	10.50%	17.75%	13.24%	12.40%
France	6.83%	0.50%	3.71%	3.06%	11.78%	4.52%
Finland	0.00%	0.09%	0.21%	0.13%	0.70%	0.04%
Estonia	0.00%	0.01%	0.05%	0.00%	0.20%	1.28%
Denmark	0.62%	1.27%	0.30%	0.24%	7.09%	8.13%
Czechia	0.59%	0.25%	0.23%	0.16%	1.76%	1.75%
Cyprus	0.00%	0.00%	0.00%	0.02%	0.68%	0.68%
Croatia	9.52%	0.07%	0.28%	0.09%	0.78%	0.46%
Bulgaria	0.13%	0.02%	0.08%	0.02%	0.52%	2.78%
Belgium	4.53%	5.59%	3.31%	3.05%	5.01%	8.95%
Austria	5.73%	3.94%	0.40%	0.94%	1.85%	4.18%

Share (%): 0, 10, 20, 30, 40

Figure A4.2: Relative sizes of the EU countries (among themselves) in import and export markets (cumulative 2019-2021)

Note: Percentages denote the EU countries' share of total EU27 imports and exports.

A.5 Additional results of the EUDR simulation

a

	Soybean		Soybean cake		Soybean oil	
	Compliance	Non-compliance	Compliance	Non-compliance	Compliance	Non-compliance
Sweden	-5.15%	-18.75%	-5.34%	-53.34%	-4.41%	-11.44%
Spain	-5.33%	-50.96%	-5.43%	-60.71%	-1.75%	-9.98%
Slovenia	-5.24%	-26.10%	-5.53%	-71.80%	-2.67%	-9.00%
Slovakia	-5.09%	-32.21%	-4.29%	-58.70%	-4.74%	-10.51%
Romania	-5.09%	-13.72%	-5.41%	-51.68%	-1.47%	-7.75%
Portugal	-5.33%	-44.63%	-5.13%	-49.12%	-4.65%	-7.40%
Poland	-5.01%	-28.57%	-5.45%	-57.70%	-2.69%	-7.48%
Netherlands	-5.32%	-40.23%	-5.57%	-68.52%	-2.30%	-11.47%
Malta	-5.24%	-40.29%	-4.58%	-38.76%	-1.13%	-8.06%
Luxembourg	-5.33%	-69.76%	-4.50%	-53.36%	-2.52%	-7.39%
Lithuania	-5.22%	-38.11%	-4.88%	-55.68%	-4.60%	-10.88%
Latvia	-5.30%	-18.61%	-4.85%	-58.99%	-4.60%	-10.67%
Italy	-5.26%	-42.21%	-5.30%	-61.00%	-1.21%	-8.40%
Ireland	-5.24%	-19.51%	-5.63%	-53.39%	-1.98%	-7.85%
Hungary	-5.17%	-47.85%	-4.35%	-57.31%	-1.42%	-7.88%
Greece	-5.26%	-36.31%	-5.51%	-58.56%	-2.72%	-9.73%
Germany	-5.26%	-27.22%	-5.09%	-62.29%	-1.27%	-8.08%
France	-5.09%	-40.77%	-5.42%	-63.81%	-2.99%	-11.54%
Finland	-5.30%	-35.89%	-4.73%	-53.43%	-3.62%	-9.59%
Estonia	-4.55%	-22.19%	-4.27%	-56.36%	-4.57%	-10.51%
Denmark	-5.17%	-27.16%	-5.30%	-57.33%	-3.52%	-7.68%
Czechia	-4.82%	-31.17%	-4.66%	-58.31%	-4.68%	-10.45%
Cyprus	-5.34%	-54.97%	-5.54%	-48.29%	-4.53%	-7.00%
Croatia	-3.43%	-32.73%	-5.13%	-58.68%	-4.21%	-10.15%
Bulgaria	-4.45%	-28.37%	-4.81%	-56.65%	-2.82%	-7.74%
Belgium	-5.20%	-33.00%	-4.81%	-57.69%	-0.99%	-7.70%
Austria	-4.95%	-34.11%	-4.92%	-58.56%	-4.12%	-10.21%

b

	Soybean		Soybean cake		Soybean oil	
	Compliance	Non-compliance	Compliance	Non-compliance	Compliance	Non-compliance
Sweden	5.43%	23.07%	5.64%	114.33%	4.61%	12.92%
Spain	5.63%	103.94%	5.75%	154.50%	1.79%	11.08%
Slovenia	5.53%	35.31%	5.85%	254.60%	2.74%	9.90%
Slovakia	5.37%	47.51%	4.48%	142.15%	4.98%	11.74%
Romania	5.37%	15.90%	5.72%	106.95%	1.50%	8.40%
Portugal	5.63%	80.60%	5.41%	96.55%	4.87%	7.99%
Poland	5.27%	40.00%	5.76%	136.39%	2.77%	8.08%
Netherlands	5.62%	67.32%	5.90%	217.69%	2.35%	12.96%
Malta	5.53%	67.48%	4.80%	63.29%	1.14%	8.77%
Luxembourg	5.63%	230.67%	4.71%	114.43%	2.59%	7.97%
Lithuania	5.51%	61.58%	5.13%	125.63%	4.82%	12.21%
Latvia	5.60%	22.86%	5.10%	143.83%	4.82%	11.94%
Italy	5.55%	73.05%	5.60%	156.42%	1.22%	9.17%
Ireland	5.53%	24.24%	5.97%	114.55%	2.02%	8.52%
Hungary	5.45%	91.77%	4.55%	134.27%	1.44%	8.56%
Greece	5.55%	57.00%	5.83%	141.30%	2.80%	10.78%
Germany	5.55%	37.41%	5.36%	165.20%	1.28%	8.79%
France	5.37%	68.85%	5.73%	176.32%	3.08%	13.05%
Finland	5.59%	55.98%	4.97%	114.74%	3.76%	10.61%
Estonia	4.77%	28.51%	4.46%	129.15%	4.78%	11.74%
Denmark	5.46%	37.29%	5.59%	134.38%	3.65%	8.32%
Czechia	5.06%	45.28%	4.88%	139.89%	4.91%	11.68%
Cyprus	5.64%	122.10%	5.86%	93.37%	4.74%	7.52%
Croatia	3.55%	48.66%	5.41%	142.04%	4.39%	11.30%
Bulgaria	4.65%	39.60%	5.05%	130.68%	2.90%	8.38%
Belgium	5.49%	49.26%	5.06%	136.36%	1.00%	8.35%
Austria	5.21%	51.78%	5.18%	141.29%	4.30%	11.37%

c

	Soybean		Soybean cake		Soybean oil	
	Compliance	Non-compliance	Compliance	Non-compliance	Compliance	Non-compliance
Sweden	5.17%	42.34%	5.17%	101.85%	1.15%	2.32%
Spain	5.43%	63.95%	5.59%	139.13%	1.44%	3.60%
Slovenia	5.53%	62.21%	3.62%	116.49%	1.91%	3.27%
Slovakia	5.27%	45.96%	4.24%	122.85%	1.13%	2.12%
Romania	4.39%	30.49%	5.02%	119.23%	1.34%	2.12%
Portugal	5.61%	91.13%	5.37%	99.50%	0.82%	1.93%
Poland	5.39%	40.02%	3.14%	117.45%	0.86%	2.29%
Netherlands	4.54%	27.56%	4.56%	129.38%	0.84%	1.96%
Malta	5.10%	52.48%	3.67%	123.85%	0.52%	1.42%
Luxembourg	5.48%	32.49%	4.58%	126.92%	2.83%	2.42%
Lithuania	4.87%	36.32%	3.25%	111.26%	1.63%	2.13%
Latvia	2.98%	21.68%	1.68%	76.45%	1.20%	1.86%
Italy	5.51%	61.91%	5.47%	141.10%	1.16%	2.82%
Ireland	0.21%	1.41%	1.40%	73.14%	0.44%	1.63%
Hungary	5.11%	52.87%	5.21%	127.02%	1.28%	2.53%
Greece	-0.09%	3.54%	5.61%	124.52%	2.73%	4.21%
Germany	5.02%	38.72%	4.87%	136.39%	1.19%	2.34%
France	5.17%	58.57%	5.27%	153.48%	1.08%	2.82%
Finland	2.92%	22.98%	4.73%	101.83%	1.94%	2.84%
Estonia	5.50%	32.44%	3.52%	111.98%	0.64%	1.57%
Denmark	4.99%	25.98%	1.22%	74.40%	1.24%	3.11%
Czechia	5.01%	35.55%	4.66%	124.21%	0.97%	2.01%
Cyprus	0.10%	5.40%	1.88%	84.13%	0.95%	1.81%
Croatia	3.41%	38.91%	5.26%	137.52%	0.71%	1.69%
Bulgaria	4.43%	32.17%	2.33%	98.89%	1.14%	2.67%
Belgium	4.81%	47.12%	5.37%	158.39%	1.43%	3.58%
Austria	5.28%	43.14%	4.56%	161.98%	1.81%	3.07%

d

	Soybean		Soybean cake		Soybean oil	
	Compliance	Non-compliance	Compliance	Non-compliance	Compliance	Non-compliance
Sweden	-0.24%	15.66%	-0.44%	-5.82%	-3.32%	-9.39%
Spain	-0.19%	-19.61%	-0.14%	-6.04%	-0.33%	-6.73%
Slovenia	0.00%	19.88%	-2.11%	-38.95%	-0.81%	-6.03%
Slovakia	-0.09%	-1.05%	-0.23%	-7.97%	-3.67%	-8.62%
Romania	-0.93%	12.59%	-0.66%	5.93%	-0.15%	-5.79%
Portugal	-0.02%	5.83%	-0.04%	1.50%	-3.87%	-5.60%
Poland	0.12%	0.02%	-2.49%	-8.01%	-1.85%	-5.36%
Netherlands	-1.02%	-23.76%	-1.27%	-27.80%	-1.48%	-9.73%
Malta	-0.41%	-8.95%	-1.08%	37.08%	-0.62%	-6.76%
Luxembourg	-0.15%	-59.93%	-0.12%	5.83%	0.24%	-5.15%
Lithuania	-0.61%	-15.63%	-1.79%	-6.37%	-3.05%	-8.98%
Latvia	-2.48%	-0.96%	-3.26%	-27.63%	-3.45%	-9.00%
Italy	-0.04%	-6.44%	-0.12%	-5.98%	-0.06%	-5.82%
Ireland	-5.04%	-18.38%	-4.31%	-19.30%	-1.55%	-6.35%
Hungary	-0.32%	-20.28%	0.63%	-3.10%	-0.15%	-5.55%
Greece	-5.34%	-34.05%	-0.21%	-6.95%	-0.07%	-5.93%
Germany	-0.50%	0.95%	-0.46%	-10.87%	-0.09%	-5.93%
France	-0.18%	-6.09%	-0.43%	-8.27%	-1.94%	-9.05%
Finland	-2.54%	-21.16%	-0.23%	-6.01%	-1.75%	-7.02%
Estonia	0.70%	3.06%	-0.89%	-7.49%	-3.95%	-9.10%
Denmark	-0.45%	-8.24%	-4.15%	-25.59%	-2.32%	-4.81%
Czechia	-0.05%	-6.70%	-0.21%	-6.54%	-3.76%	-8.65%
Cyprus	-5.24%	-52.54%	-3.76%	-4.78%	-3.62%	-5.32%
Croatia	-0.14%	-6.56%	-0.14%	-1.86%	-3.53%	-8.64%
Bulgaria	-0.21%	-5.33%	-2.59%	-13.78%	-1.71%	-5.28%
Belgium	-0.64%	-1.43%	0.30%	9.32%	0.43%	-4.40%
Austria	0.07%	-5.69%	-0.59%	8.57%	-2.39%	-7.45%

Quartile Q1 (Lowest) Q2 Q3 Q4 (Highest)

Figure A5.1: Effects of the EUDR on the EU countries, relative to a baseline without the EUDR. (a) Welfare changes (b) Price index changes (c) Producer price changes (d) Terms of trade change. Quartiles are measured at the scenario-product level.

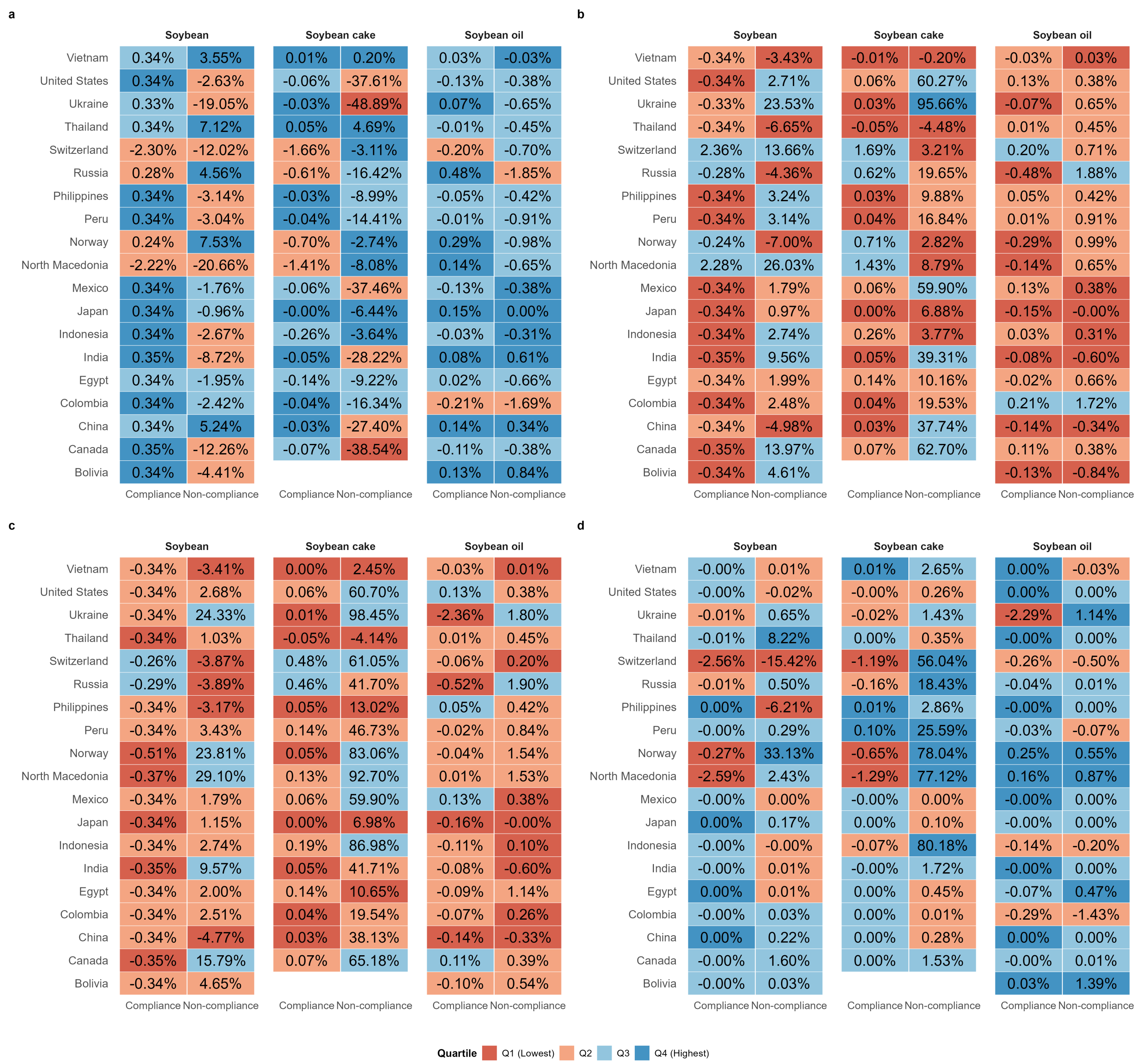

Figure A5.2: Effects of the EUDR on the selected countries, relative to a baseline without the EUDR. (a) Welfare changes (b) Price index changes (c) Producer price changes (d) Terms of trade change. Quartiles are measured at the scenario-product level.

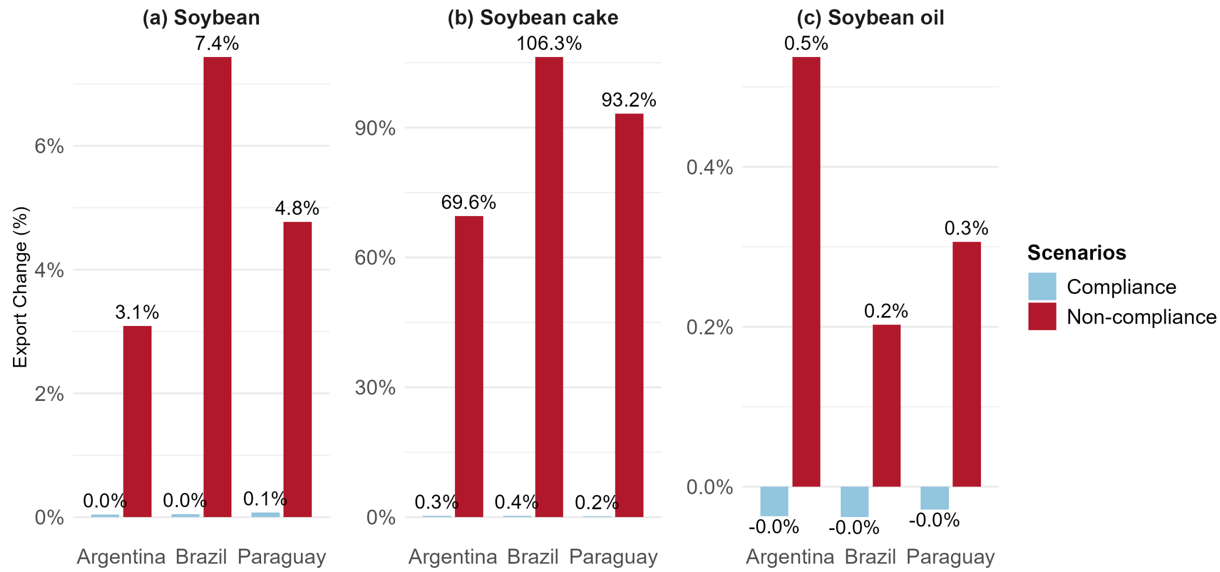

Figure A5.3: Change in exports from BAP assuming that supply remains constant, relative to a baseline without the EUDR. Quartiles are measured at the scenario-product level. The compliance and non-compliance scenarios are denoted by Com. and Non-com.

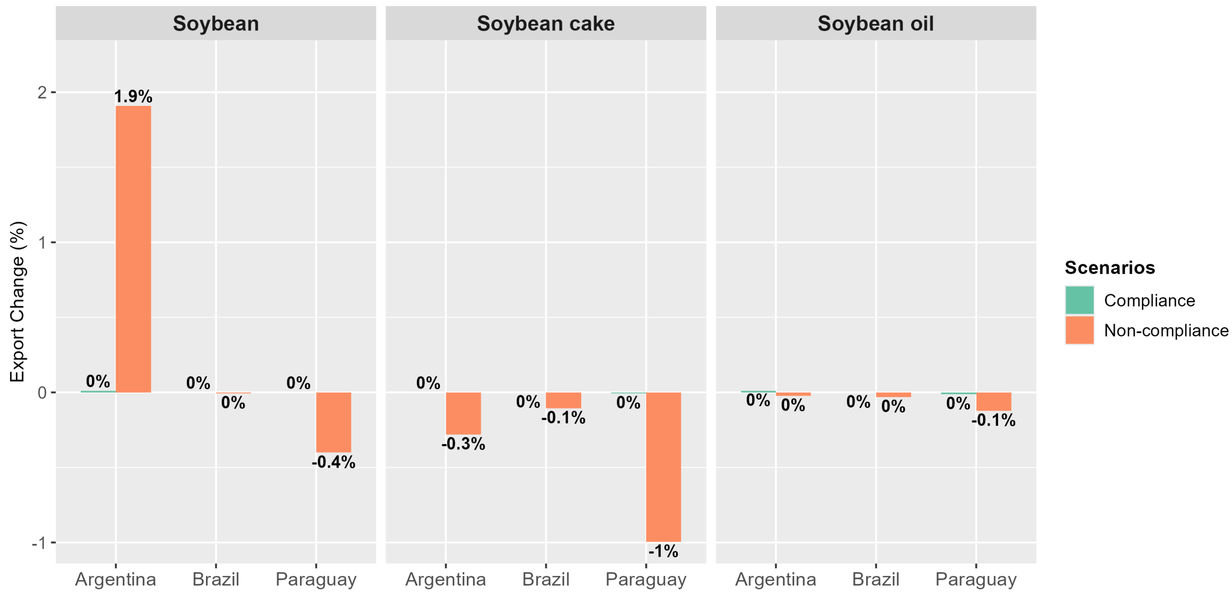

Figure A5.4: Change in exports from BAP with both supply and expenditure held constant, relative to a baseline without the EUDR. Quartiles are measured at the scenario-product level.

A.6 Sensitivity analysis

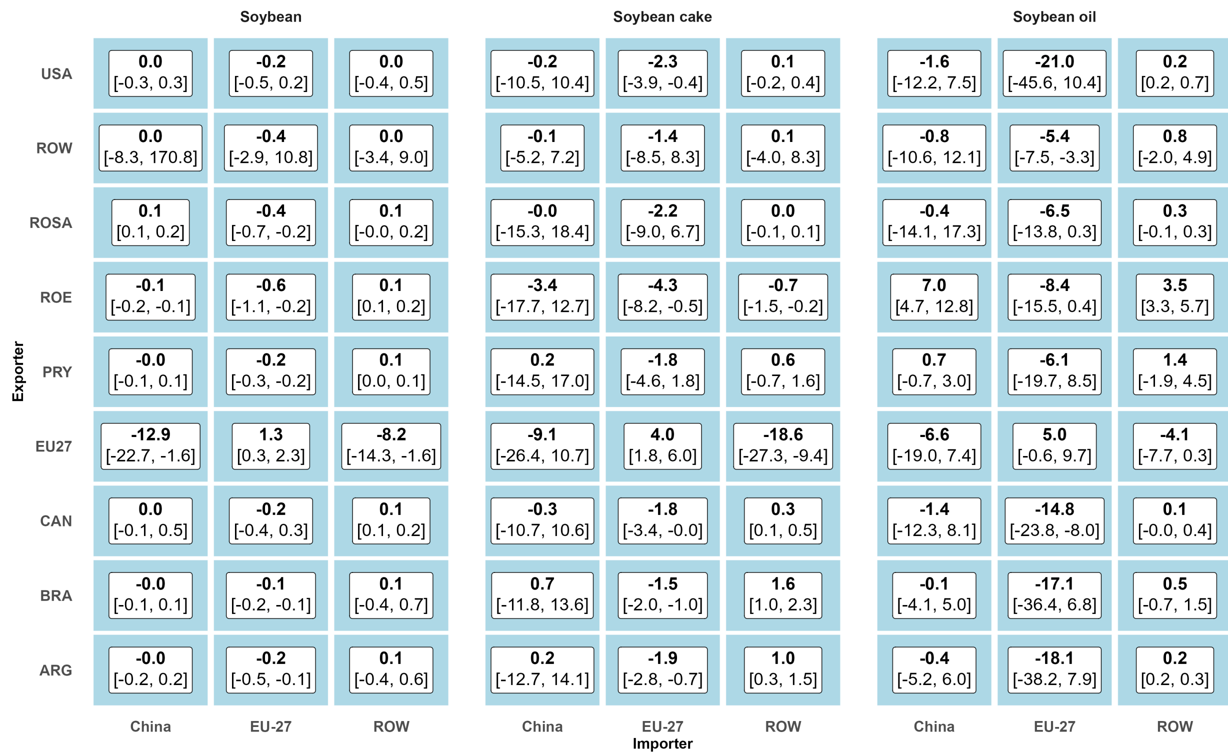

Figure A6.1: Sensitivity check under the compliance scenario. The left value in brackets denotes the minimum and the right value denotes the maximum across nine sub-scenarios, defined by three compliance cost levels (low, medium, and high) under lower, baseline, and upper-bound Armington elasticities. The bold value indicates the change in exports relative to the 2022 baseline without the EUDR, evaluated under the medium compliance cost and baseline Armington elasticities. "Low," "medium," and "high" compliance correspond to 2%, 6%, and 10% ad valorem tariff-equivalent compliance costs for EU imports, respectively.

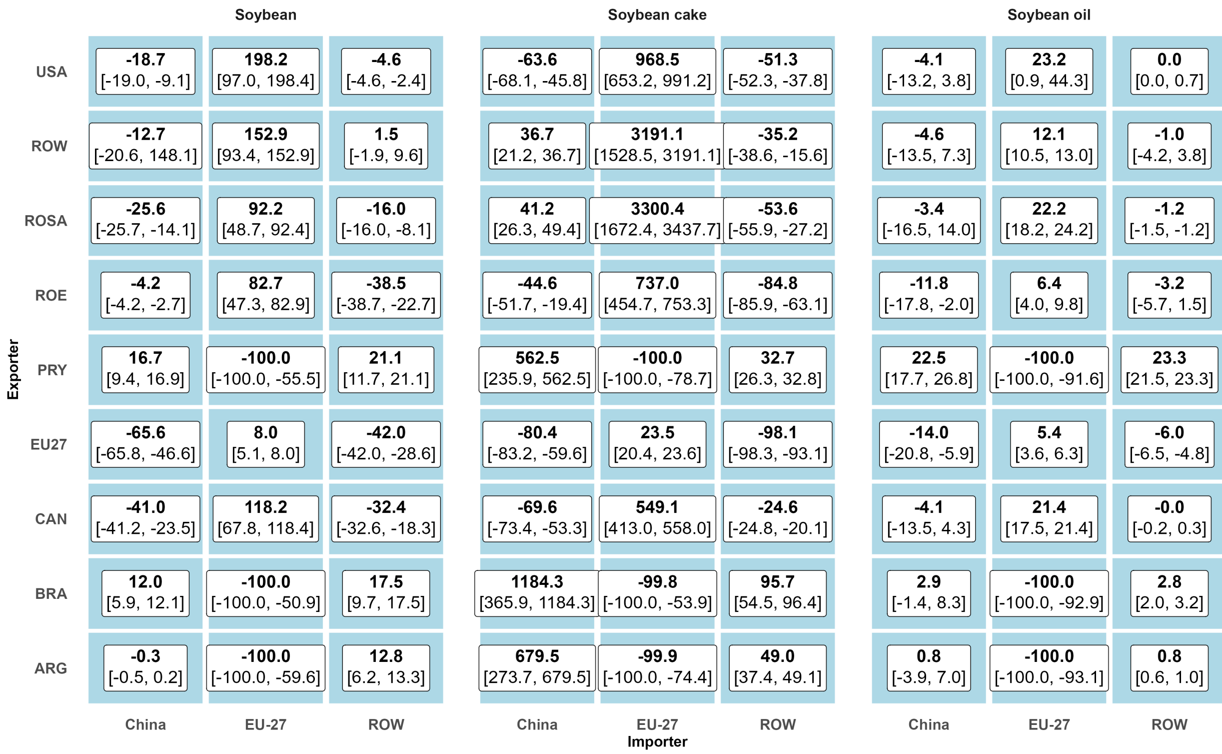

Figure A6.2: Sensitivity check under non-compliance. The left value in brackets denotes the minimum and the right value denotes the maximum across nine sub-scenarios, defined by three compliance cost levels (low, medium, and high) under lower, baseline, and upper-bound Armington elasticities. The bold value indicates the change in exports relative to the 2022 baseline without the EUDR, evaluated under the medium compliance cost and baseline Armington elasticities. “Low,” “medium,” and “high” compliance correspond to 2%, 6%, and 10% ad valorem tariff-equivalent compliance costs for EU imports, respectively.

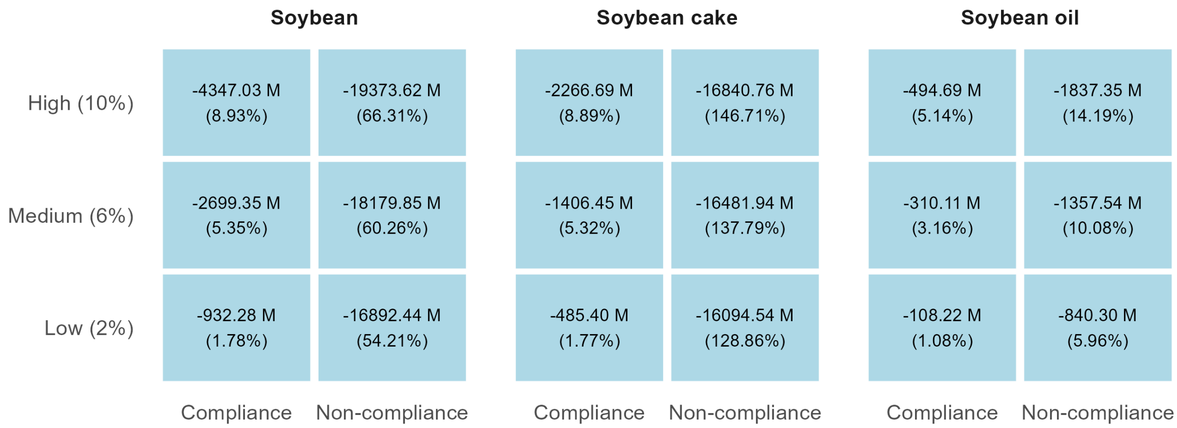

Figure A6.3: Sensitivity check for expenditure change under different compliance cost. Changes in expenditures are measured relative to the baseline year 2022 without the EUDR. Lower, medium and higher compliance denote 2%, 6% and 10% ad valorem tariff-equivalent compliance costs for EU imports.

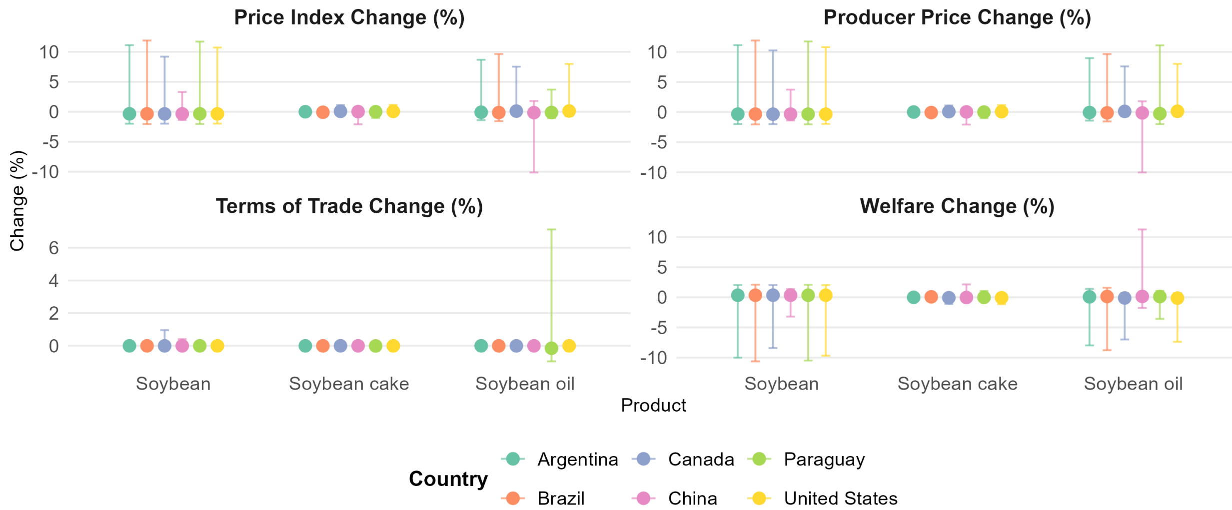

Figure A6.4: Sensitivity check for indexes under compliance. Changes in indexes are measured relative to the baseline year 2022 without the EUDR. Points in the error bar represents indices change evaluated under the medium compliance cost and baseline Armington elasticities. Error bars represents minimum and maximum across across nine sub-scenarios, defined by three compliance cost levels (low, medium, and high) under lower, baseline, and upper-bound Armington elasticities

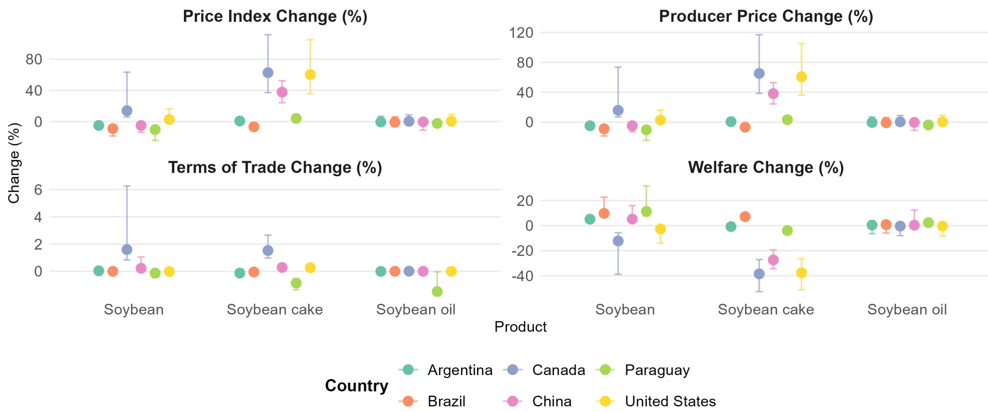

Figure A6.5: Sensitivity check for indexes under non-compliances. Changes in indexes are measured relative to the baseline year 2022 without the EUDR. Points in the error bar represents indices change evaluated under the medium compliance cost and baseline Armington elasticities. Error bars represents minimum and maximum across across nine sub-scenarios, defined by three compliance cost levels (low, medium, and high) under lower, baseline, and upper-bound Armington elasticities.

Appendix B

Appendix B: Chapter 2

A1. Selected countries by continent

Continent	Countries
Africa	Angola (AGO), Burundi (BDI), Benin (BEN), Burkina Faso (BFA), Botswana (BWA), Central African Republic (CAF), Côte d'Ivoire (CIV), Cameroon (CMR), Congo - Kinshasa (COD), Congo - Brazzaville (COG), Comoros (COM), Algeria (DZA), Egypt (EGY), Ethiopia (ETH), Gabon (GAB), Ghana (GHA), Guinea (GIN), Gambia (GMB), Guinea-Bissau (GNB), Equatorial Guinea (GNQ), Kenya (KEN), Liberia (LBR), Libya (LBY), Lesotho (LSO), Morocco (MAR), Madagascar (MDG), Mali (MLI), Mozambique (MOZ), Mauritius (MUS), Malawi (MWI), Namibia (NAM), Nigeria (NGA), Rwanda (RWA), Senegal (SEN), Sierra Leone (SLE), Somalia (SOM), Eswatini (SWZ), Chad (TCD), Togo (TGO), Tunisia (TUN), Tanzania (TZA), Uganda (UGA), South Africa (ZAF), Zambia (ZMB), Zimbabwe (ZWE)
Europe	Albania (ALB), Austria (AUT), Belgium (BEL), Bulgaria (BGR), Bosnia & Herzegovina (BIH), Belarus (BLR), Switzerland (CHE), Czechia (CZE), Germany (DEU), Denmark (DNK), Spain (ESP), Estonia (EST), Finland (FIN), France (FRA), United Kingdom (GBR), Greece (GRC), Croatia (HRV), Hungary (HUN), Ireland (IRL), Italy (ITA), Lithuania (LTU), Luxembourg (LUX), Latvia (LVA), Moldova (MDA), North Macedonia (MKD), Netherlands (NLD), Norway (NOR), Poland (POL), Portugal (PRT), Romania (ROU), Slovakia (SVK), Slovenia (SVN), Sweden (SWE), Ukraine (UKR)
North Asia	China (CHN), Kazakhstan (KAZ), Mongolia (MNG), Russia (RUS)

Continent	Countries
North and Central America	Antigua & Barbuda (ATG), Bahamas (BHS), Belize (BLZ), Canada (CAN), Costa Rica (CRI), Cuba (CUB), Dominican Republic (DOM), Guatemala (GTM), Honduras (HND), Haiti (HTI), Jamaica (JAM), St. Kitts & Nevis (KNA), St. Lucia (LCA), Mexico (MEX), Nicaragua (NIC), Panama (PAN), El Salvador (SLV), United States (USA), St. Vincent & Grenadines (VCT)
Oceania	Australia (AUS), Fiji (FJI), New Caledonia (NCL), New Zealand (NZL), Papua New Guinea (PNG), Solomon Islands (SLB), Vanuatu (VUT)
Rest of Asia	Afghanistan (AFG), Armenia (ARM), Azerbaijan (AZE), Bangladesh (BGD), Bhutan (BTN), Cyprus (CYP), Georgia (GEO), India (IND), Iran (IRN), Israel (ISR), Japan (JPN), Kyrgyzstan (KGZ), South Korea (KOR), Lebanon (LBN), Sri Lanka (LKA), Nepal (NPL), Pakistan (PAK), North Korea (PRK), Syria (SYR), Tajikistan (TJK), Turkey (TUR), Uzbekistan (UZB)
South America	Argentina (ARG), Bolivia (BOL), Brazil (BRA), Chile (CHL), Colombia (COL), Ecuador (ECU), Grenada (GRD), Guyana (GUY), Peru (PER), Paraguay (PRY), Suriname (SUR), Trinidad & Tobago (TTO), Uruguay (URY), Venezuela (VEN)
Southeast Asia	Brunei (BRN), Indonesia (IDN), Cambodia (KHM), Laos (LAO), Myanmar (Burma) (MMR), Malaysia (MYS), Philippines (PHL), Singapore (SGP), Thailand (THA), Timor-Leste (TLS), Vietnam (VNM)

A2. HS codes aggregation to commodities

Table A2.1: Aggregation of HS codes to commodities

Commodities	HS codes
Cassava	110814, 71410, 110620, 190300
Cattle	50400, 160250, 10290, 150200, 20130, 20230, 160100, 20220, 20610, 20622, 20629, 20621, 10210, 20110, 20120, 21020, 20210, 410190, 410419, 410150, 410120, 410411, 410449, 410712, 410719, 410711, 410441, 410792, 410799, 410791, 10229, 10221, 150290
Cocoa	180690, 180400, 180631, 180610, 180620, 180632, 180310, 180500, 180320, 180100, 180200
Coffee	90190, 90121, 90122, 90111, 210111, 210130, 210112, 90112
Fibre	520100, 240110, 240120, 520210, 520299, 530390, 240130, 140420, 520291, 520300, 530121, 530129, 530110, 530130, 530290, 530310, 530210, 530500
Fruits	80430, 80610, 80620, 220600, 80810, 80450, 81090, 81340, 80711, 81400, 81030, 81330, 200820, 81210, 81290, 200860, 80930, 80520, 200799, 220429, 200990, 80420, 80410, 220421, 80300, 80440, 80510, 220590, 80720, 200919, 200980, 200600, 81010, 220410, 80820, 80540, 81190, 200870, 200840, 81310, 81320, 220510, 80590, 80719, 81020, 200830, 200850, 80940, 81040, 81350, 200710, 200791, 200892, 200899, 80910, 80920, 81050, 81110, 200880, 200891, 220430, 200911, 110630, 81120, 200939, 200969, 80550, 200961, 200931, 200949, 200979, 200929, 81060, 200912, 200921, 200941, 200971, 81070, 80310, 80390, 80830, 200989, 80840, 80929, 80921, 200897, 200893, 200981

Commodities	HS codes
Maize	100590, 110220, 151529, 100510, 110313, 200580, 71040, 151521, 230210
Nuts	80250, 80211, 80212, 80119, 80240, 80231, 80290, 200819, 80122, 80221, 80222, 80132, 80232, 80131, 80121, 80260, 80251, 80252, 80241, 80242, 80261, 80262, 80270, 80280
Other cereals	190590, 100700, 220300, 110100, 121490, 110290, 100110, 230230, 190120, 190219, 190190, 100300, 100190, 190211, 100820, 110311, 110412, 110423, 110429, 190110, 190490, 190520, 230240, 100200, 100810, 100830, 100890, 110430, 110710, 190410, 190540, 100400, 110419, 110210, 110720, 121300, 190510, 110319, 190420, 110422, 230800, 190531, 190532, 110320, 190430, 100210, 100390, 100860, 100199, 100790, 100821, 100829, 100119, 100490, 100710, 100850, 100111, 100191, 100290, 100410, 100310, 100840
Other oilseeds	151590, 120799, 150990, 151211, 151219, 210330, 120600, 120720, 120220, 120740, 151511, 151519, 120210, 120400, 230630, 230620, 151229, 230610, 151530, 151221, 120760, 230690, 120791, 151550, 120890, 120750, 120730, 151411, 120510, 120590, 230641, 230649, 151499, 151419, 151491, 120241, 120770, 70992, 120729, 120230, 120721, 80112
Palm	230660, 120999, 151190, 151321, 151329, 151110
Pulses	71390, 71331, 71332, 71333, 71339, 71350, 71340, 71310, 71320, 110610, 230250, 71360, 71335, 71334
Rice	100620, 100630, 100640, 100610
Rubber	400121, 400129, 400122, 400110, 400130

Commodities	HS codes
Soybeans	210390, 150790, 150710, 120100, 230400, 210610, 120810, 210310, 120110, 120190
Stimulants	90930, 121190, 330129, 90950, 330190, 91099, 90210, 90220, 90920, 121010, 130219, 330130, 90412, 91010, 90240, 90230, 90300, 330113, 91020, 330112, 330125, 90420, 121020, 330119, 330124, 91091, 90411, 90620, 90700, 90810, 90910, 210120, 90500, 90830, 91030, 90940, 90820, 90611, 90619, 90831, 90922, 90931, 90932, 90962, 91012, 90421, 90921, 90961, 91011, 90422, 90510, 90520, 90720, 90812, 90811, 90821, 90822, 90832, 90710
Sugar crops	170290, 170410, 170490, 170199, 121291, 170112, 170310, 170230, 170390, 170219, 170111, 170211, 170240, 170191, 170260, 170220, 230320, 121293, 170114, 170113
Vegetables	71290, 70200, 70390, 70700, 70990, 70951, 71080, 71490, 121299, 70190, 70820, 71190, 200190, 200290, 200490, 200559, 70810, 70890, 71029, 71090, 200210, 200110, 70310, 70690, 70960, 70320, 70410, 70610, 71220, 70521, 200551, 70920, 200310, 200520, 200540, 70110, 71010, 71021, 71022, 71030, 110520, 200410, 70490, 70519, 70511, 70930, 70940, 110510, 200560, 200950, 70420, 71420, 121292, 70529, 200510, 70970, 71140, 200320, 200390, 70959, 71151, 71159, 71231, 71239, 71233, 71232, 200599, 200591, 70993, 70999, 121294, 70991, 71440, 71430, 71450

A3. DeDuCe model

This model combines high-resolution spatial datasets on land cover change with agricultural statistics to estimate forest loss associated with the expansion of particular commodities globally. The DeDuCE model employs a spatial attribution approach that overlays multiple spatial datasets, including cropland extent maps, forest plantation data, pasture maps, and specific commodity maps (such as soybeans, cocoa, and oil palm), with annual tree cover loss data from the Global Forest Change dataset at 30-meter resolution. This spatial overlay identifies direct forest loss pixels attributed to land use for commodity production. When forest loss pixels cannot be spatially attributed to specific commodities, the model employs a statistical land-balance approach using FAOSTAT agricultural statistics to determine the likely drivers of deforestation based on changes in harvested areas and production. For example: if spatial attribution identifies that forest loss pixels (100 ha) are attributed to cropland expansion but cannot explicitly identify specific crops, the statistical method determines what crops have expanded in that area. If maize area expanded by 60% and soybean by 40% of total crop expansion, then 60 ha are attributed to maize and 40 ha to soybean. The model accounts for land-use change dynamics including competition between cropland and pasture, incorporating a 3-year lag period to capture delays between forest clearing and agricultural establishment. In this model, roughly 42–50% of attributed deforestation is assigned using spatial attribution (about 12–15% from commodity-specific maps and about 30–35% from broader land-use layers), while the remaining 50–58% is allocated using the model's statistical land-balance procedure.

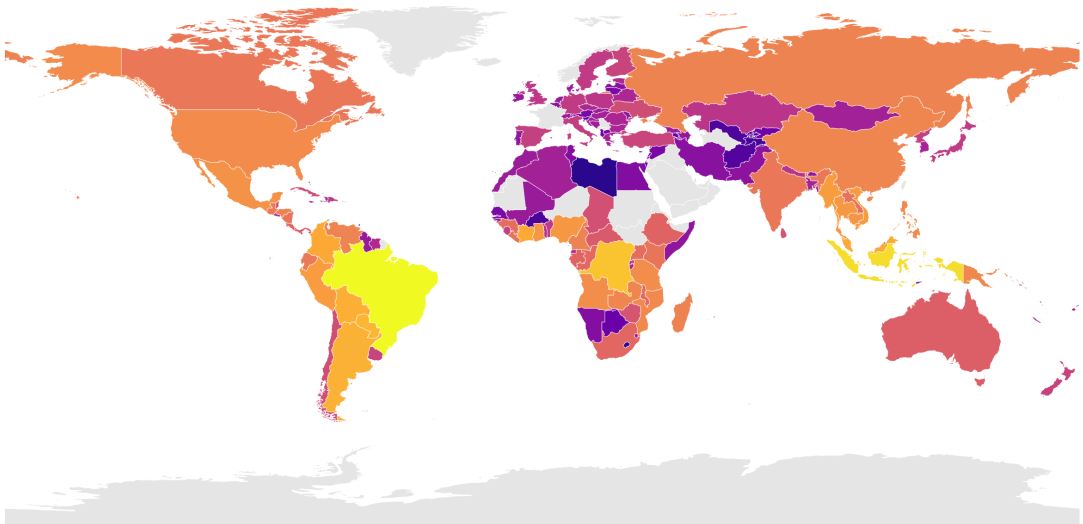

Figure A3.1: Accumulated deforestation attributed to selected commodities over the period 2000–2022. Source: Singh and Persson (2024)

A4. Primary commodities aggregation to commodities

Table A4.1: Aggregation of primary commodities to commodities

Commodity Group	Commodity from DeDuce Model	Products (FCL item code)
Cassava	Cassava, fresh; Cassava leaves	125, 126, 127, 128, 129
Cocoa	Cocoa beans	
Coffee	Coffee, green	656, 657, 658, 659, 660

Commodity Group	Commodity from DeDuce Model	Products (FCL item code)
Fibre	Seed cotton, unginned; Kenaf, and other textile bast fibres, raw or retted; Sisal, raw; Flax, processed but not spun; Other fibre crops, raw, n.e.c.; True hemp, raw or retted; Jute, raw or retted; Flax, raw or retted; Ramie, raw or retted; Agave fibres, raw, n.e.c.; Abaca, manila hemp, raw	
Fruits	Apples; Apricots; Cantaloupes and other melons; Figs; Grapes; Oranges; Other berries and fruits of the genus vaccinium n.e.c.; Other citrus fruit, n.e.c.; Other fruits, n.e.c.; Other stone fruits; Peaches and nectarines; Pears; Plums and sloes; Watermelons; Cherries; Dates; Lemons and limes; Quinces; Sour cherries; Strawberries; Tangerines, mandarins, clementines; Bananas; Pomelos and grapefruits; Pineapples; Mangoes, guavas and mangosteens; Other tropical fruits, n.e.c.; Avocados; Papayas; Blueberries; Currants; Kiwi fruit; Persimmons; Raspberries; Gooseberries; Cranberries; Plantains and cooking bananas; Cashewapple; Guavas; Mangoes; Other tropical and subtropical fruits, n.e.c.; Tangerines and mandarins; Other pome fruits; Kapok fruit	486, 489, 490, 491, 492, 495, 496, 497, 498, 499, 507, 509, 510, 512, 513, 514, 515, 517, 518, 519, 521, 523, 526, 527, 530, 531, 534, 536, 537, 541, 544, 547, 549, 550, 552, 554, 558, 560, 561, 562, 563, 564, 565, 566, 567, 568, 569, 570, 571, 572, 574, 575, 576, 577, 580, 583, 584, 587, 591, 592, 600, 603, 604, 619, 620, 622, 623, 624, 625, 626, 628
Maize	Maize (corn); Green corn (maize)	56, 57, 58, 59, 60, 61, 446, 447, 448, 636

Commodity Group	Commodity from DeDuce Model	Products (FCL item code)
Nuts	Almonds, in shell; Chestnuts, in shell; Pistachios, in shell; Walnuts, in shell; Other nuts (excluding wild edible nuts and groundnuts), in shell, n.e.c.; Cashew nuts, in shell; Hazelnuts, in shell; Areca nuts; Kola nuts	216, 217, 220, 221, 222, 223, 224, 225, 226, 229, 230, 231, 232, 233, 234, 235
Other cereals	Barley; Millet; Wheat; Oats; Rye; Canary seed; Cereals n.e.c.; Mixed grain; Buckwheat; Fonio; Quinoa; Triticale; Sorghum	15, 16, 17, 18, 19, 20, 21, 22, 41, 44, 45, 46, 47, 48, 49, 50, 51, 71, 72, 73, 75, 76, 77, 79, 80, 81, 83, 84, 85, 89, 90, 91, 92, 94, 97, 101, 103, 104, 105, 108, 109, 110, 111, 112, 113, 114, 115, 635
Other oilseeds	Linseed; Olives; Sesame seed; Sunflower seed; Groundnuts, excluding shelled; Rape or colza seed; Castor oil seeds; Safflower seed; Other oil seeds, n.e.c.; Poppy seed; Coconuts, in shell; Karite nuts (sheanuts); Mustard seed; Melonseed; Hempseed; Tallowtree seeds; Jojoba seeds; Tung nuts	242, 249, 260, 263, 265, 266, 267, 268, 269, 270, 271, 272, 275, 276, 278, 280, 281, 282, 289, 290, 291, 292, 293, 294, 295, 296, 297, 299, 306, 311, 313, 314, 329, 331, 332, 333, 334, 335, 336, 338, 339, 340, 341, 343

Commodity Group	Commodity from DeDuce Model	Products (FCL item code)
Palm	Oil palm fruit; Palm nuts and kernels	256, 257, 258, 259
Pasture	Cattle meat; Leather	
Pulses	Beans, dry; Broad beans and horse beans, dry; Other pulses n.e.c.; Chick peas, dry; Lentils, dry; Peas, dry; Pigeon peas, dry; Cow peas, dry; Lupins; Vetches; Bambara beans, dry; Pulses, n.e.c.	
Rice	Rice	27, 28, 29, 30, 31, 32, 35, 36, 37, 38, 39
Rubber	Natural rubber in primary forms	836, 837, 839
Soybeans	Soya beans	236, 237, 238, 239, 240
Stimulants	Anise, badian, coriander, cumin, caraway, fennel and juniper berries, raw; Other stimulant, spice and aromatic crops, n.e.c.; Hop cones; Unmanufactured tobacco; Chillies and peppers, dry (Capsicum spp., Pimenta spp.), raw; Maté leaves; Peppermint, spearmint; Tea leaves; Ginger, raw; Pepper (Piper spp.), raw; Nutmeg, mace, cardamoms, raw; Cinnamon and cinnamon-tree flowers, raw; Cloves (whole stems), raw; Vanilla, raw; Pyrethrum, dried flowers; Stimulant, spice and aromatic crops, n.e.c.	
Sugar	Sugar beet; Sugar cane; Other sugar crops n.e.c.	

Commodity Group	Commodity from DeDuce Model	Products (FCL item code)
Vegetables	Onions and shallots, dry (excluding dehydrated); Other vegetables, fresh n.e.c.; Potatoes; Broad beans and horse beans, green; Cabbages; Carrots and turnips; Cauliflowers and broccoli; Chillies and peppers, green (Capsicum spp. and Pimenta spp.); Cucumbers and gherkins; Eggplants (aubergines); Green garlic; Leeks and other alliaceous vegetables; Lettuce and chicory; Okra; Onions and shallots, green; Other beans, green; Peas, green; Pumpkins, squash and gourds; Spinach; Tomatoes; Artichokes; String beans; Asparagus; Sweet potatoes; Taro; Yams; Chicory roots; Edible roots and tubers with high starch or inulin content, n.e.c., fresh; Yautia	358, 366, 367, 372, 373, 388, 390, 391, 392, 393, 394, 397, 399, 401, 402, 403, 406, 407, 414, 417, 420, 423, 426, 430, 449, 450, 451, 459, 460, 461, 463, 465, 466, 469, 471, 472, 473, 474, 475, 476, 116, 117, 118, 120, 121, 122, 135, 136, 137, 149, 150, 151

A5. Statistics of shares

Table A5.1: Descriptive statistics of shares

Commodity / Variable	Minimum	Mean	Median	Maximum	SD	N
Panel A: Total						
Share (total)	0.00000	0.00192	0.00000	1.00000	0.02318	2,111,044
Panel B: By commodities						
Cassava	0.00000	0.01558	0.00014	1.00000	0.08153	12,839
Cattle	0.00000	0.00201	0.00001	1.00000	0.02059	114,623
Cocoa	0.00000	0.00327	0.00001	1.00000	0.02948	70,107
Coffee	0.00000	0.00382	0.00001	1.00000	0.02907	59,896
Fibre	0.00000	0.00415	0.00002	1.00000	0.03529	53,736
Fruits	0.00000	0.00052	0.00000	0.94237	0.00866	439,107
Maize	0.00000	0.00585	0.00001	1.00000	0.04816	38,277
Nuts	0.00000	0.00309	0.00001	1.00000	0.03079	74,210
Other cereals	0.00000	0.00088	0.00000	0.99941	0.01235	261,766
Other oilseeds	0.00000	0.00177	0.00000	1.00000	0.02191	129,434
Palm	0.00000	0.00969	0.00007	1.00000	0.05980	22,611
Pulses	0.00000	0.00404	0.00003	1.00000	0.03440	54,911

Commodity / Variable	Minimum	Mean	Median	Maximum	SD	N
Rice	0.00000	0.00922	0.00004	1.00000	0.05715	24,399
Rubber	0.00000	0.01151	0.00011	1.00000	0.07063	17,991
Soybeans	0.00000	0.00426	0.00001	1.00000	0.03521	54,001
Stimulants	0.00000	0.00087	0.00000	0.98030	0.01207	264,959
Sugar crops	0.00000	0.00237	0.00001	0.99467	0.02450	97,112
Vegetables	0.00000	0.00072	0.00000	1.00000	0.01092	321,065

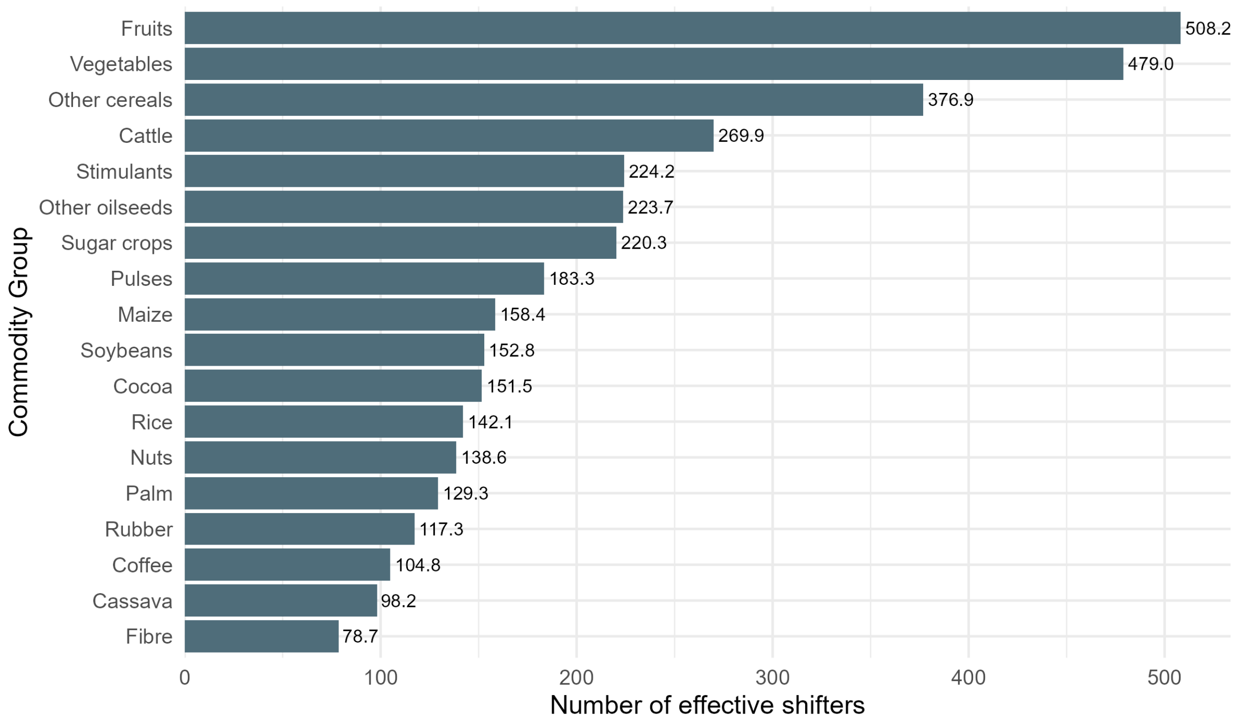

Figure A5.1: Number of effective shifters by commodity groups. Source: Own illustration.

A6. Statistics of shifts

Table A6.1: Descriptive statistics of shifts

Commodity / Variable	Mean	P10	Median	P90	SD	N
Panel A: Total						
Shift (total)	8.29767	4.27667	8.57320	11.86529	2.92173	6,920,563
Panel B: By commodities						
Cassava	6.47454	2.48491	6.82329	9.53175	2.78040	29,734
Cocoa and cocoa products	9.89053	6.10702	10.28766	13.08350	2.79632	215,031
Coffee	9.40580	4.99043	10.05878	12.87376	3.01161	226,124

Commodity / Variable	Mean	P10	Median	P90	SD	N
Fibre crops	8.09431	3.13549	8.40358	12.55261	3.52425	167,439
Fruits	8.13329	4.26268	8.33950	11.67911	2.87209	1,542,195
Maize	8.04850	4.04305	8.13535	12.00712	2.99576	162,905
Nuts	7.76191	3.40120	8.14700	11.43201	3.04384	257,304
Other cereals	8.85909	5.16479	9.10941	12.17021	2.74374	966,333
Other oilseeds	7.41397	3.46574	7.61481	11.00836	2.89482	490,566
Palm	9.44513	5.05625	9.97548	13.02262	3.13321	50,283
Pasture (Cattle meat + leather)	8.93946	5.12396	9.17585	12.56354	2.87632	161,857
Pulses and legumes	7.31647	3.55535	7.55276	10.65265	2.71470	194,117
Rice	9.12667	5.03044	9.58590	12.47222	2.82509	191,346
Rubber	8.52294	3.61092	9.09515	12.66370	3.49068	57,031
Soybeans	8.88528	4.55388	9.11295	13.03727	3.18250	107,863
Stimulants, spices and aromatic crops	7.86041	4.26268	8.06369	11.13303	2.64304	611,729
Sugar crops	8.89968	5.11199	9.34027	11.94509	2.69916	392,226
Vegetables	7.97256	4.00733	8.31214	11.36130	2.82742	1,096,480

A7. First stage and instrument strength

Table A7.1: Commodity-level first stage: predictive power of $\widehat{FD}_{ikt}$ on log exports

Commodity Group	Coefficient	Std. Error	F-statistic	Observations
Cassava	0.2602**	(0.1098)	5.62	1,016
Cocoa and cocoa products	0.2432	(0.2156)	1.27	1,039
Coffee	0.8557**	(0.3468)	6.09	1,356
Fibre crops	0.0370	(0.1646)	0.05	2,208
Fruits	0.9338***	(0.2239)	17.40	3,259
Maize	0.0354	(0.0755)	0.22	2,326
Nuts	0.5359***	(0.1146)	21.85	2,144
Other cereals	0.1828	(0.1739)	1.10	2,706
Other oilseeds	0.4198***	(0.0974)	18.57	2,848
Palm	-0.1143	(0.1607)	0.51	922
Pasture (Cattle meat + leather)	0.4505**	(0.1932)	5.44	2,791
Pulses and legumes	0.2583**	(0.1181)	4.79	2,526
Rice	-0.0383	(0.1311)	0.09	1,799
Rubber	0.1283	(0.1261)	1.03	597
Soybeans	0.4671***	(0.1520)	9.44	1,957

Commodity Group	Coefficient	Std. Error	F-statistic	Observations
Stimulants, spices and aromatic crops	0.5673***	(0.1489)	14.52	2,863
Sugar crops	0.8243***	(0.2548)	10.46	2,453
Vegetables	0.4384***	(0.1110)	15.61	3,138

Note: Each row is a separate OLS regression of log exports on $\widehat{FD}_{ikt}$ with country and year fixed effects. Standard errors are clustered at country–commodity and year levels. * $p < 0.10$, ** $p < 0.05$, *** $p < 0.01$.

Table A7.2: Continent-level first stage: predictive power of $\widehat{FD}_{ikt}$ on log exports

Continent	Coefficient	Std. Error	F-statistic	Observations
Africa	0.8835***	(0.0942)	87.88	10,257
Europe	0.5922***	(0.2221)	7.11	8,146
North and Central America	0.8565***	(0.1594)	28.89	4,645
North Asia	0.3748	(0.2480)	2.28	1,053
Oceania	1.1175***	(0.2540)	19.35	1,328
Rest of Asia	0.6482***	(0.1454)	19.87	5,463
South America	1.0638***	(0.2182)	23.78	3,959
Southeast Asia	0.2828*	(0.1631)	3.01	3,097

Note: Each row is a separate OLS regression of log exports on $\widehat{FD}_{ikt}$ for all country-commodity observations within the continent, with country and year fixed effects. Standard errors are clustered at country–commodity and year levels. * $p < 0.10$, ** $p < 0.05$, *** $p < 0.01$.

Table A7.3: Strength check of instrument $\widehat{FD}_{ikt}$

	Level	log(def+1)	asinh(def)	log(def)
Instrument	$\widehat{FD}_{ikt-1}$	$\widehat{FD}_{ikt-1}$	$\widehat{FD}_{ikt-1}$	$\widehat{FD}_{ikt-1}$
First-stage F-stat	3382.74	3382.74	3382.74	2971.78
Observations	37,948	37,948	37,948	30,809
Country × Year FE	Yes	Yes	Yes	Yes
Commodity × Year FE	Yes	Yes	Yes	Yes

Note: First-stage F-statistics from 2SLS using $\widehat{FD}_{ikt}$ as instrument for log exports across alternative deforestation outcome transformations. Standard errors are clustered at country–commodity and year levels.

A8. Cumulative export growth between 2001-2003 and 2020-2022

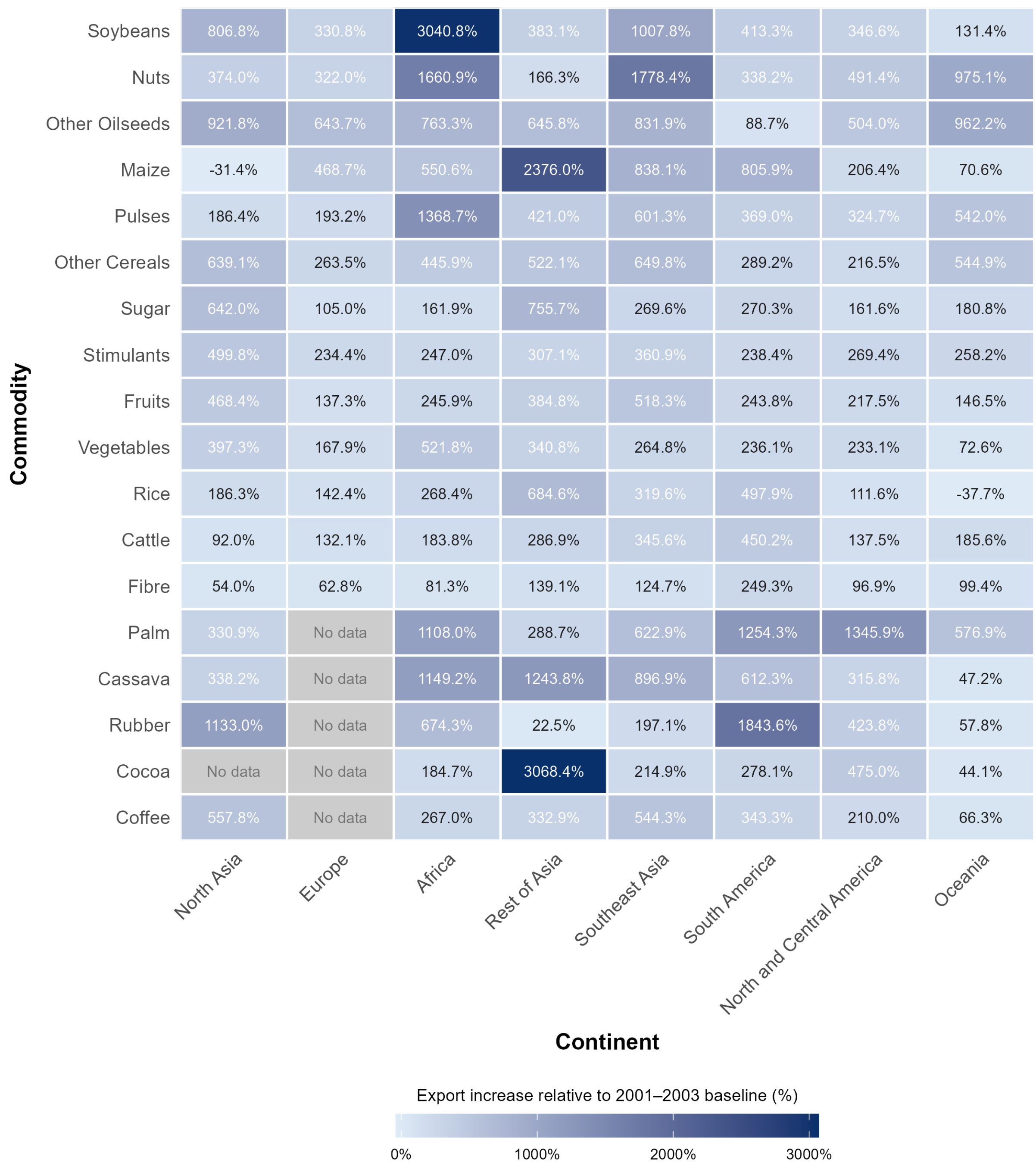

Figure A8.1: Cumulative export growth of commodity by region between 2001-2003 and 2020-2022

Note: Export growth of commodities across region taking cumulative export of 2001–2003 as intial value and cumulative export of 2020-2022 as final value. Grey cells indicate no data taken for study.

A9. Bootstrap procedure

We obtain inference for the CF–PPML estimator via a block bootstrap aligned with the panel structure of the data. The full-sample control-function (CF) model is first estimated as described in the empirical strategy section, using the same country-by-year and commodity-by-year fixed effects in both stages.

- **First stage:** We regress $\log X_{ikt}$ on $\widehat{FD}_{ikt}$ and the fixed effects to produce residuals $\hat{\nu}_{ikt}$.
- **Second stage:** We estimate the PPML including $\log X_{ikt}$, $\hat{\nu}_{ikt}$, and the same fixed effects, yielding estimates of $\hat{\alpha}$ (the elasticity of deforestation with respect to foreign demand/exports) and $\hat{\delta}$ (the control-function coefficient used for the endogeneity test).

Resampling proceeds by treating each country–commodity panel (i, k) as a block containing its complete time series. Our dataset consists of 2001 such blocks. For each bootstrap replication, we sample, with replacement, 2001 blocks (the same number as in the original data), stack the selected panels to form the bootstrap sample (allowing duplicates), and re-estimate both stages exactly as in the full-sample procedure, recomputing the first-stage residuals within the bootstrap sample. We repeat this 1000 times, and use the resulting covariance matrix of the bootstrap draws to obtain "bootstrap standard errors" for $\hat{\alpha}$ and $\hat{\delta}$:

$$\widehat{\text{SE}}_{\text{boot}}(\hat{\alpha}) = \sqrt{\widehat{\text{Var}}_{\text{boot}}(\hat{\alpha})}, \qquad \widehat{\text{SE}}_{\text{boot}}(\hat{\delta}) = \sqrt{\widehat{\text{Var}}_{\text{boot}}(\hat{\delta})}.$$

In our main results, we report these bootstrap-based standard errors together with significance stars derived from the same bootstrap distribution. For each coefficient (e.g. $\hat{\alpha}$), we construct its empirical bootstrap distribution, center this distribution on the full-sample estimate, and compute a two-sided bootstrap p-value as

$$p_{\text{boot}}(\hat{\alpha}) = 2 \times \min\left\{ \Pr(\tilde{\alpha}^* \leq 0),\, \Pr(\tilde{\alpha}^* \geq 0)\right\},$$

where $\tilde{\alpha}^*$ denotes draws from the centered bootstrap distribution of $\hat{\alpha}$, and the probabilities are calculated as empirical proportions over the 1000 replications. The same procedure is applied to

$\hat{\delta}$. Significance stars in the results are then assigned according to these bootstrap p-values: $***$ if $p_{\text{boot}} < 0.01$, $**$ if $p_{\text{boot}} < 0.05$, $*$ if $p_{\text{boot}} < 0.10$, and no star otherwise. Because both the 95% confidence intervals and the p-values are derived from the same bootstrap distribution (via percentiles and tail probabilities, respectively), a coefficient whose 95% bootstrap percentile interval excludes zero will correspondingly receive at least two stars ($**$). This block bootstrap design preserves within-panel serial correlation and arbitrary heteroskedasticity and is consistent with our maintained assumption that unobserved shocks are most strongly correlated within country–commodity panels over time.

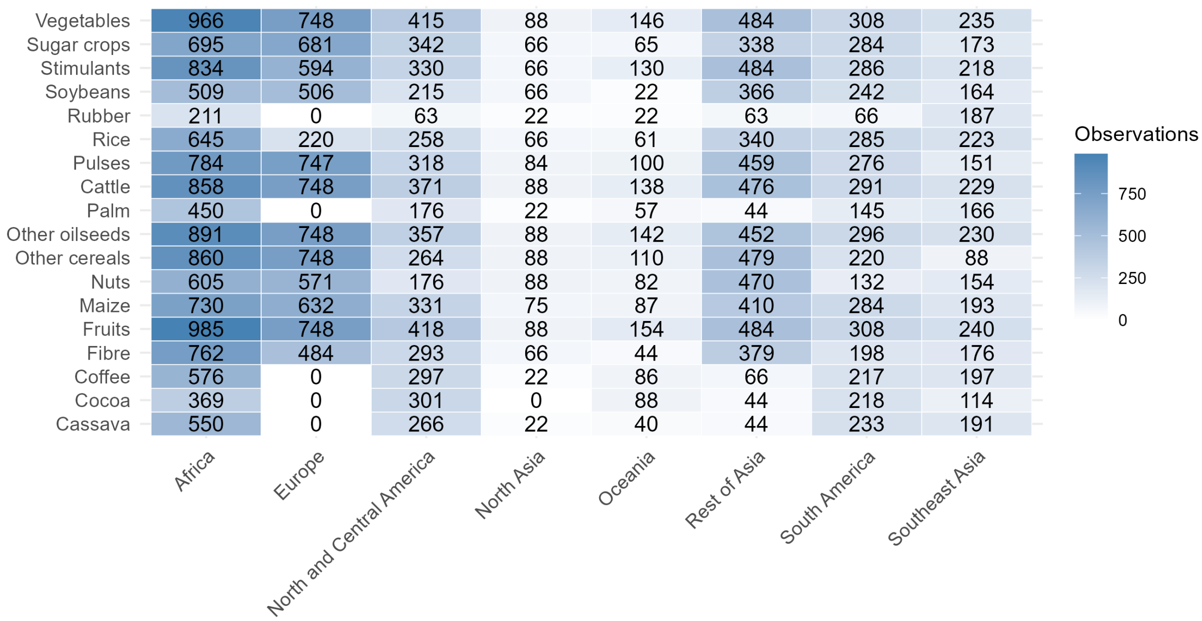

Figure A10.1: Number of observations by continent and commodity group. Source: Own illustration.

A10. Panel structure of country-commodity

A11. Specifications to estimate effects of export sales

First, we estimate the first-stage estimation as shown in equation (6). Then, we estimate the residuals from first-stage, and then use it in second stage regression, which is called as two-stage residual inclusion (2-SRI).

Specification 1: Pooled effect estimation:

$$C_{ikt} = \exp(\gamma \log X_{ikt} + \alpha_{it} + \alpha_{kt} + \delta \widehat{\nu_{ikt}})\varepsilon_{ikt}. \qquad (A11.1)$$

Specification 2: Heterogeneous effect by commodity group: Let $g \in G$ index commodity groups and $\mathbb{1}_{k=g}$ be the indicator for group g. Then:

$$C_{ikt} = \exp(\sum_{g \in G} \gamma_g \log X_{ikt} \mathbb{1}_{k=g} + \alpha_{it} + \alpha_{kt} + \delta \widehat{\nu_{ikt}})\varepsilon_{ikt}. \qquad (A11.2)$$

Specification 3: Heterogeneous effect by continent: Let $r(i) \in R$ index continent of country i and $\mathbb{1}_{r(i)=r}$ be the indicator for continent r. Then:

$$C_{ikt} = \exp(\sum_{r \in R} \gamma_r \log X_{ikt} \mathbb{1}_{r(i)=r} + \alpha_{it} + \alpha_{kt} + \delta \widehat{\nu_{ikt}})\varepsilon_{ikt}. \qquad (A11.3)$$

Specification 4: Heterogeneous effect by continent-commodity pair:

$$C_{ikt} = \exp(\sum_{g \in G} \sum_{r \in R} \gamma_{gr} \log X_{ikt} \mathbb{1}_{k=g} \mathbb{1}_{r(i)=r} + \alpha_{it} + \alpha_{kt} + \delta \widehat{\nu_{ikt}})\varepsilon_{ikt}. \qquad (A11.4)$$

A12. Alternative specifications

Table A12.1: Effect of export sales on deforestation across multiple forms of deforestation

	Level	log(def+1)	asinh(def)	log(def)
Log Exports	1017.836**	0.306***	0.325***	0.591***
	(458.983)	(0.042)	(0.046)	(0.131)
Observations	37948	37948	37948	30809
Country × Year FE	X	X	X	X
Commodity × Year FE	X	X	X	X

* p < 0.1, ** p < 0.05, *** p < 0.01

Notes: 2SLS estimates. Standard errors clustered by country–commodity and year. * p<0.10, ** p<0.05, *** p<0.01.

Notes: Standard errors clustered by country and year in parentheses. All models use 2SLS with country-year and commodity-year fixed effects, instrumenting exports with $\widehat{FD}_{ikt}$. * $p < 0.1$, ** $p < 0.05$, *** $p < 0.01$.

Table A12.2: Effect of export sales on deforestation by commodity across multiple forms of deforestation

	Level	Log(def+1)	Asinh(def)	Log(def)
Cassava	-2531.676	-0.109	-0.111	0.152
	(1905.129)	(0.115)	(0.123)	(0.284)
Cocoa	-940.997	0.099	0.104	0.755*
	(1869.069)	(0.116)	(0.125)	(0.380)
Coffee	-592.799	0.259**	0.277**	0.580*
	(1348.940)	(0.098)	(0.106)	(0.323)
Fibre	234.909	0.259***	0.276***	0.354
	(731.642)	(0.070)	(0.075)	(0.208)
Fruits	475.140	0.309***	0.328***	0.630***
	(473.049)	(0.054)	(0.058)	(0.135)
Maize	363.713	0.258***	0.273***	0.589**

	Level	Log(def+1)	Asinh(def)	Log(def)
	(586.383)	(0.064)	(0.069)	(0.213)
Nuts	-80.287	0.352***	0.386***	0.501**
	(969.407)	(0.082)	(0.088)	(0.203)
Other Cereals	733.902	0.539***	0.577***	1.032***
	(467.570)	(0.064)	(0.069)	(0.161)
Other Oilseeds	489.271	0.461***	0.496***	0.799***
	(534.372)	(0.057)	(0.061)	(0.152)
Palm	4507.083	0.411**	0.435**	0.617**
	(4634.436)	(0.158)	(0.169)	(0.233)
Cattle	7050.486	0.295***	0.290***	0.671***
	(5297.887)	(0.076)	(0.082)	(0.148)
Pulses	212.573	0.345***	0.375***	0.764***

	Level	Log(def+1)	Asinh(def)	Log(def)
	(625.296)	(0.069)	(0.074)	(0.186)
Rice	34.347	0.263***	0.280***	0.222
	(817.116)	(0.070)	(0.075)	(0.241)
Rubber	2034.572	0.859***	0.901***	1.193***
	(2513.188)	(0.213)	(0.222)	(0.291)
Soybeans	1413.161**	0.442***	0.470***	0.824***
	(649.157)	(0.081)	(0.087)	(0.270)
Stimulants	397.078	0.329***	0.351***	0.557***
	(636.366)	(0.066)	(0.072)	(0.194)
Sugar	506.948	0.292***	0.307***	0.289
	(503.931)	(0.063)	(0.068)	(0.228)
Vegetables	433.872	0.297***	0.319***	0.655***

	Level	Log(def+1)	Asinh(def)	Log(def)
	(471.737)	(0.052)	(0.056)	(0.145)
Observations	37948	37948	37948	30809

* p < 0.1, ** p < 0.05, *** p < 0.01

Notes: Standard errors clustered by country and year in parentheses. All models use 2SLS with country-year and commodity-year fixed effects, instrumenting exports with $\widehat{FD}_{ikt}$. * p < 0.1, ** p < 0.05, *** p < 0.01.

Table A12.3: Effect of export sales on deforestation by continent across multiple forms of deforestation

	Level	Log(def+1)	Asinh(def)	Log(def)
Africa	326.205	0.209***	0.222***	0.320*
	(502.981)	(0.060)	(0.064)	(0.161)
Europe	15.532	0.240***	0.255***	0.825***
	(598.126)	(0.066)	(0.072)	(0.191)
North and Central America	1073.070**	0.465***	0.497***	1.008***
	(411.884)	(0.084)	(0.090)	(0.247)
North Asia	657.888	0.640***	0.657***	0.616*
	(695.252)	(0.170)	(0.183)	(0.348)
Oceania	698.910	0.436***	0.463***	1.108**
	(417.135)	(0.120)	(0.131)	(0.435)
Rest of Asia	221.048	0.280***	0.312***	0.785***

	Level	Log(def+1)	Asinh(def)	Log(def)
	(477.046)	(0.070)	(0.076)	(0.244)
South America	5792.198	0.438***	0.457***	0.786***
	(3525.877)	(0.097)	(0.102)	(0.215)
Southeast Asia	1286.595	0.390**	0.402**	0.132
	(790.641)	(0.142)	(0.151)	(0.259)
Observations	37948	37948	37948	30809

* p < 0.1, ** p < 0.05, *** p < 0.01

Notes: Standard errors clustered by country and year in parentheses. All models use 2SLS with country-year and commodity-year fixed effects, instrumenting exports with $\widehat{FD}_{ikt}$. * p < 0.1, ** p < 0.05, *** p < 0.01.

A13. Back-of-envelope calculations for deforestation attributable to export sales

The calculation uses two inputs: the commodity-group $\times$ continent export elasticity $\hat{\gamma}_{gr}$ estimated in equation (A11.4), and observed log-export growth since 2001.

The PPML second stage gives the conditional mean of deforestation as

$$\mathbb{E}[C_{ikt}] = \exp\bigl(\hat{\gamma}_{gr} \ln X_{ikt} + \hat{\alpha}_{it} + \hat{\alpha}_{kt} + \hat{\delta}\hat{\nu}_{ikt}\bigr). \qquad (A13.1)$$

The counterfactual holds exports at the baseline level X_{ik,t_0} (year $t_0 = 2001$) while leaving the fixed effects and the CF residual unchanged. The CF residual is held constant to isolate the effect of export growth driven by foreign demand, as the CF residual captures unobserved supply shocks that are correlated with exports and deforestation. The counterfactual mean is therefore:

$$\mathbb{E}[C^0_{ikt}] = \exp\bigl(\hat{\gamma}_{gr} \ln X_{ik,t_0} + \hat{\alpha}_{it} + \hat{\alpha}_{kt} + \hat{\delta}\hat{\nu}_{ikt}\bigr). \qquad (A13.2)$$

Taking the ratio, the fixed effects $\hat{\alpha}_{it}$, $\hat{\alpha}_{kt}$ and the residual term $\hat{\delta}\hat{\nu}_{ikt}$ cancel identically, yielding

$$\frac{\mathbb{E}[C^0_{ikt}]}{\mathbb{E}[C_{ikt}]} = \exp\bigl(-\hat{\gamma}_{gr}\, \Delta \log X_{ikt}\bigr),$$

where $\Delta \log X_{ikt} \equiv \log X_{ikt} - \log X_{ik,t_0}$ is cumulative log-export growth since baseline. The attributable share — the fraction of observed deforestation explained by export growth above baseline — is therefore

$$\widehat{s^X_{ikt}} \;=\; 1 - \frac{\mathbb{E}[C^0_{ikt}]}{\mathbb{E}[C_{ikt}]} \;=\; 1 - \exp\bigl(-\hat{\gamma}_{gr}\, \Delta \log X_{ikt}\bigr). \qquad (A13.3)$$

By construction, $\widehat{s^X_{ikt}} \in [0, 1)$ when exports grew and is negative when exports fell below baseline.

We apply the share to observed deforestation C_{ikt}, aggregate over all country–commodity pairs

(i, k) and years $t \in [2002, 2022]$, and divide by 10^6 to report million hectares (Mha):

$$\widehat{A_{ikt}^{X}} \;=\; C_{ikt}\, \widehat{s_{ikt}^{X}}, \qquad (A13.4)$$

$$A_{\text{total}}^{X} \;=\; \frac{1}{10^6} \sum_{i,k,t} \widehat{A_{ikt}^{X}} \quad \text{(Mha)}. \qquad (A13.5)$$

A14. Cumulative deforestation shares by commodity and region

Figure A14.1: Cumulative share of global agricultural deforestation (ha) by continent and commodity, 2001–2022. Grey cells indicate no data taken for the study. Source: Singh and Persson (2024). Note: Shares are based on the cumulative sum of deforestation across selected countries between 2001 and 2022, computed for each commodity–region cell.

A15. Cumulative export shares by commodity and region

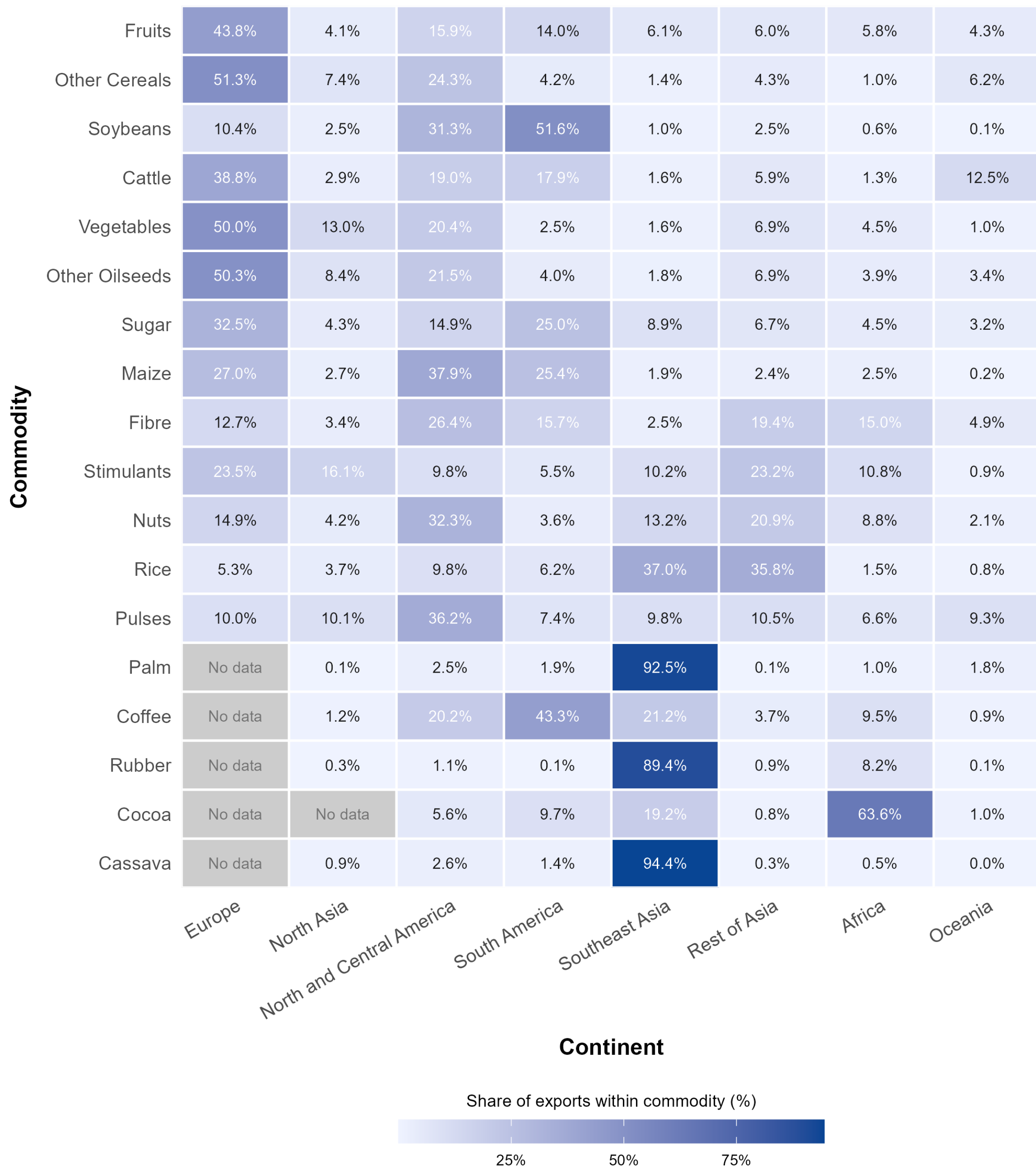

Commodity	Europe	North Asia	North and Central America	South America	Southeast Asia	Rest of Asia	Africa	Oceania
Fruits	43.8%	4.1%	15.9%	14.0%	6.1%	6.0%	5.8%	4.3%
Other Cereals	51.3%	7.4%	24.3%	4.2%	1.4%	4.3%	1.0%	6.2%
Soybeans	10.4%	2.5%	31.3%	51.6%	1.0%	2.5%	0.6%	0.1%
Cattle	38.8%	2.9%	19.0%	17.9%	1.6%	5.9%	1.3%	12.5%
Vegetables	50.0%	13.0%	20.4%	2.5%	1.6%	6.9%	4.5%	1.0%
Other Oilseeds	50.3%	8.4%	21.5%	4.0%	1.8%	6.9%	3.9%	3.4%
Sugar	32.5%	4.3%	14.9%	25.0%	8.9%	6.7%	4.5%	3.2%
Maize	27.0%	2.7%	37.9%	25.4%	1.9%	2.4%	2.5%	0.2%
Fibre	12.7%	3.4%	26.4%	15.7%	2.5%	19.4%	15.0%	4.9%
Stimulants	23.5%	16.1%	9.8%	5.5%	10.2%	23.2%	10.8%	0.9%
Nuts	14.9%	4.2%	32.3%	3.6%	13.2%	20.9%	8.8%	2.1%
Rice	5.3%	3.7%	9.8%	6.2%	37.0%	35.8%	1.5%	0.8%
Pulses	10.0%	10.1%	36.2%	7.4%	9.8%	10.5%	6.6%	9.3%
Palm	No data	0.1%	2.5%	1.9%	92.5%	0.1%	1.0%	1.8%
Coffee	No data	1.2%	20.2%	43.3%	21.2%	3.7%	9.5%	0.9%
Rubber	No data	0.3%	1.1%	0.1%	89.4%	0.9%	8.2%	0.1%
Cocoa	No data	No data	5.6%	9.7%	19.2%	0.8%	63.6%	1.0%
Cassava	No data	0.9%	2.6%	1.4%	94.4%	0.3%	0.5%	0.0%

Figure A15.1: Cumulative share of global agricultural exports (%) by continent and commodity, 2001–2022. Grey cells indicate no data taken for the study. Source: BACI database (Gaulier and Zignago 2010). Note: Shares are based on the cumulative sum of export sales across selected countries between 2001 and 2022, computed for each commodity–region cell.

A16. Results based on alternative instrument ($\widehat{FD2}_{ikt}$)

Table A16.1: Pooled CF-PPML estimate using gravity-predicted demand ($\widehat{FD2}_{ikt}$) instrument

	Deforestation
Log(Exports)	0.514***
	(0.081)
	[0.302, 0.610]
Residual	-0.103
	(0.000)
Observations	30,255
Pseudo R-squared	0.851
Country × Year FE	Yes
Commodity × Year FE	Yes
Instrument	$\widehat{FD2}_{ikt}$

Notes: Bootstrap standard errors (1,000 replications) in parentheses. 95% bootstrap percentile CIs in brackets. Instrument: gravity-predicted demand FD2 (equation 9). Fixed effects: country x year, commodity x year. * p<0.10, ** p<0.05, *** p<0.01.

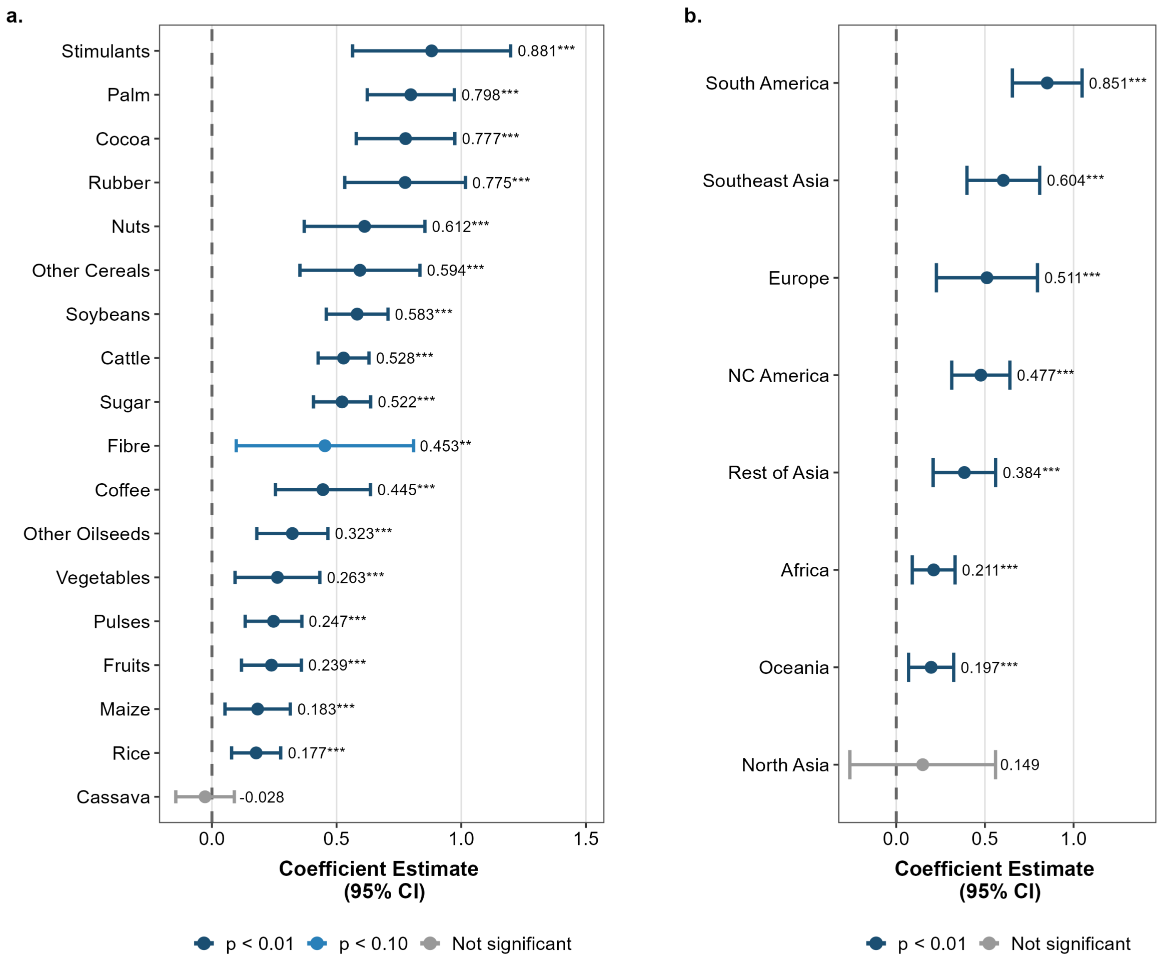

Figure A16.1: Heterogeneous deforestation elasticities using the $\widehat{FD2}_{ikt}$ instrument. Panel (a) shows CF-PPML estimates by commodity group; Panel (b) by continent. All specifications include country–year and commodity–year fixed effects. Standard errors are clustered at country–commodity and year levels. Significance levels: *** p<0.01, ** p<0.05, * p<0.1.

A17. Results based on alternative shares (1996–2000)

This appendix reports the pooled and heterogeneous CF-PPML results using the pre-sample instrument $\widehat{FD}^{pre}_{ikt}$, which replaces the main-sample export shares with shares computed from 1996–2000 BACI data. The importer fixed effects $\hat{\psi}_{jkt-1}$ are identical to those in the main specification.

	Deforestation
Log(Exports)	0.376**

	Deforestation
	(0.179)
	[0.003, 0.709]
Residual	0.066
	(0.168)
	[-0.274, 0.382]
Observations	36,598
Pseudo R-squared	0.863
Country × Year FE	Yes
Commodity × Year FE	Yes
Instrument	$\widehat{FD}_{ikt}^{pre}$

Notes: Bootstrap standard errors (1,000 replications) in parentheses. 95% bootstrap percentile CIs in brackets. Fixed effects: country×year, commodity×year. * p<0.10, ** p<0.05, *** p<0.01.

Table A17.1: Pooled CF-PPML deforestation elasticity using pre-sample shares (1996–2000). Bootstrap standard errors (1,000 replications) in parentheses; 95% bootstrap percentile confidence intervals in brackets. Fixed effects: country×year and commodity×year. * p<0.10, ** p<0.05, *** p<0.01.

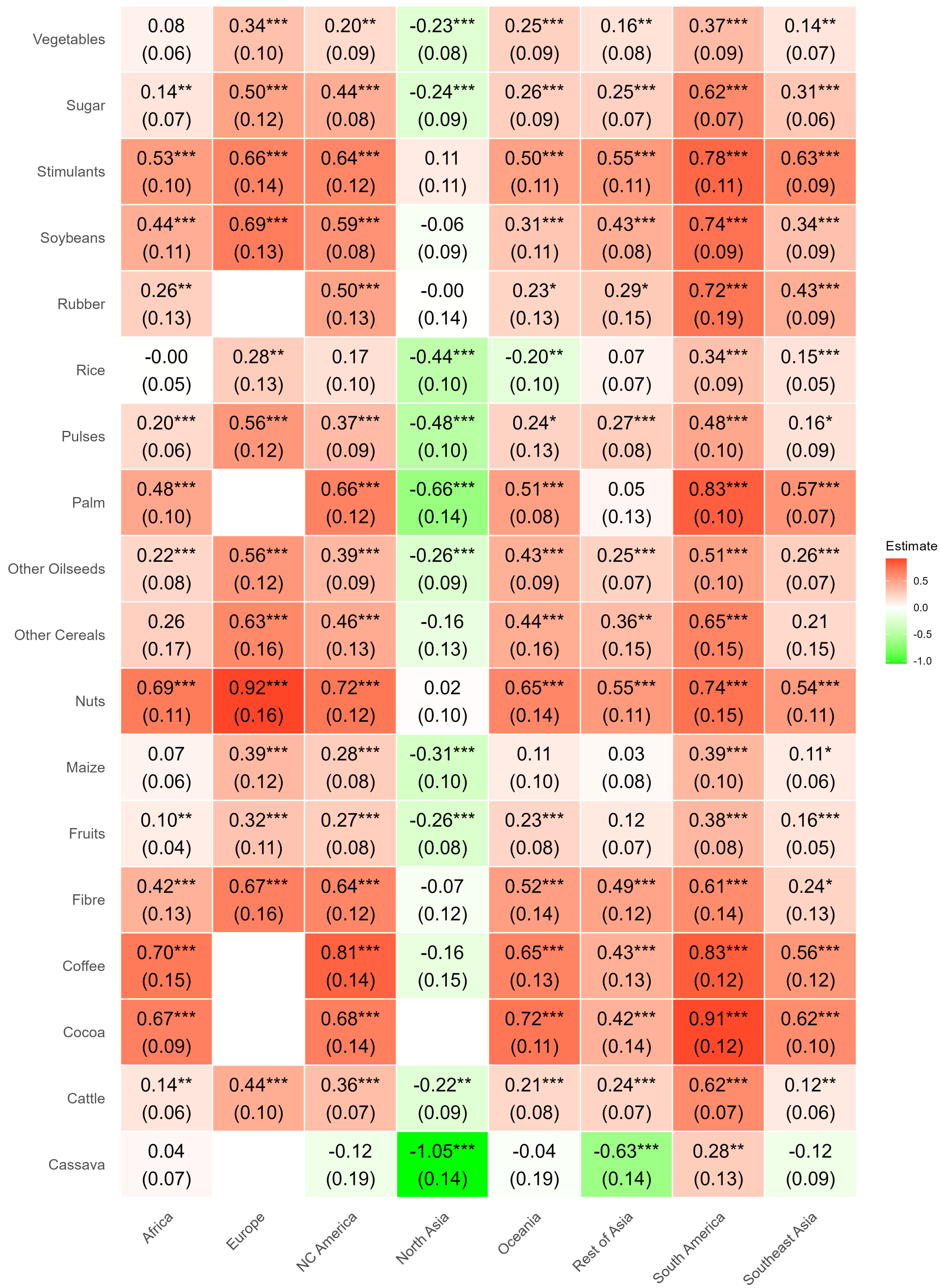

Figure A16.2: CF-PPML elasticity by continent $\times$ commodity using the $\widehat{FD2}_{ikt}$ instrument. Red indicates positive elasticities; green indicates negative elasticities. Fixed effects: country–year and commodity–year. Significance levels: *** p<0.01, ** p<0.05, * p<0.1.

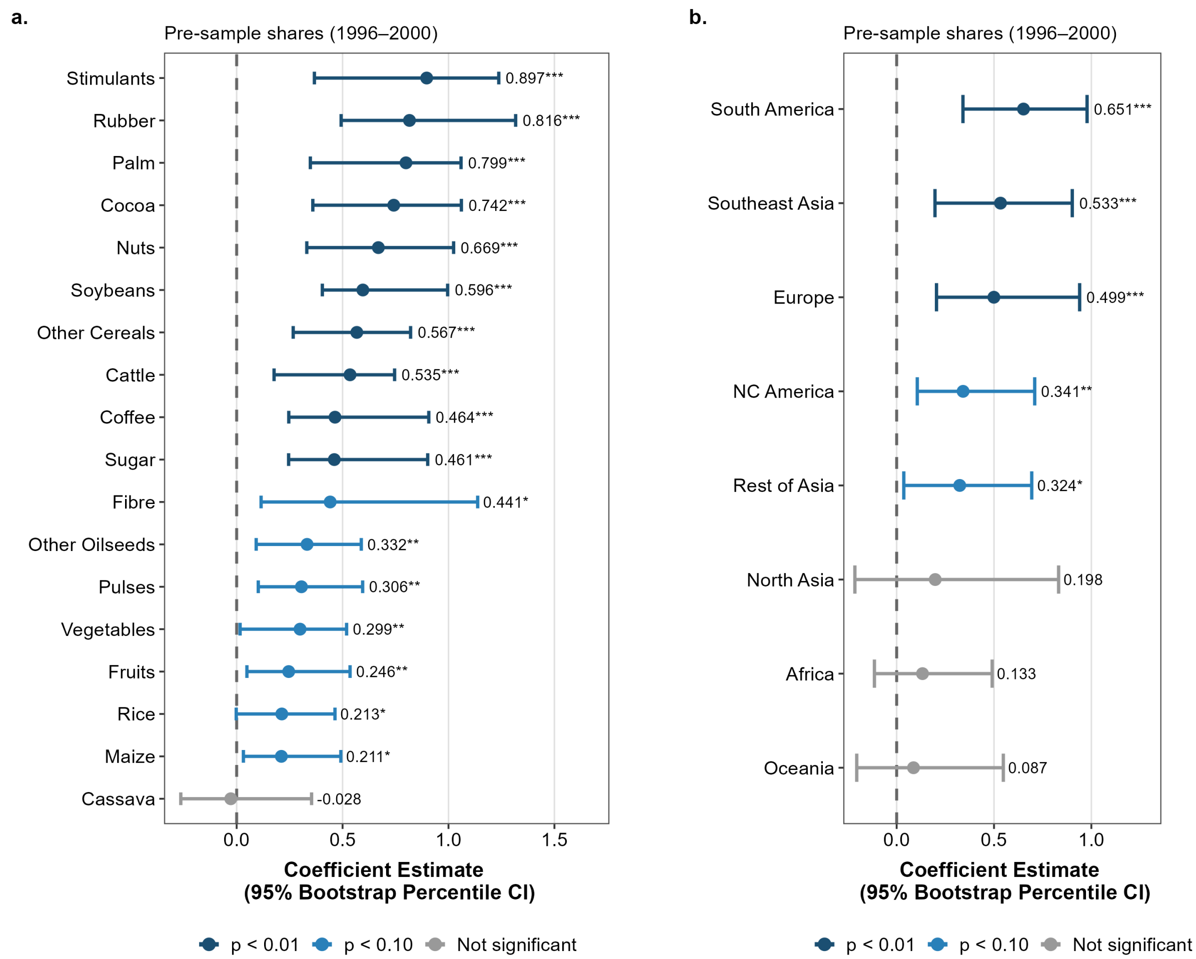

Figure A17.1: CF-PPML export–deforestation elasticity by commodity and continent using pre-sample shares (1996–2000). Error bars show 95% bootstrap percentile confidence intervals (1,000 replications). Fixed effects: country–year and commodity–year. Significance levels: *** p<0.01, ** p<0.05, * p<0.1.

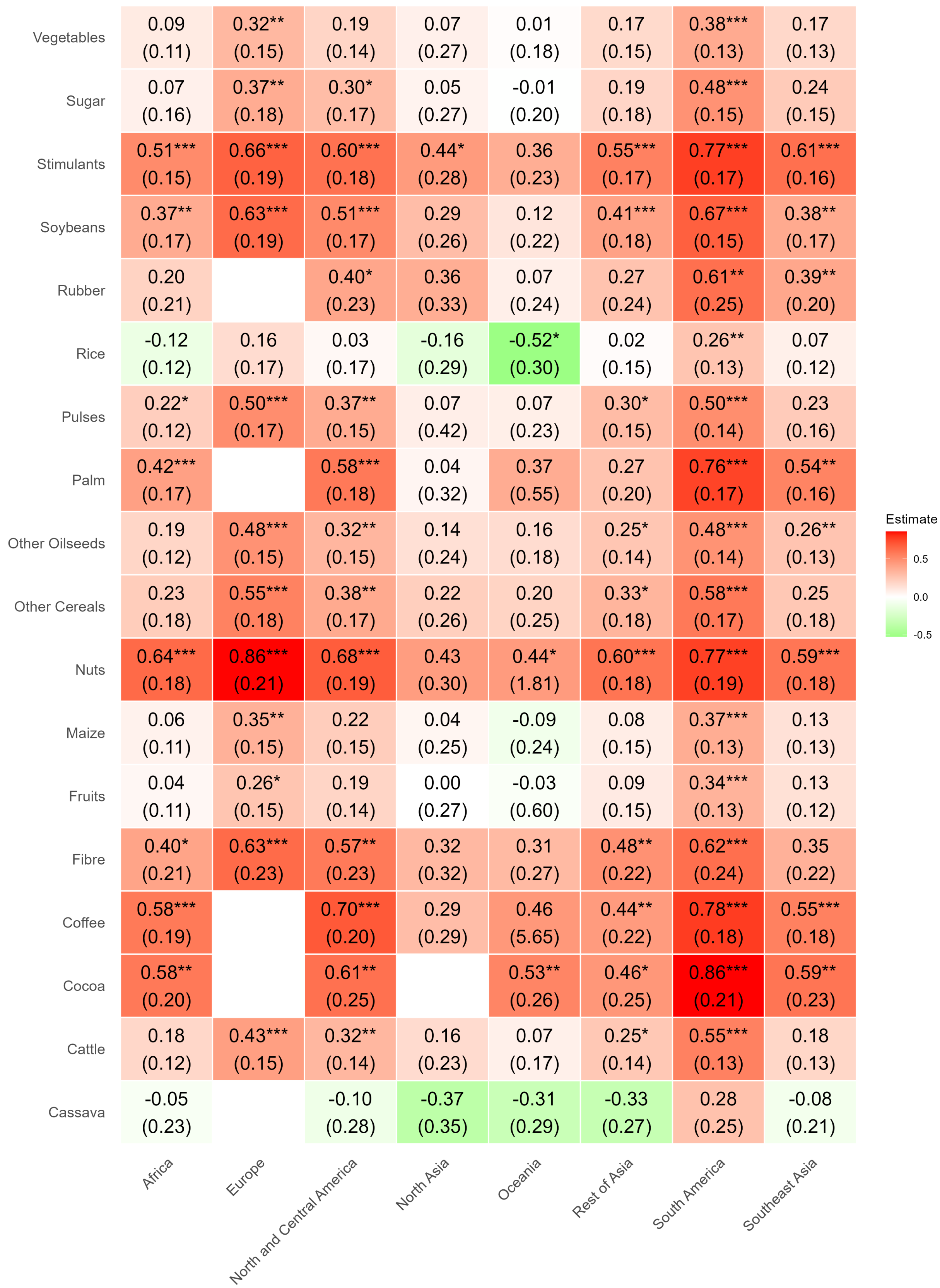

Figure A17.2: CF-PPML deforestation elasticity by continent and commodity using pre-sample shares (1996–2000). Red indicates positive elasticities; green indicates negative elasticities. Bootstrap standard errors (1,000 replications) in parentheses. Fixed effects: country–year and commodity–year. Significance levels: *** p<0.01, ** p<0.05, * p<0.1.